

Chromophore-independent roles of *Drosophila* opsin apoproteins and visual cycle components

Dissertation
for the award of the degree
"Doctor rerum naturalium" (Dr.rer.nat.)
of the Georg-August-Universität Göttingen

within the doctoral program
of the Georg-August University School of Science (GAUSS)

submitted by
Radoslaw Katana

from Zielona Góra, Poland

Göttingen, 2018

Thesis Committee**Prof. Dr. Martin Göpfert**

Department of cellular neurobiology,
University of Göttingen

Prof. Dr. André Fiala

Department of molecular neurobiology of behavior,
University of Göttingen

Members of the Examination Board**Prof. Dr. Martin Göpfert**

Department of cellular neurobiology,
University of Göttingen

Prof. Dr. André Fiala

Department of molecular neurobiology of behavior
University of Göttingen

Further members of the Examination Board:**Dr. Manuela Schmidt**

Emmy Noether-Nachwuchsgruppe somatosensory signaling and systems biology,
Max Planck Institute of Experimental Medicine

Prof. Dr. Jörg Großhans

Institute of biochemistry and molecular cell biology,
University Medical Center Göttingen

Dr. Jan Clemens

Neural computation and behavior group,
European Neuroscience Institute

Dr. Gerd Vorbrüggen

Department of molecular development,
Max Planck Institute for Biophysical Chemistry

Date of oral examination: November 23rd, 2018

I herewith declare that the Phd thesis entitled “Chromophore-independent roles of *Drosophila* opsin apoproteins and visual cycle components” was written independently, with no other sources and aids than quoted.

Radoslaw Katana

Göttingen, October 19th, 2018

I. Preface.....	8
I.I. Hearing in <i>Drosophila melanogaster</i>	9
I.II. Chordotonal neurons	10
I.III. Molecular basis of fly hearing	11
II. Materials and methods	13
II.I. Generation of transgenic flies.....	13
II.I.I Promoter-GAL4 fusion lines.....	13
II.I.II. Genomic rescue flies.....	16
II.I.III. <i>santa-maria</i> ^{TGEM} line.....	16
II.I.IV. Trojan-GAL4 lines	17
II.II. Reverse transcriptase PCR	17
II.III. Laser Doppler vibrometry:	18
II.IV. Prolonged depolarizing afterpotential (PDA) recordings:	20
II.V. Immunohistochemistry:	21
II.V.I. Adult Johnston’s organ staining:	21
II.V.II. Larva Ich5 staining.....	21
II.VI. Fly husbandry	22
II.VI.I. Regular fly food	22
II.VI.II. Vitamin A depleted food.....	22
II.VII. Fly stocks used	23
II.VIII. List of antibodies used	24
Chapter 1: Chromophore-independent roles of <i>Drosophila</i> opsin apoproteins and visual cycle components.	25
1.1. Introduction	25
1.1.1. The <i>Drosophila</i> visual system.	25
1.1.1.1. Rhodopsin.....	26
1.1.1.2 Visual chromophore	26
1.1.1.3 Chromophore generation pathway and recycling	27
1.1.2. Non visual roles of rhodopsins	29
1.2. Results:	32
1.2.1 Scavenger receptor class B - SANTA-MARIA in <i>Drosophila</i> hearing	32

1.2.1.1 Auditory defects of <i>santa-maria</i> ¹ mutant flies	32
1.2.1.2 <i>santa-maria</i> expression pattern	35
1.2.1.3. Localization of TRP channels in <i>santa-maria</i> ¹ mutants.....	37
1.2.1.4. Tissue specific rescue of <i>santa-maria</i> mutants	40
1.2.2. Relevance of the chromophore generation pathway for fly audition	42
1.2.2.1. Vitamin A depletion.....	44
1.2.3. Auditory importance of the genes implicated in chromophore processing and recycle..	47
1.2.3.1. PINTA is functionally involved in auditory process.....	47
1.2.3.2 <i>ninaG</i> function and expression in chordotonal organs.....	51
1.2.3.3 Genes of chromophore recycling pathway in fly hearing	56
1.2.4. Possible roles of Rhodopsin1 in <i>Drosophila</i> hearing.....	60
1.2.4.1. Probing Johnston’s organ function in <i>ninaE</i> ¹⁷ mutants.....	61
1.3. Discussion	64
1.3.1. Eliminating key genes of chromophore synthesis left hearing unaffected.....	64
1.3.2. Santa-Maria scavenger receptor is crucial for JO function	65
1.3.3. Auditory organ function is dependent on the proteins previously implicated is chromophore processing	66
1.3.4. Genes of chromophore recycling pathway are functionally involved in hearing.....	67
1.3.5. Rhodopsin1 has no function in JO	69
Chapter 2: Identifying novel genes in <i>Drosophila</i> hearing.....	70
2.1. Introduction:.....	70
2.1.1. MiMIC as a powerful tool in <i>Drosophila</i> genetics	70
2.1.1.1. MiMIC features.....	70
2.1.1.2. RMCE	71
2.2. Results.....	72
2.2.1. Selection of candidate genes	72
2.2.2. <i>Sosie</i>	73
2.2.2.1. Hearing in <i>sosie</i> mutant flies is severely impaired.....	73
2.2.2.2. <i>Sosie</i> is present in auditory neurons	75
2.2.2.3. Morphology of JO neurons in <i>sosie</i> mutants.....	76
2.2.3 <i>CG14085</i> – the unknown <i>Drosophila</i> gene.....	77
2.2.3.1 Hearing deficits in <i>CG14085</i> mutant flies.....	77

2.2.2.2. <i>CG14085</i> is expressed in chordotonal organs	79
2.3 Discussion	80
3. Summary	82
Bibliography:	83
List of figures:	92
List of abbreviations:	93
<i>Curriculum Vitae</i>	94
Acknowledgements	96

I. Preface

Animal perception of surrounding environment relies on sensing external sensory information with different sensory modalities (Keeley, 2002). This includes: vision, hearing, taste, smell and touch. Between these, hearing and touch are based on conversion of mechanical stimuli into electrochemical activity in the process called mechanotransduction (Albert et al., 2007). To facilitate detection of the mechanical force animals developed specialized mechanosensory organs such as chordotonal organs found in insects. The most extensively studied chordotonal organ in *Drosophila* is Johnston's organ (JO), which plays a major role in fly hearing (Yack, 2004). Although, anatomically fly auditory organs and vertebrates ears are vastly different, they actually share numerous genetic and functional parallels (Senthilan et al., 2012). The most remarkable example of genetic resemblance is interchangeable role of *Drosophila* helix-loop-helix transcription factor *atonal* (*ato*) that specifies JO sensory neurons and its mammalian homolog *Math* that determine development of hair cells in vertebrate ears (Wang et al., 2002). Mouse *Math1* can functionally substitute *ato* in the flies lacking *ato* and vice versa, suggesting conserved role of both proteins (Wang et al., 2002). Furthermore, mechanotransduction machinery of JO neurons and hair cells seem to be based on the same components including gating springs that convey force to the mechanically gated ion channels and adaptation motors (Senthilan et al., 2012).

Interestingly, mechanosensory organs as they may seem very distinct from photoreceptors in *Drosophila* eye, actually were shown to share the same evolutionary origin (Fritsch et al., 2007). Early in the development they are specified by previously mentioned proneural gene *atonal* (Jarman and Groves, 2013). Moreover, molecules that previously were solely known as photosensors in *Drosophila* retina – Rhodopsins seem to be involved in sensing more cues than light (Leung and Montell, 2017). This canonical light sensors are also involved in adult hearing, larval proprioception and thermosensation (Senthilan et al., 2012; Shen et al., 2011; Sokabe et al., 2016; Zanini et al., 2018).

I.I. Hearing in *Drosophila melanogaster*

Hearing in insect serves two main roles: communication and courtship (Todi et al., 2004). In *Drosophila* mating behavior male flies produce a courtship song by extending and fanning one of its wings to attract a female and stimulate other males to sing and court (Greenspan, 2000; Yoon et al., 2013). These songs are species specific and compose of two main components: sine and pulse which fall in the frequency range of 100-300 Hz (Dickson, 2008).

In *Drosophila* adults hearing organs are located on both sides of the head, between the eyes and are called Antennae (Yack, 2004). Each antenna is composed of three main segments. The first segment (scape) is the smallest one and comprises muscles to actively position the whole organ (Figure 1). The second antennal segment (pedicel) harbors the Johnston's organ, an array of ca. 500 stretch receptive chordotonal neurons that are used to detect sound, wind and gravity (Göpfert and Robert, 2002). The third segment (funicel) serves for olfaction and together with stiffly coupled branched structure called arista forms a sound receiver (Göpfert and Robert, 2002). The sound receiver is connected with the second antennal segment via a hook which allows rotational movement of the whole structure in response to particle velocity of sound (Albert and Göpfert, 2015). These vibrations result in mechanical stress that is applied on chordotonal neurons in 2nd antennal segment leading to their activation (Göpfert and Robert, 2001).

JO neurons can be classified into 5 classes (A-E) based on their projections in the antennal mechanosensory and motor center (AMMC) in the brain (Azusa Kamukouchi, Tkashi Shimada, 2006). The most sensitive subpopulation of neurons belong to class A and B, they mainly respond to sound-induced antennal deflections and are needed for hearing (Kamikouchi et al., 2009). In the other hand, CE class of neurons are activated by higher antennal deflection caused by gravity and wind (Yorozu et al., 2009).

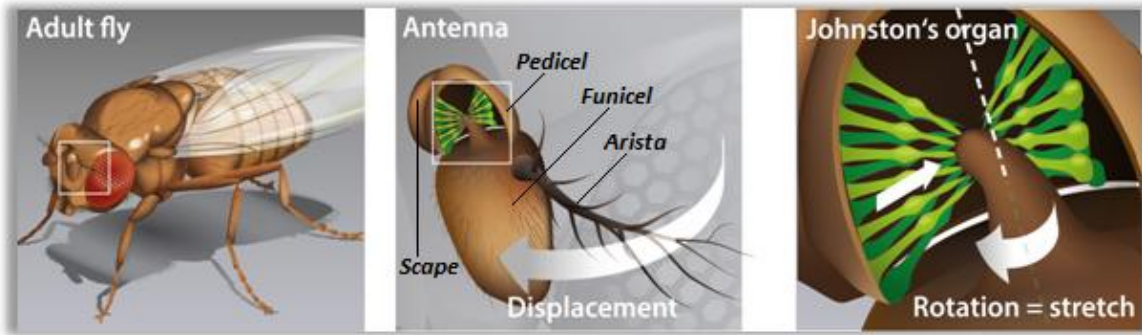


Figure 1. Hearing organ of *Drosophila*.

On the right: sketch of *Drosophila* adult fly. Magnified view on antenna: the first segment (scape), the second segment (pedicel), the third segment (funicel) and the arista. On the left: 2nd antennal segment anatomy. In green are mechanosensitive JO neurons which are suspended between the antennal hook and the cuticula. Rotation of the sound receiver causes activation of the neurons. Modified from Dr. C. Spalhoff.

I.II. Chordotonal neurons

The biggest chordotonal organ (cho) in adult *Drosophila* is JO that consists of mechanosensory neurons organized in units called scolopidia (Figure 2) (Kamikouchi et al., 2009). Each scolopidium comprises of two to three monodendric, ciliated sensory neurons associated with three accessory cells: ligament cell, scolopale cell and cap cell (Brewster and Bodmer, 1995). The ligament cell supports the neuron by attaching it to the cuticula on its proximal end, whereas the cap cell is responsible for apical attachment to the 3rd antennal segment joint (Albert and Göpfert, 2015). The scolopale cells on the other hand wraps around cilium forming a sealed scolopale space filled with an extracellular lymph enriched in K⁺ ions that creates a proper environment for mechanotransduction (Caldwell and Eberl, 2002). Additionally, scolopale cells are endowed with actin enriched rods which protects the neuronal dendrite and presumably creates initial tension of the cilium (Todi et al., 2004).

Chordotonal sensory neurons can be also found in *Drosophila* larvae where they form: lateral pentaloscolopodial organ LCh5 (Figure 2 right), single lateral organ LCh1, and two ventral organs VChA and VChB that are used for proprioception (Halachmi et al.,

2016). The most extensively studied is LCh5 organ that consists of an array of 5 scolopidia units and set of accessory cells that share the same morphological and functional properties as the ones seen in adult JO (Styczynska-Soczka and Jarman, 2015).

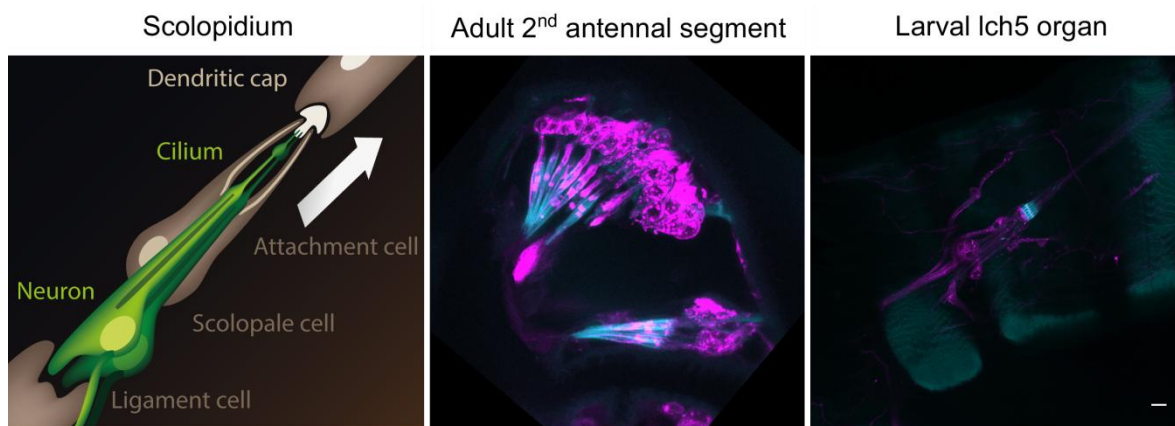


Figure 2. Chordotonal organs in *Drosophila*

Left: Sketch of the scolopidium. Mechanosensory chordotonal neurons are colored green and accessory cell in brown. Modified from Dr. Spalthoff. Middle and right: Immunohistochemical staining of the adult JO and larval pentaloscolopidial (lch5), respectively. Neurons are shown in magenta and scolopale rods in cyan. Scale bar 10 μ m.

I.III. Molecular basis of fly hearing

The mechanical force that acts on the sound receiver causes vibrations on the joint between funiculus hook and dendritic cap attachment of auditory neurons in the 2nd antennal segment (Albert and Göpfert, 2015). These vibrations are conveyed to the mechano-electrical transduction (MET) channels which resides in the distal part of the chordotonal sensory neuron (Bokolia and Mishra, 2015). In flies, these mechanotransduction channels of JO neurons are considered to be directly gated as their electrical response to sound stimuli show a delay of less than 1 ms, which is too short for second-messenger cascade (Albert et al., 2007). Direct gating of these channels is further supported by observation of characteristic gating compliance in response to rapid deflection of sound receiver (Nadrowski et al., 2008).

Even though, cilia of Johnston's organ mechanosensory neurons display '9+0' microtubule axonemes arrangement, which are usually considered as immotile due to lack of central pair of microtubules, they are endowed with dynein arms that support their motility (Karak et al., 2015). Thus, *Drosophila* sound receiver show spontaneous, self sustained motions in absence of stimulus (Göpfert and Robert, 2003). These motions can be monitored by tracking the antennal movement using the laser Doppler vibrometer, that permits direct and noncontact measurements of antennal vibration velocity (Robert and Göpfert, 2002). Fly antennae are broadly tuned, with the highest peak at the frequency of around 250Hz, which matches the dominant frequency of the courtship song (Göpfert and Robert, 2002). In response to sound stimuli JO neurons actively boost antennal vibrations enhancing the antennal sensitivity to faint sounds by a factor of ~10 (Göpfert et al., 2006). The origin of this mechanical amplification derives from the coaction between the mechanotransduction channels and previously mentioned axonemal dyneins motors (Karak et al., 2015).

There are 3 known MET ion channels implicated in *Drosophila* hearing: No mechanoreceptor potential C (NOMPC), Inactive (*Iav*) and Nanchung (*Nan*) (Bokolia and Mishra, 2015). They belong to transient receptor potential (TRP) superfamily of ion channels, whereas NOMPC is a single member of TRPN subfamily, *Iav* and *Nan* belongs to TRPV subfamily (Bokolia and Mishra, 2015). NOMPC was proposed to play a main role in mechanotransduction complex of JO neurons (Effertz et al., 2011). In absence of NOMPC hearing is severely impaired as evidenced by complete loss of JO neurons motility, abolished mechanical amplification and lack of sound-evoked action potentials in antennal nerve (Effertz et al., 2011). However, when stimulated with louder sounds *nompC* mutants show residual nerve potential that probably comes from activation of less sensitive mechanotransduction channels in CE class of JO neurons (Effertz et al., 2012). NOMPC occurs at the dendritic tips of JO neurons, whereas *Iav* and *Nan* are present more proximal in the cilium forming heteromultimeric transduction channel (Kim et al., 2003). Thus, these two TRPV channels are not considered as main mechanotransduction channels, rather they act downstream of NOMPC (Zhang et al., 2015). They seem to negatively control NOMPC dependent amplification as *nan* and *iav* mutants flies show excessive fluctuation power and increase of the mechanical amplification gain (Göpfert et al., 2006).

II. Materials and methods

II.I. Generation of transgenic flies

II.I.I Promoter-GAL4 fusion lines

To generate the GAL4 promoter fusion construct of particular genes their upstream genomic regions of ~2kb were amplified. The primers were design as follows:

pinta	F: 5'-CCTCTAGAGCAACCAGTTGCAGCAAAAC-3' R: 5'-CCGGATCCCGTTGATCTGCGGATTGG-3'
ninaG	F: 5'-CCTCTAGAGCCATTGAGCCACTGGATA-3 R: 5'-CCGGATCCACTCCCATTGCTGTTTTTGG-3'
Pdh	F: 5'-CCTCTAGACAATGCCCACTAGATGGG R: 5'-CCGAATCCGCGAAAGGACATCTTGGTCT-3'

The forward and reverse primer contains XbaI and BamHI restriction site respectively. Extra CC was added to 5' end of each primer to facilitate enzymatic digestion.

Genomic DNA extraction

Genomic DNA was extracted from flies using DNeasy Blood & Tissue Kit from Qiagen. Homogenization was made by crushing 20 *w¹¹¹⁸* flies in 180µl of buffer ALT together with 20µl of proteinase K using the QiagenTissueLyser LT homogenizator. The homogenate was incubated at 56°C 1000rpm overnight on the Thermoshaker. Following washing steps were done according to the DNeasy protocol. After DNA elution in the pure water the nucleic acid concentration was measured using the Thermo Scientific Nanodrop 1000.

PCR amplification:

Desired DNA sequences were amplified using GoTaq® G2 Green Master Mix.

The reaction mixes were prepared on ice as follows:

For a 50µl reaction volume:

Component:	Volume	Final conc.
GoTaq® G2 Green Master Mix, 2x	25µl	1x
Upstream primer	1µl	0,5 µM
Downstream primer	1µl	0,5 µM
DNA template	2µl	~500ng
Nuclease-Free Water	21µl	N.A

PCR tubes were placed in the Bio-Rad MyIQ thermal cycler and PCR conditions were set.

Protocol for PCR reaction:

Step	Time (min:sec)	Temperature (°C)
Initialization	3:00	95
Dentaturation	0:15	95
Annealing	0:30	57
Elongation	1:30	72
Final elongation	7:00	72

Steps B1,B2,B3 were repeated 30 times

Restriction digestion:

After PCR the samples were cleaned using a NucleoSpin® Gel and a PCR Clean-up kit from Machery-Nagel. DNA samples and pPTGAL vector were then digested in 1x Fast digest buffer containing BamH1 and Xba1 restriction enzymes at 37°C for 2 hours.

Gel electrophoresis:

Digested DNA samples and pPTAGAL vector were loaded in the 1% agarose gel containing 2.5µl of Roti®-GelStain reagent for detection of nucleic acids. The gel was placed in the Bio-Rad Wide Mini Sub Cell GT electrophoresis apparatus filled with 1x TBE buffer. A Thermo Scientific Gen ruler DNA ladder was added into one of the wells. The gel was run at 100V for 1 hour. A single bands of DNA construct and pPTAG vector of correct size was excised from the gel, weight and cleaned using the NucleoSpin® Gel and the PCR Clean-up kit from Machery-Nagel.

Ligation:

The insert and the vector (5µl each) were added to 10x ligation buffer in presence of 1µl T4 DNA ligase. Ligation was carried overnight at 4°C.

Transformation:

Aliquots of XL1-Blue competent cells were thawed on ice for 20min. 15µl of the ligation reaction was carefully added to the cells and incubated on ice for 15min. Then, the cells were heat shocked at 42°C for 60sec and incubated for 10min on ice. Then, 200µl of SOB medium was added and incubated for 1hour in the Innova 40 shaker incubator with 1000rpm agitation. The bacteria cultures were poured on the LB agar plates containing ampicillin antibiotic, streaked to obtain single bacterial colonies and left to grow in 37°C chamber overnight. On the next day single colonies were picked and added to liquid LB medium and incubated overnight in 37°C bacteria shaker.

Mini-prep from bacterial culture:

After successful transformation, 2ml of bacterial overnight cultures were spun down, and the supernatant was taken out. The next steps were performed according to the NucleoSpin® Plasmid kit from Machery-Nagel. The final samples were digested and run on the gel as in previous steps for verification of correct insert and vector sizes.

Sequencing:

Samples of total volume of 16µl and concentration of 100ng/µl were sequenced by the MPI-Sequencing Facility in Hermann-Rein-Str. 3, 37075 Goettingen, Germany. After sequence verification constructs were sent to BestGene® for embryo injections.

II.I.II. Genomic rescue flies

Genomic rescue flies were made using BACPAC clones ordered from P(acman) resource centre. To generate *pinta* rescue a clone no. CG321-22H03 was used that contains ~65kb of the 3rd chromosome of wild-type fly including *pinta* locus. For generation of *pdh* rescue CH322-23P06 clone was used that contains ~22kb including *pdh* locus. The clones were directly send for embryo injection to BestGene.

II.I.III. *santa-maria*^{TGEM} line

TGEM vector phase 0 (addgene #62891) was targeted into 1st coding intron of *santa-maria* gene by homologous recombination using CRISPR/Cas strategy (Diao et al., 2015). The guide RNA was: GACTCGCGCCAATTGAGAGG CGG and the primers to amplify the left and the right homology arms were as follows:

Left arm:

Forward primer: TCCCGATAAGCGATAAGTGC

Reverse primer: GGCACCTCCCAGTTGTTCTTC

Right arm:

Forward primer: AAGCAATAGCATCACAAATTTTAC

Reverse primer: TCCACAGTTTCCACATAATCCA

The experiment was carried out by GenetiVision.

II.I.IV. Trojan-GAL4 lines

MiMIC flies: *sosie*^{M11265} and *CG14085*^{M111086} were obtained from Bloomington Stock Centre. *in vivo* Recombinase Mediated Cassette Exchange (RMCE) was performed to replace MiMIC cassette with triple donor construct pC-(loxP2-attB2-SA-T2A-Gal4-Hsp70)3 cassette through series of genetic crosses (Diao et al., 2015). The detailed crossing scheme can be find in Figure S1B. (Diao et al., 2015). YFP-positive larvae were collected and the lines were established.

II.II. Reverse transcriptase PCR

RNA extraction:

To extract total RNA from the antenna and the heads, 50 *w*¹¹¹⁸ flies were transferred to a 10ml falcon tube and snap frozen using liquid nitrogen. In order to disintegrate different body parts, flies were vortexed for 5sec then incubated in liquid nitrogen. This step was repeated several times. Set of sieves with mesh sizes of: 710µm, 425µm, 250µm, 125µm were pre-chilled in -80°C for 30min and kept on dry ice. Whole material from falcon tubes was transferred on to the upper sieve. After vigorous shaking pure heads were retained on the 425µm sieve whereas 2nd antenna segments passed through all sieves on the bottom sieve pan. Material was then collected to eppendorf tubes containing a lysis buffer and homogenized in the TissueLyser LT. RNA was extracted using NucleoSpin[®] RNA Clean-up XS kit according to a manufacture protocol. RNA concentration was determined using Nanodrop spectrophotometer.

cDNA synthesis and PCR:

The RNA was converted to complementary cDNA using Qiagen QuantiTect[®] Reverse Transcription Kit. The cDNA was amplified by PCR using following primers:

F: 5'-CAAAACACAATGGAGAGGTACG-3'

R: 5'-GCACATGGACCAGATGGA-3'

II.III. Laser Doppler vibrometry:

Fly mounting:

The fly was mounted on the top of plastic rod using Icosane. In order to minimized any vibration coming from head, abdomen and wings they were fixed using dental glue. In order to avoid antenna movement the 1st segment was fixed to head capsule. As a results, the only vibrating part was a sound receiver made of 3rd antennal segment and its arista. To diminish any external vibration the whole setup was placed on the air table.

Free fluctuations recordings:

The free fluctuations were recorded using Politec Leaser Doppler Vibrometer (PSV-400) by pointing the laser beam on the tip of the arista. In the absence of any external stimuli the only forces that act on the arista are thermal motions and intrinsic properties of sound receiver. The LDV allows very precise measurements of antennal velocity. A Fast Fourier Transform (FFT) of the velocity time trace was performed by the LDV software to extract frequency dependent velocity characteristic of the antenna fluctuations and power spectra. The power spectral density (PSD) of the fluctuations was calculated by integrating

fluctuation power of frequencies between 100 and 1,500 Hz. The frequency where antennal fluctuations reached its peak was considered as individual best frequency (Ibf).

Sound-induced antennal responses:

A loudspeaker was used to generate pure tones of desired frequency. An attenuator was used to manipulate the sound intensity from 6-96 dB. An Emkay NR 3158 pressure-gradient microphone was used to directly measure sound particle velocity at the position of the fly antenna. The antennal displacements were measured at the frequency matching fly Ibf. Amplification gains were calculated by dividing antennal displacement by microphone response. The ratio between the lowest and the highest gain was considered as a amplification gain. Compound action potentials (CAP) were monitored via electrolytically sharpened tungsten electrodes. The recording electrode was placed between 1st antennal segment and the head capsule near the antennal nerve and the reference electrode in the thorax. The antennal CAP responses of each individual were normalized, plotted against sound particle velocity or antennal displacement and fitted using Hill-equation. The hearing thresholds were defined as a sound particle velocity or antennal displacement that correlates to 10% of maximum CAP amplitude from the Hill fit.

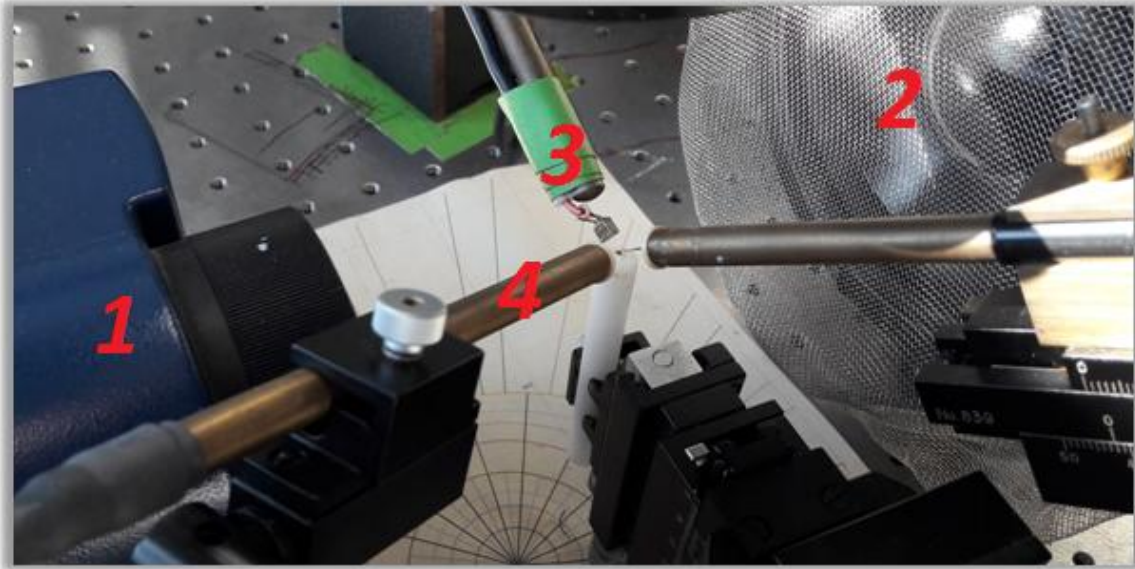


Figure 3. Experimental setup to probe antennal mechanics and electrophysiology.

Picture showing experimental setup. Fly is mounted on the top of plastic rod. (1) Laser Doppler Vibrometer (LDV), (2) speaker, (3) microphone, (4) electrodes.

II.IV. Prolonged depolarizing afterpotential (PDA) recordings:

In order to observe PDA phenotype in flies, ERG recordings were performed. *Drosophila* fly was mounted on plastic rod in similar way as described in (2.3.1). The blue light (470nm) and orange light (590nm) was delivered by Superluminescent LED (catalog no. LB W5SN-GYHZ-25-Z, LY W5SN-JYKY-46, Mouser electronics). LED's were mounted ca. 10cm in front of the fly. The resulted ERG traces were recorded via tungsten electrode inserted in the eye and reference electrode placed in thorax. Fly was adopted in complete darkness for 5min and stimulated with sequence of light pulses orange-blue-blue-orange-orange, each pulse 10s long with 10 seconds dark intervals.

II.V. Immunohistochemistry:

II.V.I. Adult Johnston's organ staining:

The flies were anaesthetized on the CO₂ pad. The heads were dissected and fixed in 4% PFA + 0,3% PBST pH 7.4 for 1 hr RT. Then, the heads were embedded in preheated gelatin-albumin solution in small silicon moulds, cooled down at 4°C for 5 min and post fixated in 6% PFA at 4 °C overnight. On the next day blocks were incubated for 20 min in methanol and then transferred to PBS pH 7.4. The fly antennae were then cut in 40µm slices using Leica vibrotome and proceed with antibody staining.

The section were blocked in blocking solution for 1 hr RT and then incubated with primary antibody diluted in the same solution at 4°C overnight with constant agitation. On the next day sections were washed 4 times in 0,05% PBST for 20 min, followed by incubation with secondary antibodies diluted in 0,05% PBST for 3 hr. Then, the sections were washed 4 times in 0,05% PBST for 20 min and once in DABCO solution for 10 min. The samples were then mounted on the glass slides in DABCO and stored at 4°C until subjected for confocal imaging using Leica SP2 confocal microscope. The images were analyzed and processed using ImageJ software.

II.V.II. Larva Ich5 staining

Larva was put on the petri dish filled with PBS pH 7.4 and cut parallel to the body axis, the guts were removed leaving body wall neurons exposed. The preparation was washed 3 times for 10 min in PBS and then, fixed with 4% PFA in 0,3% PBST for 40 min RT. The tissue was washed 3 times for 30 min in PBS pH 7.4 then, washed once again with 0.3% PBST for 20 min. Larval filet was then incubated in the blocking solution for 1 hr RT. The primary antibodies were diluted in the blocking solution and incubated with the sample overnight at 4°C with agitation. On the next day samples were washed 5 times with 0.1% PBST for 20 min. Secondary antibodies were diluted in PBST and incubated with samples for 4 hr RT and washed again in PBST thrice for 20 min, and finally mounted on the glass slides with DABCO.

II.VI. Fly husbandry

II.VI.I. Regular fly food

Standard fly composition:

Ingredients:	Quantity:
dry yeasts	1000g
sugar	1000g
salt	40g
agar	120g
flour	500g
apple juice	2l
propionic acid	60ml

Ingredients needed to prepare 14l of fly food.

To prepare 14l of standard fly food, 120g of Agar was soaked in 5l of water overnight. On the next day 500g flour, 1000g yeast 40g salt, 1000g sugar were mixed in 6 liters of water and 2l of apple juice was added. The whole mixture was boiled at 100 °C in the Varioklav® Steampot DT44580604. When the temperature lowers to 65°C 60ml of propionic acid was added. Immediately after that empty vials were filled with ~10ml of food. After cooling down overnight at 4°C the vials were closed with mite free plugs.

The flies were grown at 18°C or 25°C incubator with 60% humidity in 12h light dark cycles. The flies were kept in plastic vials ¼ filled with fly food.

II.VI.II. Vitamin A depleted food

To prepare Vitamin A free fly food 2g of agar was added to 100ml of water and boiled for 2 min. 10g of dry yeast and 10g of sugar was added and boiled for 10 more

minutes with stirring. After the temperature drops to ~60°C 20mg of cholesterol was added. Then the food was poured to vials and used in deprivation assays.

II.VII. Fly stocks used

Genotype:	Symbol:	Source:
<i>w</i> ¹¹¹⁸	<i>w</i> ¹¹¹⁸	Lab stock
<i>w</i> [*]; <i>ninaD</i> [1]/ <i>SM1</i>	<i>ninaD</i> ¹	BL 42244
<i>w</i> [*]; <i>santa-maria</i> [1]	<i>santa-maria</i> ¹	BL 24520
<i>w</i> [1118]; <i>P</i> { <i>y</i> + <i>t</i> 7.7} <i>w</i> [+ <i>mC</i>]= <i>GMR90A05-GAL4</i> } <i>attP2</i> <i>santa-maria GAL4</i>	<i>santa-maria-GAL4</i>	BL 46905
<i>w</i> [*]; <i>santa-maria</i> [1]; <i>P</i> { <i>w</i> [+ <i>mC</i>]= <i>UAS-santa-maria.W</i> }3	<i>UAS-santa-maria</i>	BL 24519
<i>w</i> [*]; <i>ninaB</i> ^{360d}	<i>ninaB</i> ^{360d}	Kindly provided by Prof. O'Tousa
<i>w</i> [*]; <i>sna</i> [<i>Sco</i>]/ <i>CyO</i> ; <i>pinta</i> [1]	<i>pinta</i> ¹	BL 24860
<i>w</i> [*]; <i>pinta-GAL4/TM3</i>	<i>Pinta-GAL4</i>	self made
<i>w</i> [*]; <i>ninaG</i> ^{P330}	<i>ninaG</i> ^{P330}	Kindly provided by Prof. O'Tousa
<i>w</i> [*]; <i>ninaG-GAL4/TM3</i>	<i>ninaG-GAL4</i>	self made
<i>w</i> [*]; <i>P</i> { <i>w</i> [+ <i>mC</i>]= <i>Pdh</i> [+ <i>t</i> 1.5]}2; <i>TI</i> { <i>w</i> [+ <i>mW.hs</i>]= <i>TI</i> } <i>Pdh</i> [1] <i>st</i> [1]	<i>Pdh</i> ¹	BL 32077
<i>w</i> [*]; <i>Pdh-GAL4/TM3</i>	<i>Pdh-GAL4</i>	Self made
<i>w</i> [*]; <i>sr</i> [1] <i>ninaE</i> [17]	<i>ninaE</i> ¹⁷	Kyoto DGGR 109599
<i>y</i> [1] <i>w</i> [*]; <i>sr</i> [1] <i>ninaE</i> [17]	<i>ninaE</i> ¹⁷	Kindly provided by Prof. Britt
<i>w</i> [*]; <i>rdhB</i> ¹	<i>rdhB</i> ¹	Kindly provided by Prof. Montell
<i>P</i> { <i>w</i> [+ <i>mC</i>]= <i>rdhB-GAL4.W</i> }1, <i>w</i> [1118]; <i>sna</i> [<i>Sco</i>]/ <i>CyO</i> ; <i>TM2/MKRS</i>	<i>rdhB-GAL4</i>	BL 24501
<i>w</i> [*]; <i>Dnai2-GAL4</i>	<i>Dnai2-GAL4</i>	Kindly provided by Dr. Karak
<i>y</i> [1] <i>w</i> [*]; <i>wg</i> [<i>Sp-1</i>]/ <i>CyO</i> , <i>P</i> { <i>Wee-P.ph0</i> } <i>Bacc</i> [<i>Wee-P20</i>]; <i>P</i> { <i>y</i> + <i>t</i> 7.7} <i>w</i> [+ <i>mC</i>]= <i>20XUAS-6XGFP-Myc</i> } <i>attP2</i>	<i>UAS-GFP</i>	BL 52261
<i>w</i> [1118]; <i>P</i> { <i>w</i> [+ <i>mC</i>]= <i>UAS-RedStinger</i> }4/ <i>CyO</i>	<i>UAS-nuclear RFP</i>	BL 8546
<i>w</i> [*]; <i>so</i> [1]	<i>so</i> ¹¹	BL 401
<i>w</i> [*]; <i>P</i> { <i>pinta</i> } ⁺	<i>pinta</i> ⁺	Self made
<i>w</i> [*]; <i>P</i> { <i>Pdh</i> } ⁺	<i>Pdh</i> ⁺	Self made
<i>w</i> [*]; <i>P</i> { <i>Rh1</i> [<i>y</i> ⁺]} <i>ninaE</i> ¹⁷	<i>ninaE rescue</i>	Kindly provided by Prof. Britt
<i>y</i> [1] <i>w</i> [*]; <i>Mi</i> { <i>PT-GFSTF.0</i> } <i>alphaTub85E</i> [<i>MI08426-GFSTF.0</i>]	<i>Tub85E-GFP</i>	BL 60267
<i>w</i> [*]; <i>Santa-maria</i> ^{TGEM}	<i>Santa-maria</i> ^{TGEM}	Made by GenetiVision

$y[1] w[*]; Mi\{MIC\} sosie^{MII265}$	$sosie^{MiMIC}$	BL 58547
$y[1] w[*]; Mi\{MIC\} CG14085^{MII1086}$	$CG14085^{MiMIC}$	BL 56121
$y[1] w[*]; sosie^{Trojan}-GAL4$	$sosie^{Trojan}-GAL4$	Self made
$y[1] w[*]; CG14085^{Trojan}-GAL4$	$CG14085^{Trojan}-GAL4$	Self made

II.VIII. List of antibodies used

Anti-GFP chicken, catalog no. GTX13970 GeneTex (1:1000)

Anti-RFP Rat, catalog no. 5F8, Chromotek (1:1000)

Anti- α Tub85E, kindly provided by Prof. Dr. A. Salzberg, (Halachmi et al., 2016) (1:500)

Anti-NOMPC rabbit, kindly provided by Prof. Dr. Yuh-Nung Jan (1:300)

Anti-Iav rat, kindly provided by Prof. Dr. Changsoo Kim (1:300)

Cy3-conjugated goat anti-HRP, catalog no. 123165021 Jackson ImmunoResearch (1:500)

Alexa Fluor 488 anti-chicken catalog no. A21316 ThermoFisher Scientific (1:300)

Alexa Fluor 488 anti-rabbit catalog no. A11008 ThermoFisher Scientific (1:300)

Alexa Fluor 633 anti-rabbit catalog no. A21094 ThermoFisher Scientific (1:300)

Alexa Fluor 633 Phalloidin catalog no. A22284 ThermoFisher Scientific (1:300)

Chapter 1: Chromophore-independent roles of *Drosophila* opsin apoproteins and visual cycle components.

1.1. Introduction

1.1.1. The *Drosophila* visual system.

As in most insects the *Drosophila* vision is based on compound eye made of approximately 750 hexagonal, columnar units called ommatidia (Pak et al., 2012). Each ommatidium consists of 20 cells in which there are 8 photoreceptor cells (R1-R8) and set of accessory cells (Leung and Montell, 2017). The main photoreceptors R1-R6 occupy the outer part of ommatidium, whereas photoreceptors R7/R8 are located in the centre part (Montell, 2012). There are also two types of accessory cells surrounding the photoreceptor cells: secondary retinal pigment cells (2° PC) and tertiary retinal pigment cells (3° PC) (Pak et al., 2012). Each photoreceptor contains rhabdomere, which is a densely packed stack of membranes (microvilli) where phototransduction takes place. These membranes are filled with the light sensor molecules – rhodopsins (Montell, 2012). The *Drosophila* genome encodes for 7 different rhodopsins with 6 expressed in photoreceptors (Grebler et al., 2017). The most abundant rhodopsin is Rhodopsin1 (Rh1) which is a product of the *ninaE* gene. It is present in photoreceptors R1 - R6 and absorbs maximally at 486nm (O'Tousa et al., 1985). Minor rhodopsins Rh3-R6 are expressed in photoreceptors R7-R8 and show maximal spectral sensitivity at 331, 355, 442 and 512 nm respectively (Salcedo et al., 2003).

1.1.1.1. Rhodopsin

Rhodopsins belong to the G protein-coupled receptor (GPCR) family. They are made of an apoprotein molecule opsin and covalently linked light sensitive unit chromophore (Figure 4) (Wald, 1938, 1968). Opsins are expressed in photoreceptor cells and after maturation are embedded in the cell membrane by seven transmembrane domains (Ozaki et al., 1993). The chromophore, 11-*cis*-hydroxy-retinal binds to lysine in the seventh transmembrane domain via Schiff base linkage (Vogt and Kirschfeld, 1984). Upon light stimulation, rhodopsin is activated to metarhodopsin by *cis* to *trans* photo-isomerization of the chromophore. This in turn leads to conformational changes in the opsin subunit that triggers GDP-GTP exchange in a heteromeric G-protein (Dolph et al., 1993). The effector molecule of heteromeric G-protein in *Drosophila* is phospholipase C (PLC), which hydrolyzes phosphatidylinositol 4,5-bisphosphate (PIP₂) resulting in opening of the TRP and TRPL ion channels (Scott et al., 1995).

1.1.1.2 Visual chromophore

All animals depend on dietary intake of Vitamin A and its precursors (provitamins, mainly β -carotene) to support the synthesis of the visual chromophore (Kiefer et al., 2002). In contrast to vertebrates where Vitamin A is implicated in multiple processes besides vision (Lane and Bailey, 2005), in *Drosophila* it is exclusively used in the retina for the chromophore synthesis (Wang, 2005). There, the visual chromophore serves two main functions. First, as mentioned previously, it captures light photons which activates rhodopsin and starts the visual cascade. Second, the chromophore is necessary for opsin synthesis in endoplasmic reticulum, where it acts as a molecular chaperone (Colley et al., 1991). In absence of the chromophore opsin cannot exit the ER and eventually gets degraded (Wang et al., 2007). As a consequence, diminished rhodopsin levels leads to a severe vision deficiency and degeneration of photoreceptors R1 – R6. (O'Tousa JE1, Leonard DS, 1989).

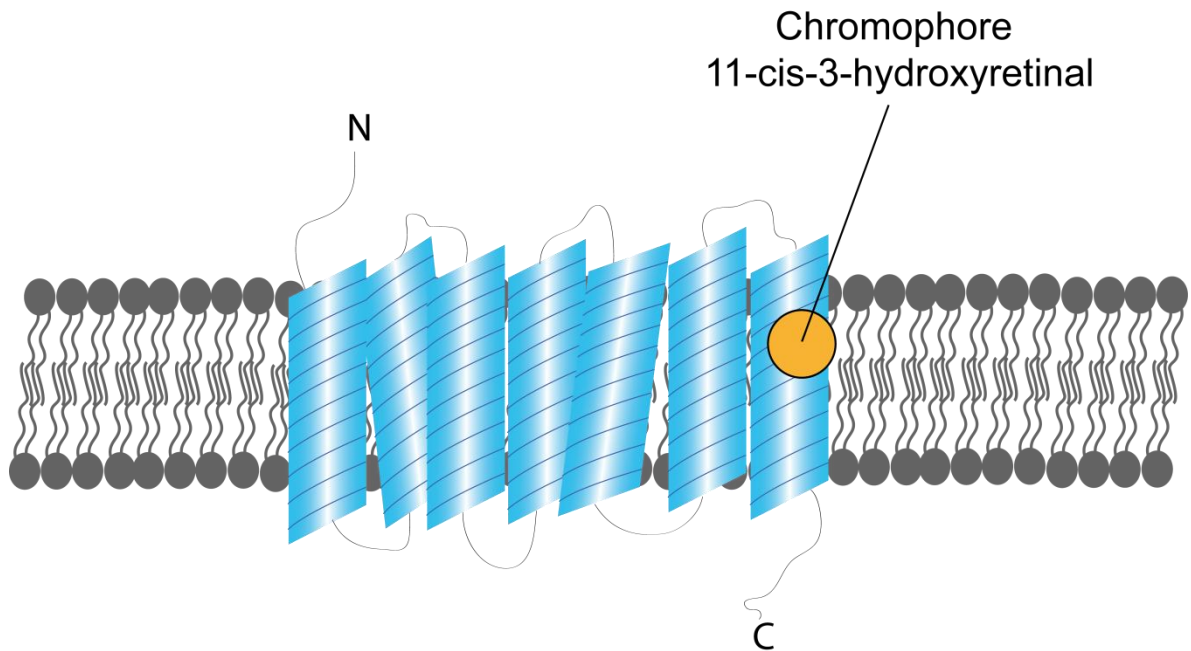


Figure 4. Rhodopsin sketch

Rhodopsin is composed of seven transmembrane domain protein- opsin and a light-sensitive chromophore 11-cis-3-hydroxyretinal.

1.1.1.3 Chromophore generation pathway and recycling

The 11-*cis*-3-hydroxy-retinal synthesis pathway involves several proteins responsible for β -carotene uptake, cleavage, transport and multistep enzymatic reactions. The intake of carotenoids take place in the midgut, and depends on specialized scavenger receptor NINAD (Kiefer et al., 2002). It has a significant sequence homology to mammalian class B scavenger receptors, SR-BI and CD36 which besides participation in carotenoid uptake are also implicated in lipoproteins metabolism (Steinbrecher, 1999). However, flies seem to utilize it exclusively for β -carotene intake (Kiefer et al., 2002).

Later, β -carotene can be hydroxylated to form zeaxanthin (3,3-dihydroxy β , β -carotene) and subsequently stored in fat body or immediately used for further chromophore production (Giovannucci and Stephenson, 1999). Circulating β -carotene is then taken up by another scavenger receptor class B - SANTA-MARIA expressed in the neurons and glia in

1.1 Introduction

the brain (Wang et al., 2007). Subsequently, the C₄₀ carotenoid backbone chain is symmetrically cleaved yielding two C₂₀ retinoids (all-trans retinal). This crucial reaction in chromophore synthesis is catalyzed by β,β -carotene-15,15'-monooxygenase (BCO) encoded by *ninaB* gene (Lintig and Vogt, 2000). Moreover, it was shown that NINAB also catalyzes the isomerization of all-trans to 11-cis retinal that can directly serve as a chromophore for opsin (Oberhauser et al., 2008). In blind *ninaB* mutant flies vision can be restored by supplying the flies with all-trans retinal, whereas *ninaD* and *santa-maria* mutants need β -carotene to bring back normal light perception (Wang et al., 2007).

The next player in biogenesis of the visual chromophore is PINTA- a retinoid binding protein (RBP) which belongs to CRAL-TRIO family of proteins (Wang, 2005). It is expressed in the retinal pigment cells in the eye where it preferentially binds retinol (Wang, 2005). Nonetheless, the cellular function of PINTA is still not well-defined (Pak et al., 2012). Subsequent steps of chromophore synthesis involve activity of NinaG (Sarfare et al., 2005). This protein belongs to the glucose-methanol-choline (GMC) oxidoreductase enzyme family and participates in the conversion of (3R)-3-hydroxyretinol to the 3S enantiomer (Ahmad et al., 2006). In flies, only Rh1 utilize (3S)-3-hydroxyretinol as its chromophore, other rhodopsins use the 3R enantiomer. Thus, only Rh1 production is affected in *ninaG* mutant flies.

In flies, as in vertebrates, the photoconverted chromophore product 3-OH-all-trans-retinal dissociate from rhodopsin and is regenerated through the visual pathway (Wang et al., 2010). This pathway is crucial in *Drosophila* to maintain chromophore levels under carotenoid deficiency conditions that prevent them from generating the new chromophore. So far two dehydrogenases have been discovered to participate in the chromophore recycling: PDH (pigment cell dehydrogenase) and RDHB (retinal dehydrogenase) (Wang et al., 2010, 2012). The pathway also includes an unknown isomerase that converts all-trans-3-hydroxyretinol to 11-cis-3-hydroxyretinol (Montell, 2012). All these enzymatic reactions occur in the photoreceptor accessory cells- retinal pigment cells (RPC). When exposed to constant light *Pdh* and *rdhB* mutant flies show progressive retinal degeneration caused by chromophore depletion and as a consequence reduced Rh1 levels (Wang et al., 2012).

1.1.2. Non visual roles of rhodopsins

During past 130 years rhodopsins were investigated extensively. Series of studies focused on describing protein structure, activation mechanism and the visual transduction cascade (Leung and Montell, 2017; Montell, 2012; Sakmar et al., 2002). A dogma was that opsins act exclusively as light sensors in photoreceptor cells. However, over the last years this has changed as more evidence suggests that *Drosophila* opsins also serve non visual functions.

In larvae, the main visual rhodopsin Rh1 was found to be implicated in temperature sensing (Shen et al., 2011). Wild-type larvae have a strong thermal preference to 18°C and their comfortable range is 19° to 24°C (Kwon et al., 2008). Unexpectedly, *rh1* mutants turned out to be defective in temperature discrimination between 18° and 24°C (Shen et al., 2011). This thermotactic behavior was independent of light, but turned out to require a chromophore since eliminating β -carotene from a diet or disrupting chromophore synthesis in *santa-maria*¹ mutants cause comparable effects to *rh1* mutants. Hence, both opsin and its chromophore are needed for larval thermosensation. The authors suggested that in this case the chromophore may play a similar role as in adult photoreceptors, where besides being a light sensitive molecule it also serves as a chaperone for maturing opsin (Ozaki et al., 1993).

Later studies proposed that Rh5 and Rh6 are not only required in larval Bolwig's organ for light perception but also for thermal selection during last stage of larval development (Sokabe et al., 2016). Larvae experience a switch from Rh1 mediated thermosensation in early to mid 3rd instar to multiple opsins like Rh5 and Rh6 in late 3rd instar. These two opsins seem to function in *trpA1* expressing neurons in the brain and body wall. As with Rh1, Rh5 and Rh6 functions are light independent and depend on visual chromophore (Sokabe et al., 2016).

Another surprising finding was that opsins are crucial for mechanotransduction in adult flies (Senthilan et al., 2012). The work of Senthilan and colleagues in 2012 revealed that Rh5 and Rh6 are implicated in *Drosophila* auditory processing. Both are expressed in JO neurons where they contribute to mechanical amplification and sound-evoked electrical

1.1 Introduction

responses. Mutation of either *rh5* or *rh6* results in almost complete loss of JO neuron motility, abolished amplification gain and reduction in sound evoked potentials. Likewise, opsins in larval temperature discrimination, Rh5 and Rh6 also seem to require the visual chromophore for hearing in adults (Senthilan et al., 2012). Mutant flies for *santa-maria* gene show comparable auditory impairments to *rh6* and *rh5* mutants (Senthilan et al., 2012). Moreover, SANTA-MARIA seem to also operate in JO neurons since driving *UAS-santa-maria* transgene with chordotonal neurons specific driver *JO15-GAL4* in *santa-maria*¹ mutant background restored normal hearing (Senthilan et al., 2012).

Few years later opsins were reported to be involved in proprioception in *Drosophila* larvae (Zanini et al., 2018). Authors showed that lack of Rh1 and Rh6 lead to severe crawling defects including reduction of speed, increase in turning frequency and longer time to advance one body length. Both opsins were shown to be present in proprioceptive pentameric chordotonal organs (*lch5*), the main organs providing locomotory feedback in larvae (Caldwell et al., 2003; Zanini et al., 2018). Each *lch5* organ is comprised of five monodendritic sensory neurons and set of accessory cells, and Rh1 and Rh6 expression was restricted to dendrites of these neurons (Zanini et al., 2018). Interestingly, the correct ciliary localization of mechanotransduction channels NOMPC and IAV seem to depend on Rh1 and Rh6. In absence of these opsins NOMPC mislocalize from the ciliary tip leaking down into endolymph space, whereas IAV was absent in some cilia (Zanini et al., 2018). Furthermore, *rh1* and *rh6* mutants show strong defects in cilium ultrastructure (Zanini et al., 2018). Larvae that lack SANTA-MARIA showed similar crawling phenotype to this of opsin mutants, thus their functions seem to be chromophore dependent. Unlike opsin function in larval thermosensation where they were proposed to act as a thermosensors, in larval locomotion Rh1 and Rh6 seem to play structural role keeping a proper ciliary organization.

Based on these findings one can clearly say that rhodopsins are not just light sensors. Besides vision, they are used to sense different modalities like hearing, thermosensation and proprioception. To serve these non visual functions, rhodopsins seem to require a visual chromophore, most probably for rhodopsin maturation and trafficking. Chromophore necessity for non-visual functions was investigated either by retinal depletion

or testing *santa-maria* mutants. However, even though SANTA-MARIA is needed for β -carotene uptake in the brain, the initial substrate intake takes place in the gut and is mediated by the NINAD scavenger receptor.

This thesis focused on testing the hypothesis of chromophore dependent auditory roles of opsins. This was achieved by analyzing genes involved in chromophore synthesis, their expression patterns and by nutritional depletion of β -carotene. I also tested whether the main visual opsin Rh1 is needed for hearing, as in larval chordotonal organs for proprioception.

1.2. Results:

Rhodopsins were long considered to exclusively act in light detection. Recent studies, however, showed that this might not necessarily be the case as various *Drosophila* rhodopsins were found to be involved in sensory modalities other than vision and light detection (Leung and Montell, 2017). Besides light-dependent functions Rh1, Rh5 and Rh6 were found to play light-independent roles in larval thermosensation (Shen et al., 2011; Sokabe et al., 2016); Rh5 and Rh6 in fly hearing (Senthilan et al., 2012) and Rh1, Rh6 in larval proprioception (Zanini et al., 2018). Thermosensory rhodopsin functions seem to involve the chromophore as eliminating the Santa-Maria receptor, or removing β -carotene from a diet, causes thermosensory defects as observed in rhodopsin mutants (Shen et al., 2011; Sokabe et al., 2016). Loss of Santa-Maria also impairs larval proprioception and fly hearing, and it was accordingly hypothesized that the chromophore would also be required for mechanosensory opsin functions (Senthilan et al., 2012; Sokabe et al., 2016).

The aim of this thesis was to systematically test this hypothesis using nutritional and genetic approaches. I started with re-analyzing hearing in mutant flies lacking Santa-Maria, which reportedly cause hearing defects (Senthilan et al., 2012).

1.2.1 Scavenger receptor class B - SANTA-MARIA in *Drosophila* hearing

1.2.1.1 Auditory defects of *santa-maria*¹ mutant flies

First, free fluctuations of the fly's antennal sound receiver were monitored using laser Doppler vibrometry. Antennae of wild-type flies show self sustained oscillations in absence of external stimuli that arise from thermal motion and mechanical activity of Johnston's organ neurons (Göpfert and Robert, 2003). Fast Fourier transforms (FFT) of the velocity traces were used to compute power spectra of the fluctuations. Motile JO neurons actively feed energy supporting antennal vibrations (Göpfert et al., 2005) that can be

estimated by integrating the power spectral density (PSD) of the fluctuations for frequencies between 100 and 1500 Hz. For control *w¹¹¹⁸* flies, the respective fluctuation power was $1189 \pm 403 \text{ nm}^2/\text{Hz}$ (mean \pm 1 S.D., N = 5) (Figure 5A). The frequency at which velocity of fluctuations reaches its peak was considered as the individual mechanical best frequency (Ibf) of the antennal receiver, which for controls was $227 \pm 12 \text{ Hz}$. As expected, *santa maria¹* mutant displayed ca. 10 times lower PSD ($136 \pm 13 \text{ nm}^2/\text{Hz}$) and a higher Ibf ($595 \pm 81 \text{ Hz}$) than the controls.

To further characterize mutant effects on hearing, the flies were exposed to pure tones of different intensities matching the antennal best frequency and the resulting receiver vibrations and compound action potentials were recorded (Figure 5B). For loud and faint sound stimuli, antennal displacements in controls linearly scaled with intensity, whereas a nonlinear scaling was found at intermediate intensities, boosting the vibrational response to faint sounds with an amplification gain of 10.5 ± 1.7 . In *santa-maria¹* mutants, the antenna's displacement response was linearized, reducing the amplification gain to 1.65 ± 0.4 .

The sound-evoked antennal nerve responses were measured as compound action potential (CAP). The measurements of maximum CAP responses showed high variability that comes from restrictions of the recording method. Main factors that influence measured values are the quality of the electrode and the distance of the inserted electrode from antennal nerve. Wild-type maximum CAP response was $16.1 \pm 10.8 \text{ }\mu\text{V}$, and in *santa-maria¹* mutants the amplitude was reduced ($5.7 \pm 3.9 \text{ }\mu\text{V}$) (Figure 5C).

The recorded nerve responses were normalized, plotted against the sound particle velocity, and then fitted with a Hill equation (Figure 5C). The sound particle velocity threshold (SPV threshold) defined as 10% of the maximum CAP amplitude, was $63 \pm 2 \text{ nm/s}$ for control flies. Antennae of *santa-maria¹* flies were less sensitive to sound with thresholds of $0.12 \pm 0.06 \text{ mm/s}$. Another parameter tested was antennal displacement threshold, which refers to antennal displacement needed to elicit 10% of the maximum CAP response (Figure 5C). For wild-type flies, this displacement threshold was $78 \pm 5 \text{ nm}$. Mutant *santa-maria¹* flies showed higher displacement thresholds of $62 \pm 7 \text{ nm}$.

1.2 Results

The hearing deficits in *santna-maria*¹ mutants are consistent with previous findings (Senthilan et al., 2012). Johnston's organ function is severely impaired, most prominent being a strong reduction in JO neuron motility as witnessed by the loss of mechanical amplification.

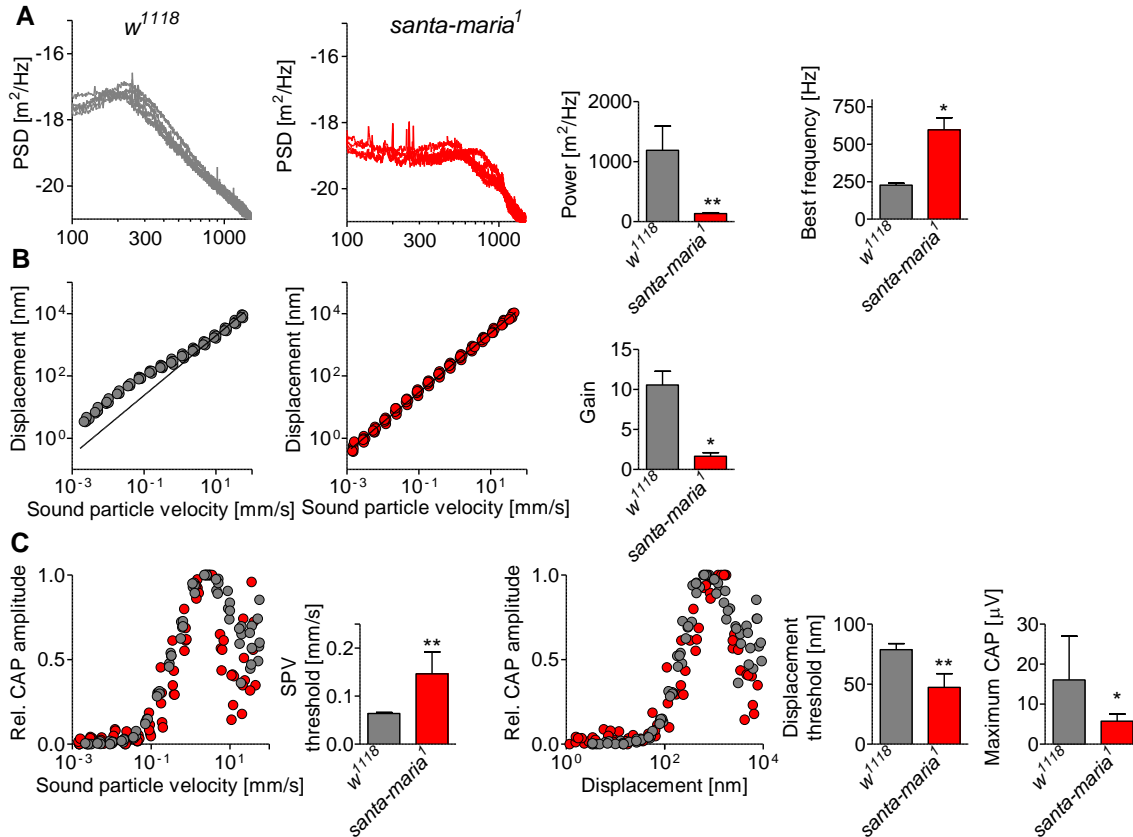


Figure 5. Biomechanical and sound evoked nerve responses analyses of wild-type and *santa-maria*¹ mutant flies.

- A)** Left: power spectral density (PSD) of the free mechanical fluctuation of the antenna in the wild-type (gray) and *santa-maria*¹ mutants (red) (N=5 per strain). Right: respective fluctuation powers and antennal best frequency.
- B)** Left: Tone-evoked antennal displacement as a function of the particle velocity of the tone. The black line indicates linearity. Right: respective mechanical amplification gain.
- C)** Left: Relative amplitude of toned-evoked CAPs as a function of the particle velocity of the tone and respective particle velocity threshold. Right: CAP amplitude plotted against the respective antennal displacement and corresponding displacement threshold.

Data are presented as a mean values \pm 1 SD, N=5, *P < 0.05, **P < 0.01 two-tailed Mann Whitney U-test.

1.2.1.2 *santa-maria* expression pattern

To assess the pattern of *santa-maria* expression, an existing *santa-maria-Gal4* driver was used that was reported previously to target neurons and glia in the brain (Wang et al., 2007). After crossing this line to *20xUAS-6xGFP* fluorescent reporter, no signal was detected in chordotonal organs of both larvae and adults. To enhance fluorescence signal I also generated flies carrying two copies of each transgene, but also here no expression in chordotonal organs could be seen (Figure 6). Thus, a recently developed method of generating Gal4 driver lines was employed that uses MiMIC-like Trojan exon constructs (T-GEM) that can be targeted via Crispr/Cas to the coding intron of the gene of interest enabling Gal4 expression in a pattern that mimics the native expression pattern (Diao et al., 2015). This approach enables to express GAL4 in the pattern that mimic the native site of gene expression (Diao et al., 2015). After crossing *santa-maria*^{T-GEM}-*Gal4* flies to flies carrying a *20xUAS-6xGFP* reporter, the expression pattern in larvae was examined. Already without anti-GFP staining, GFP fluorescence could be detected (Figure 7).

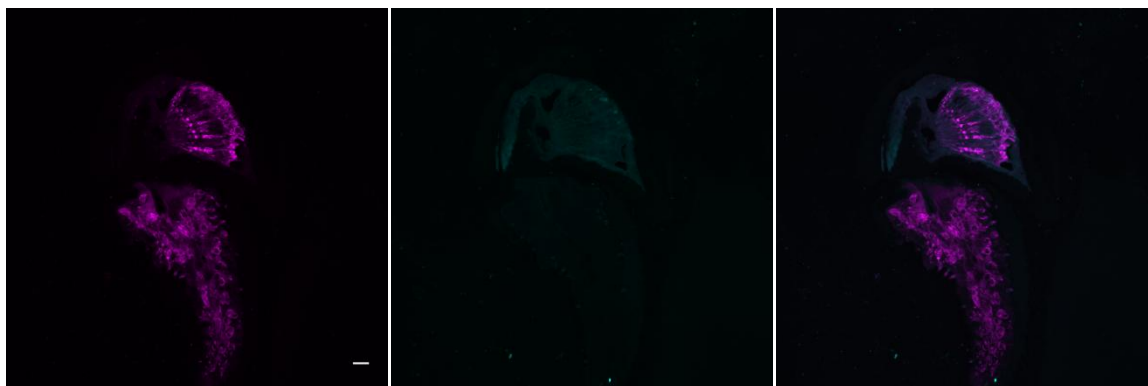


Figure 6. *santa-maria-Gal4* expression pattern. Two copies of both *santa-maria Gal-4* and *20xUAS-6xGFP* were used. Anti-GFP staining of adult antennae did not yield any detectable signal (cyan) in the 2nd or 3rd antennal segments. Neurons are marked with anti-HRP (magenta). Scale bar = 10 μ m.

1.2 Results

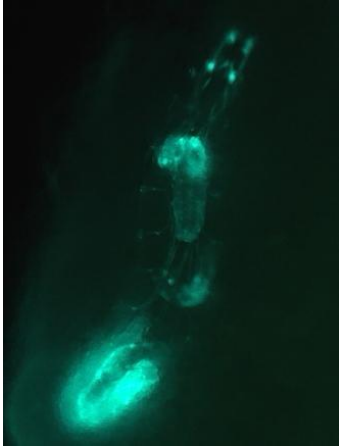


Figure 7. Epifluorescent image of the *santa-maria*^{T-GEM}-*Gal4* expression pattern in larva. GFP signals can be observed in Bolwig's organ, the brain, segmental nerves and the intestines.

To address whether Santa-Maria occurs in larval chordotonal neurons, immunohistochemistry staining on pentameric chordotonal organ (Ich5) was performed. The GFP signal seems to surround the cell bodies of Ich5 neurons, their axon bundles, and other body wall sensory neurons (Figure 8). Counterstaining neurons with anti-HRP suggests that, within Ich5, the peripheral glial cell that enwraps neuronal cell bodies and axons is Santa-Maria-positive.

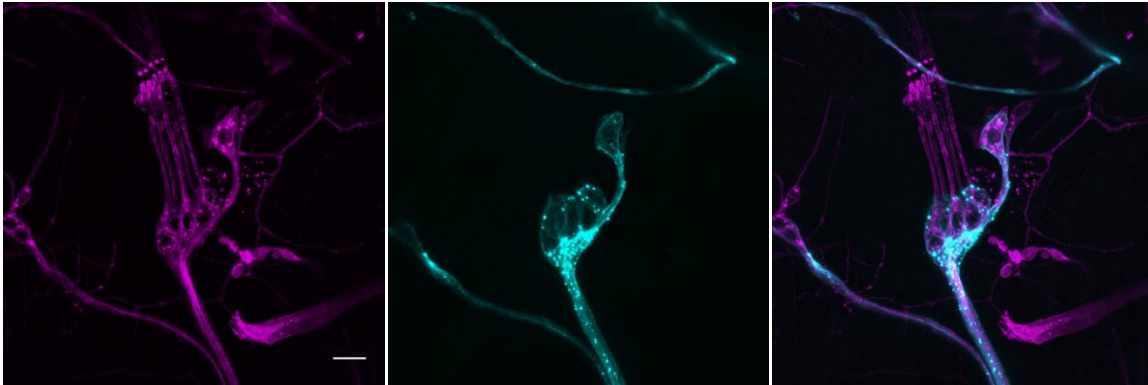


Figure 8. *santa-maria*^{T-GEM}-*Gal4* expression in larval Ich5 chordotonal organ. Neurons of Ich5 organ marked with anti-HRP neuronal marker (magenta). GFP signal showed in cyan. On the right overlap picture. Scale bar = 10µm.

Immunohistochemical staining on sliced 2nd antennal segment of adult flies also revealed broad *santa-maria* expression around somata and axons (Figure 9). Most probably stained structures are ligament cells and other glia cells.

The expression data suggests that *santa-maria* is expressed more broadly as suggested previously (Wang et al., 2007). Expression includes glia cells of chordotonal neurons and other sensory neurons in larvae as well as in adults (e.g. 3rd antennal segment olfactory neurons, data not shown) and the larval gut, where expression was excluded based on the old driver (Wang et al., 2007).

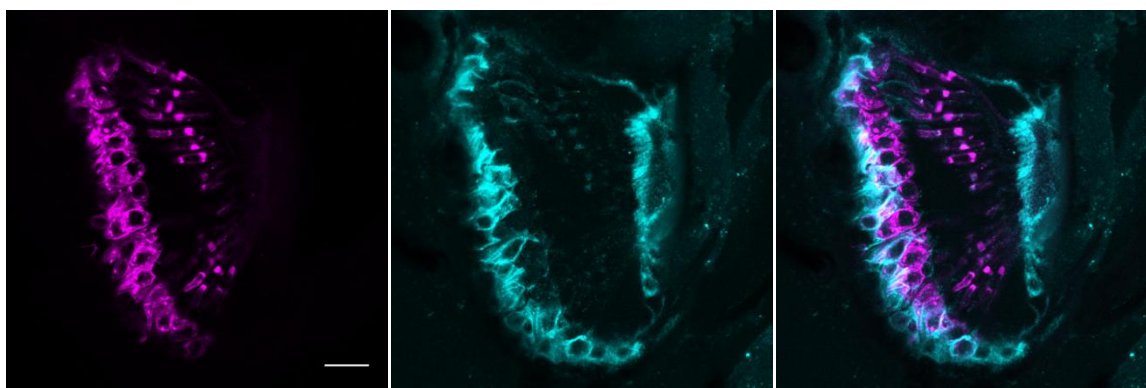


Figure 9. *santa-maria*^{T-GEM}-*Gal4* expression in Johnston's organ.

Anti-GFP staining of 2nd antennal segment slices. Neurons are stained with HRP - magenta, GFP signal is shown in cyan. GFP signal was detected in glia cells enwrapping neuronal cell bodies and axons. Scale bar = 10µm.

1.2.1.3. Localization of TRP channels in *santa-maria*¹ mutants

In *Drosophila* larvae, mutations in *ninaE* and *Rh6* cause mislocalization of NOMPC and Nan-Iav TRP channels in lch5 cilia and impair cilium ultrastructure (Zanini et al., 2018). To test whether such phenotypes also arise from the loss of Santa-Maria, lch5 and JO of *santa-maria*¹ mutants were stained with antibodies against NOMPC and Iav. HRP staining revealed no gross structural defects of the mechanosensory neurons, and the localization of TRP channels seemed normal with NOMPC being present in the tips of the

1.2 Results

cilia and *Iav* localizing more proximally to the basal cilium region (Figure 10, 11). Apparently, loss of opsins and *santa-maria* both affect hearing, but only the loss of opsins causes TRP channel mislocalization and ultrastructural cilium defects.

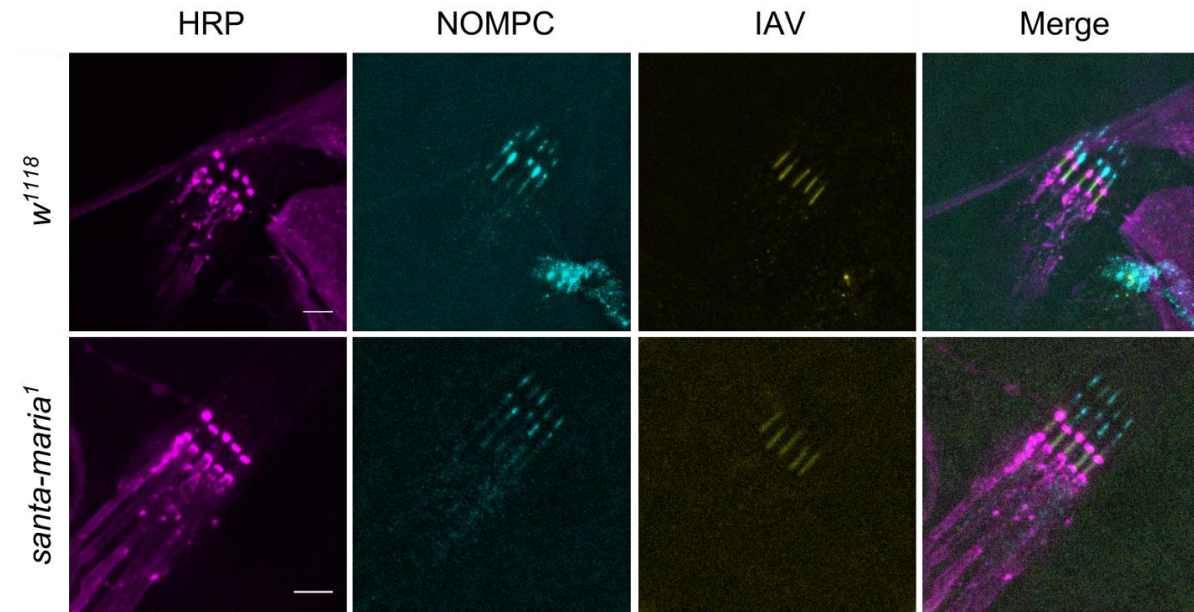


Figure 10. Localization of TRP channels in Ich5 organ in wild type and *santa-maria¹* mutant larvae.

Neurons are stained with HRP (magenta), anti-NOMPC staining is shown in cyan and anti-Iav staining in yellow. In the wild type, NOMPC is detected in the ciliary tip, whereas Iav resides more proximal between two HRP bands. No alterations of this pattern were detected in *santa-maria¹* mutants. Scale bars: 5 μ m.

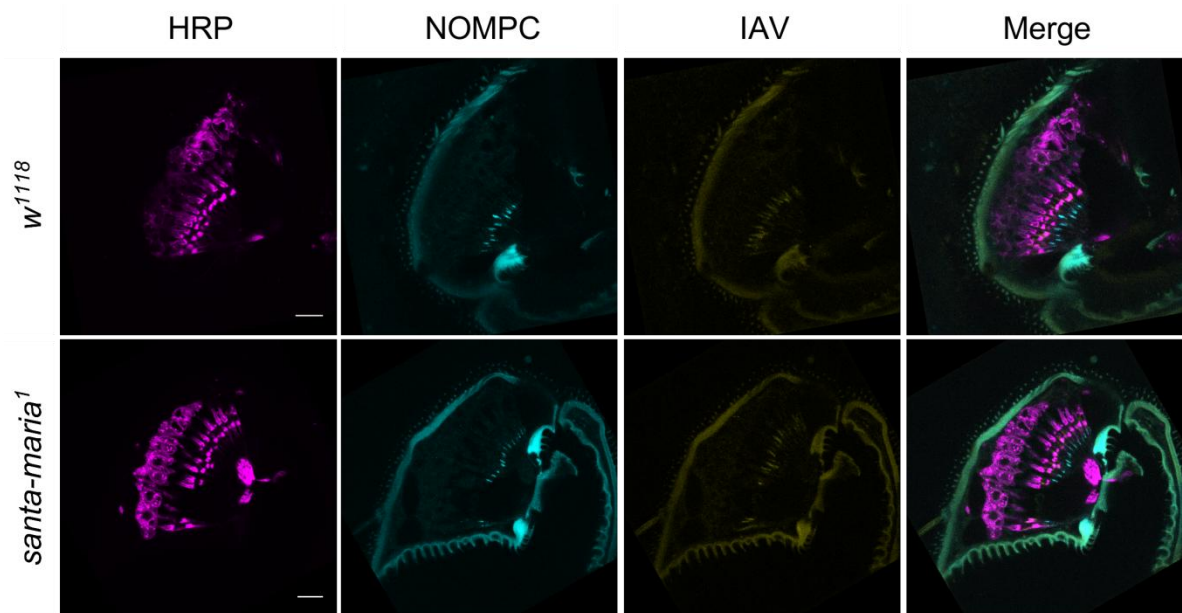


Figure 11. Localization of TRP channels in JO of wild type and *santa-maria*¹ mutants.

Neurons are stained with HRP (magenta), anti-NOMPC staining is shown in cyan and anti-Iav staining in yellow. In the wild type, NOMPC is detected in the ciliary tip, whereas Iav resides more proximal between two HRP bands. No alterations of this pattern were detected in *santa-maria*¹ mutants. Scale bars: 10 μ m.

1.2.1.4. Tissue specific rescue of *santa-maria* mutants

To test if genetic rescue of *santa-maria* restores normal hearing in *santa-maria*¹ mutants, a rescue construct containing wild-type *santa-maria* was expressed in the *santa-maria*¹ mutant background under the control of different Gal-4 drivers. First, I wanted to replicate the results of Senthilan et al (2012) and tested for rescue of hearing using a chordotonal neuron-specific driver. Instead of using *JO1-Gal4*, I decided to use the stronger driver *Dnai2-Gal4* that was reported previously to specifically label chordotonal neurons (Karak et al., 2015). Second, because *santa-maria*^{TGEM}-*Gal4* showed staining in glia cells, I wanted to check whether expressing *santa-maria* under the control of the glial driver *repo-Gal4* can restore hearing *santa-maria*¹ mutants. Driving the expression of *UAS-santa-maria* with either of these two Gal4 drivers partially rescued hearing. Compared to the mutants, antennal fluctuation powers and best frequencies were increased in the rescue flies (Figure 12A), and so was the mechanical amplification gain (Figure 12B). Also auditory sensitivity was partly restored, as witnessed by diminished particle velocity and displacement thresholds of sound-evoked CAPs (Figure 12C).

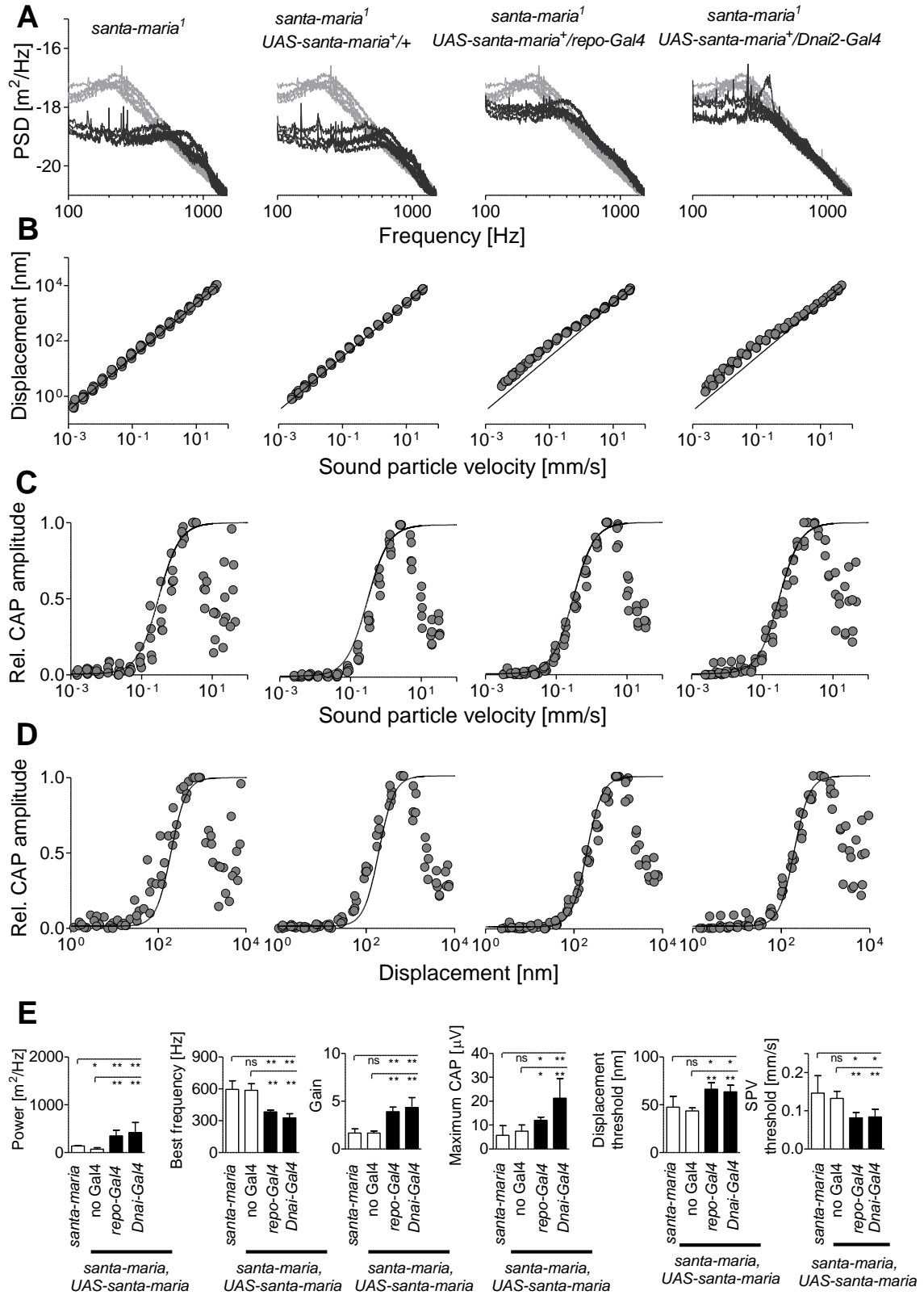


Figure 12. Laser Doppler analysis of *santa-maria* GAL4-UAS rescue.

1.2 Results

- A) Power spectral density (PSD) of the free mechanical fluctuation of the antenna in *santa-maria*¹ mutants; *santa-maria*¹, *UAS-santa-maria* mutants, *santa-maria repo-GAL4* rescue and *santa-maria Dnai2-GAL4* rescue flies (N=5 per strain). Control *w*¹¹¹⁸ traces in grey.
- B) Tone-evoked antennal displacement as a function of the particle velocity of the tone. The black line indicates linearity.
- C) Relative amplitude of toned-evoked CAPs as a function of the particle velocity of the tone.
- D) Relative CAPs amplitudes plotted against the respective antennal displacement.
- E) Respective: fluctuation powers, antennal best frequencies, mechanical amplification gains, maximum CAP amplitudes, sound particle velocity thresholds and displacement thresholds.

Data are presented as a mean values \pm 1 SD, N = 5, *P < 0.05, **P < 0.01, ns = not significant, two-tailed Mann Whitney U-test.

1.2.2. Relevance of the chromophore generation pathway for fly audition

The first step in the de novo synthesis of the chromophore is the uptake of dietary beta-carotenoids in the gut. This uptake requires the scavenger receptor NinaD (Kiefer et al., 2002). Subsequently, beta-carotenoids are taken up in a Santa-Maria-dependent manner into neurons and glia in the brain, where they are cleaved into retinal by the beta,beta-carotene-15,15'-oxygenase (BCO) NINAB (Kiefer et al., 2001). Eliminating NINAD or NINAB proteins abolishes chromophore synthesis, leading to blindness and retinal degeneration (Voolstra et al., 2010).

If the chromophore were needed for fly audition, *ninaD*¹ and *ninaB*³⁶⁰ null mutants should show similar hearing impairments as observed in *santa-maria*¹ mutants. Compared to controls, however, antennal free fluctuation measurements revealed no significant changes in both fluctuation power and antennal best frequency in *ninaD*¹ (PSD=1130 \pm 329 nm²/Hz, Ibf=185 \pm 6 Hz) and *ninaB*³⁶⁰ (PSD=1604 \pm 385 nm²/Hz, Ibf=183 \pm 6 Hz) mutants (Figure 13A). Also amplification gains resembled those of controls, with gains of ca. 10.5 and 8.4 for *ninaD*¹ and *ninaB*³⁶⁰ mutants, respectively (Figure 13B). Recorded antennal nerve responses were similar to the once observed for *w*¹¹¹⁸ controls (Figure 13C and D). Maximum CAP responses (*ninaD*¹ 23.1 \pm 6.2 μ V and *ninaB*³⁶⁰ 26.7 \pm 10.5 μ V), sound particle velocity thresholds (*ninaD*¹ 0.058 \pm 0.01 mm/s and *ninaB*^{360d} 0.054 \pm 0.005 mm/s) and displacement thresholds (*ninaD*¹ 68.89 \pm 10.14 nm and *ninaB*^{360d} 77.85 \pm 9.35nm)

were in normal range. Hence, disrupting chromophore synthesis leaves fly hearing unaffected.

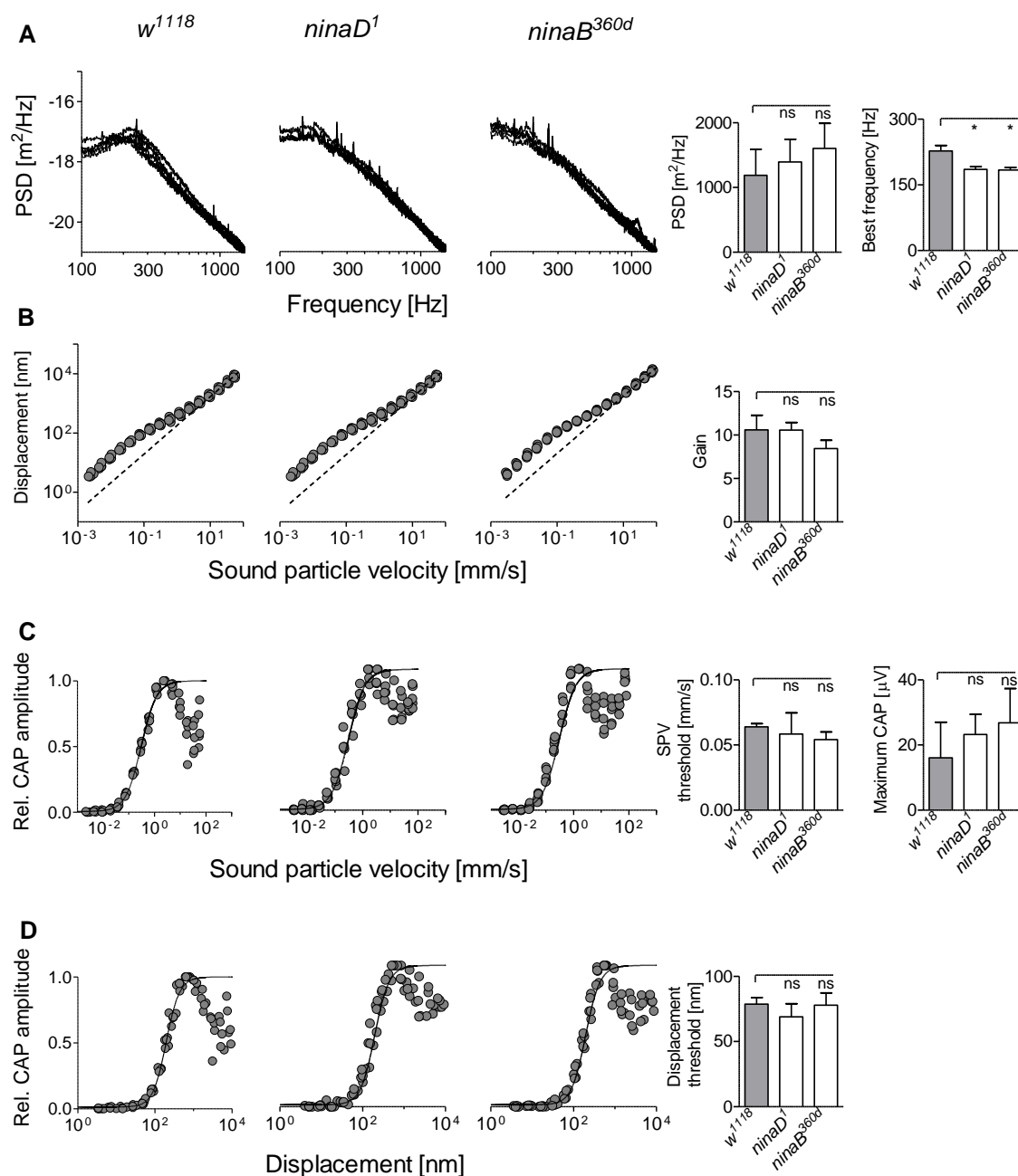


Figure 13. Auditory performance of *ninaD¹* and *ninaB^{360d}* mutant flies.

A) Left: power spectral density (PSD) of the free mechanical fluctuation of the antenna in the wild-type, *ninaD¹* and *ninaB^{360d}* flies (N=5 per strain). Right: respective fluctuation powers and antennal best frequencies.

1.2 Results

- B)** Left: Tone-evoked antennal displacement as a function of the particle velocity of the tone. The black dashed line indicates linearity. Right: respective mechanical amplification gains.
- C)** Left: Relative amplitude of toned-evoked CAPs as a function of the particle velocity of the tone. Right: respective particle velocity threshold and maximum CAP amplitudes.
- D)** Left: Relative CAP amplitude plotted against the respective antennal displacement. Right: corresponding displacement thresholds.

Data are presented as a mean values \pm 1 SD, N=5, *P < 0.05, ns = not significant, two-tailed Mann Whitney U-test.

1.2.2.1. Vitamin A depletion

To further test the relevance of the chromophore for *Drosophila* audition, w^{1118} flies were kept for six generations on medium depleted of vitamin A. As mentioned previously, eliminating vitamin A from a diet will disrupt the de novo synthesis of the chromophore and, in electroretinogram recordings (ERGs), eliminate the prolonged depolarizing afterpotential (PDA) (Dolph et al., 1993; Pak et al., 2012). PDA arises from the bi-stable nature of rhodopsin where blue light photoconverts rhodopsin to its active form called metharhodopsin (M*) generating a depolarizing receptor potential (PDA) that persist even in the dark (Figure 14 left). Metharhodopsin can be photoconverted back to its inactive state by exposure to orange light. ERG measurements confirmed that the vitamin A-depleted flies, but not control flies raised on standard medium, lacked PDA (Figure 14 right).

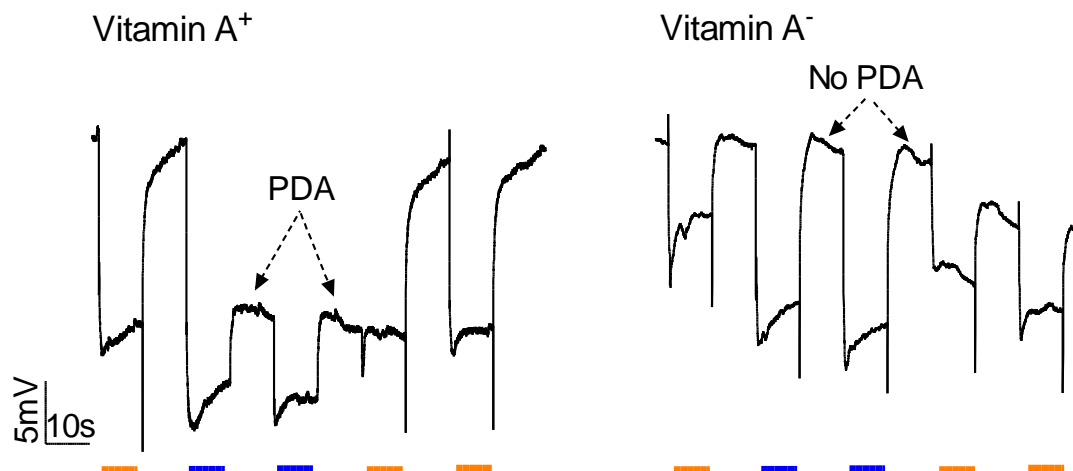


Figure 14. ERG recording from wild type and vitamin A depleted flies.

Left: responses to an orange and a blue stimulus of control flies raised on the normal medium (Vit A⁺). The first blue light pulse generates a large response during the stimulus, photoconverting rhodopsin to metarhodopsin. When light is switched off, PDA (Prolonged depolarizing afterpotential) is generated, with photoreceptor cells R1-6 staying depolarized and being inactivated. The next blue light pulse elicits only small response that comes from photoreceptors R7-8. Orange light terminates PDA, metarhodopsin is photoconverted back to rhodopsin and the response goes back to the resting potential. **Right:** PDA is lost in flies raised for 6 generations on vitamin A-depleted food (Vit A⁻). There is no rhodopsin that can be photoconverted, so PDA cannot be generated.

To test whether vitamin-deprivation affects hearing, antennal mechanics were examined. Antennal fluctuation powers and best frequencies of vitamin A-depleted flies were indistinguishable from those of controls, and the same applied to the mechanical amplification gain and hearing thresholds (Figure 15). Hence, unlike vision, hearing seems independent of vitamin A and, accordingly, the chromophore.

1.2 Results

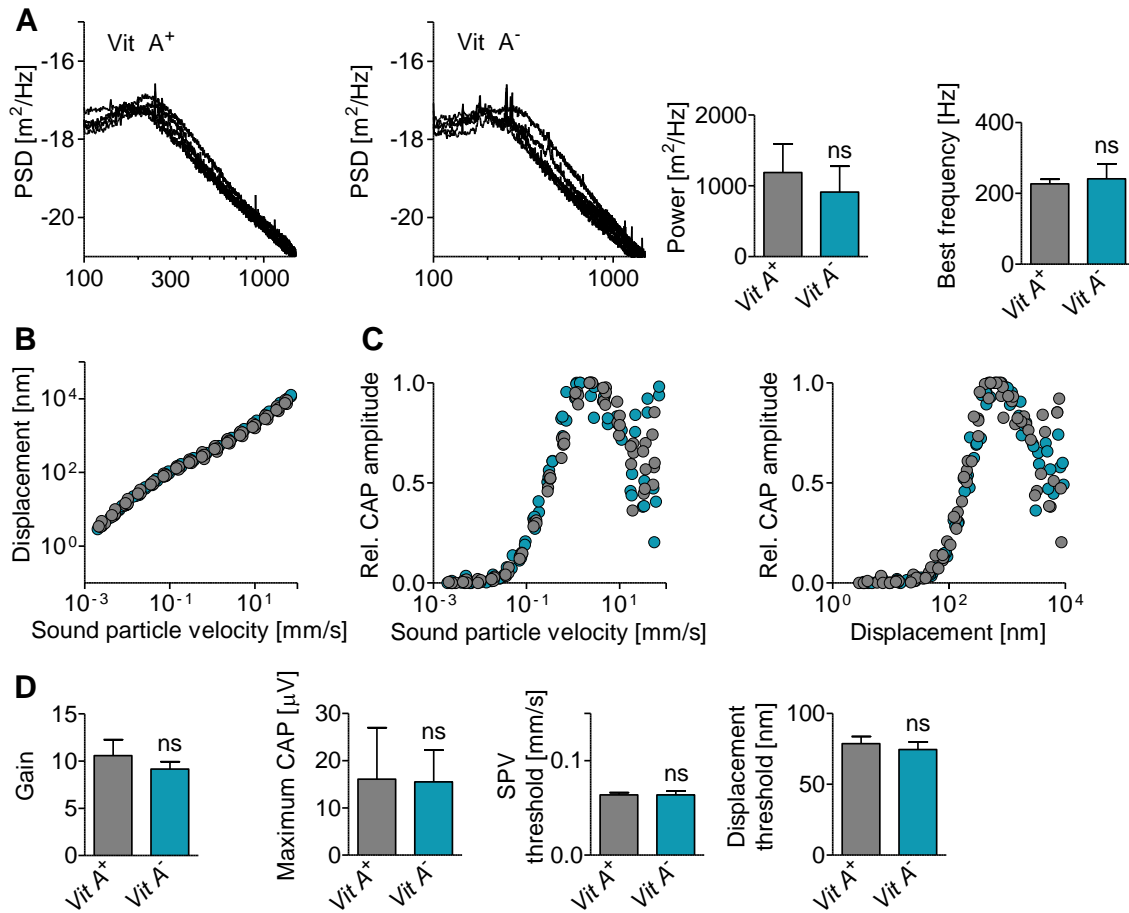


Figure 15. LDV measurements of Vitamin A depleted flies.

- A)** Left: power spectral density (PSD) of the free mechanical fluctuation of the antenna in the Vitamin A depleted (Vit A⁻) and flies raised on normal food (Vit A⁺) (N=5 per strain). Right: respective fluctuation powers and antennal best frequencies.
- B)** Sound receiver displacement in response to sound stimuli. Superimposed data, VitA⁺ (gray) and VitA⁻ blue
- C)** Left: Relative amplitude of toned-evoked CAPs as a function of the particle velocity of the tone. Right: CAP amplitude plotted against the respective antennal displacements.
- D)** Respective mechanical amplification gains, maximum CAP amplitudes, sound particle velocity thresholds and antennal displacement thresholds.

Data are presented as a mean values \pm 1 SD, N = 5, * P < 0.05, ns = not significant, two-tailed Mann Whitney U-test.

1.2.3. Auditory importance of the genes implicated in chromophore processing and recycle

In the last chapter I showed that blocking chromophore synthesis by eliminating its dietary substrate β -carotene, or disrupting genes involved in de novo chromophore generation pathway (*ninaD* and *ninaB*) does not affect *Drosophila* hearing. Therefore, auditory rhodopsin functions seem chromophore-independent. Interestingly, the scavenger receptor Santa-Maria operating in the chromophore synthesis pathway between NINAD and NINAB turned out to be crucial for JO function. Following this path it was intriguing to probe auditory performance and expression patterns of other genes involved in visual chromophore synthesis and the chromophore recycling pathway.

1.2.3.1. PINTA is functionally involved in auditory process

The next protein operating in de novo visual chromophore synthesis is PINTA. It is a member of CRAL-TRIO family of proteins that is involved in all-trans-retinal binding in retinal pigment cells within the eye (Wang, 2005).

*pinta*¹ null mutant flies were subjected to LDV analysis. Surprisingly, auditory phenotypes were observed that resembled those of *santa-maria*¹ mutants. The most prominent effect was a drop in fluctuation power to $164 \pm 59 \text{ nm}^2/\text{Hz}$ and an increase of the antennal best frequency to $354 \pm 22\text{Hz}$ (Figure 16A). Along with the impaired antennal fluctuations, amplification gains were reduced to 2.9 ± 0.3 (Figure 16B). Electrophysiological recordings from the antennal nerve showed no significant differences of maximum CAP amplitudes and sound particle velocity thresholds (Figure 16C). Larger antennal displacements, however, were required to elicit nerve responses in *pinta*¹ mutant flies, signaling that sound transduction is impaired (Figure 16D). Normal hearing was restored when a genomic *pinta* rescue construct, $P\{pinta^+\}$ was expressed in the *pinta*¹ mutant background.

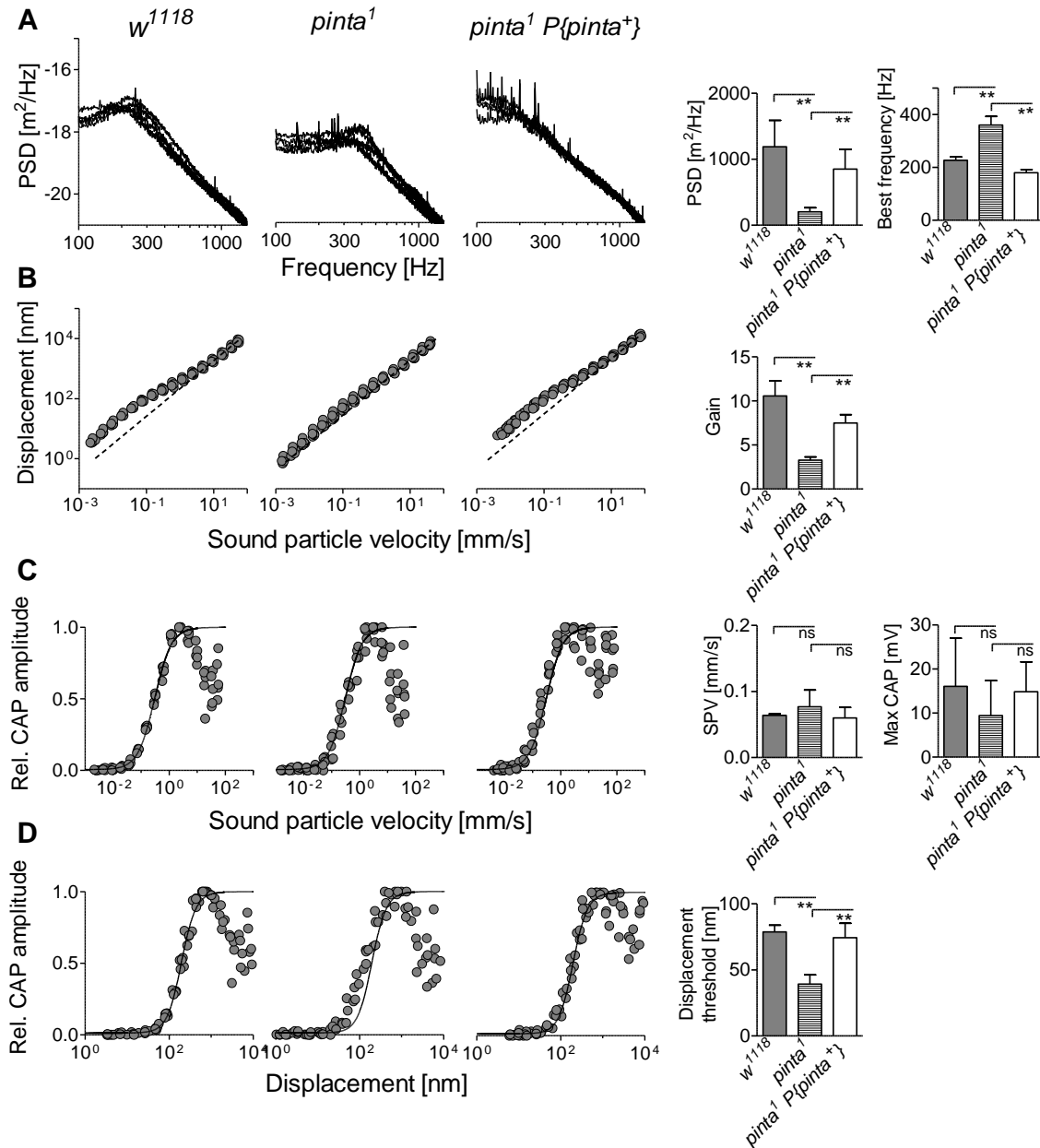


Figure 16. JO function in *pinta*¹ mutants and rescue flies.

- A) Left: power spectral density (PSD) of the free mechanical fluctuation of the antenna in the wild-type, *pinta*¹ and *pinta* genomic rescue flies (N=5 per strain). Right: respective fluctuation powers and antennal best frequencies.
- B) Left: Tone-evoked antennal displacement as a function of the particle velocity of the tone. The black dashed line indicates linearity. Right: respective mechanical amplification gains.
- C) Left: Relative amplitude of toned-evoked CAPs as a function of the particle velocity of the tone. Right: respective particle velocity thresholds and maximum CAP amplitudes.
- D) Left: CAP amplitude plotted against the respective antennal displacement. Right: corresponding displacement thresholds.

Data are presented as a mean values \pm 1 SD, N=5, *P < 0.05, **P < 0.01 two-tailed Mann Whitney U-test.

To assess cell types where *pinta* is expressed, a Gal4 promoter fusion construct was generated (*pinta-Gal4*). *pinta-Gal4* flies were used to drive expression of *20xUAS-6xGFP* in larva and adult *Drosophila*. In larvae, GFP signals were detected in cap cells of *lch5* organs and other chordotonal neurons (*lch1*, *vchA*, *vchB*) (Figure 17 top). These elongated cells create tendon-like structures that apically support the cilium of chordotonal neurons (Hartenstein, 1988). Additionally, very faint signals were observed in the scolopale cells that surround the distal part of the neurons. To further test whether *pinta-Gal4* also labels scolopale cells, another fluorescent reporter expressing RFP with nuclear localization was used. Nuclear RFP signals in cells surrounding the distal parts of the cilia confirmed that *pinta*, besides being expressed in cap cells, is also present in scolopale cells (Figure 17 bottom).

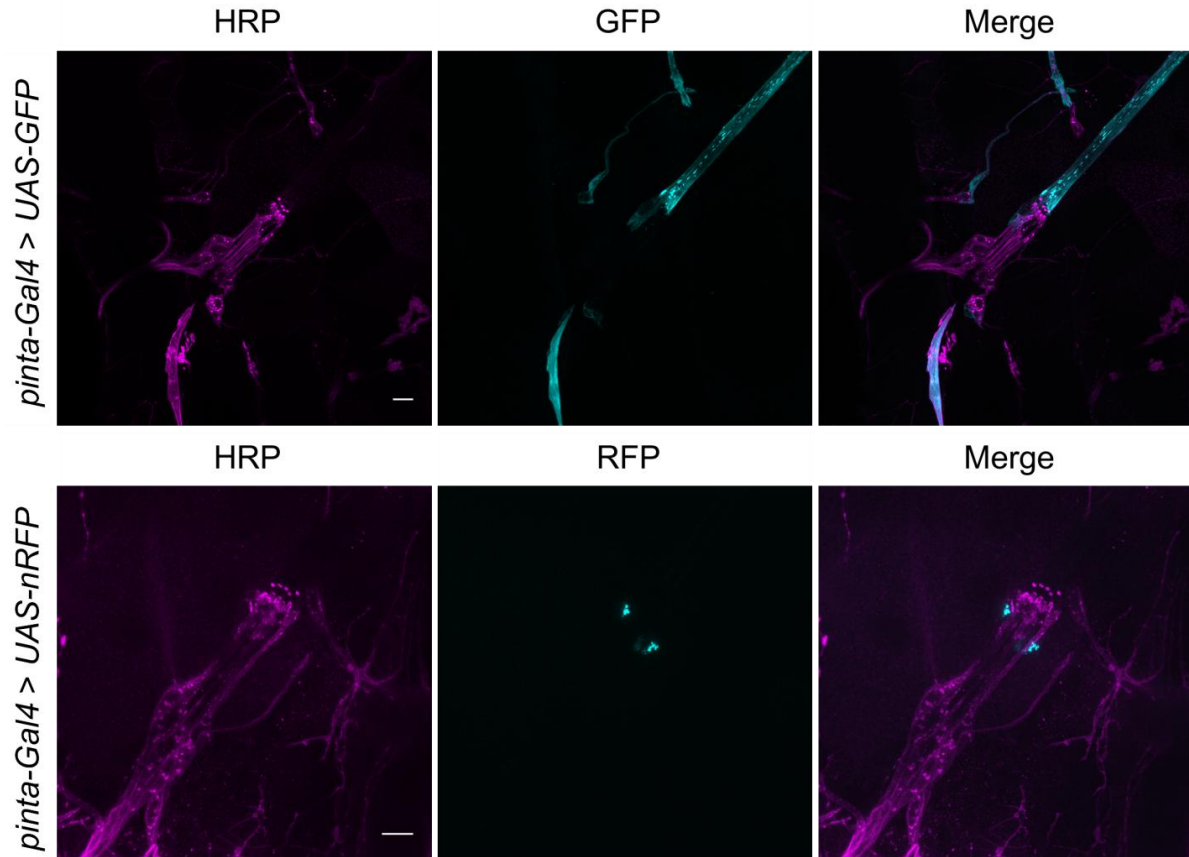


Figure 17. *pinta* expression in larval Ich5 organ.

Top panel: *pinta-Gal4 > 20xUAS-6xGFP*, neurons of Ich5 organ marked with anti-HRP neuronal marker showed in magenta. GFP signal showed in cyan. Overlap picture on the right. Scale bar = 10 μ m.

Bottom panel: *pinta-Gal4 > UAS-nRFP*, neurons of Ich5 organ marked with anti-HRP neuronal marker showed in magenta. RFP signal showed in cyan. Overlap picture on the right. Scale bar = 10 μ m

Next, the expression pattern of *pinta-Gal4* in the adult 2nd antennal segment was investigated. GFP signals were spotted as stripes on the both sides of the scolopidium (Figure 18 top). Like in *Ich5*, these structures are most probably cap cells of JO neurons. To test this impression, *pinta-Gal4* was crossed to flies expressing *UAS-nuclearRFP* and additionally counterstained with DAPI to mark all nuclei on the slice. The RFP signals colocalized with DAPI positive nuclei next to the proximal ciliary region, where also the GFP signals had been observed, identifying the respective cells as supporting cap cells (Figure 18 bottom). Nuclear RFP additionally labeled cell nuclei of scolopale cells, some JO neurons and hypodermal cells beneath the cuticle.

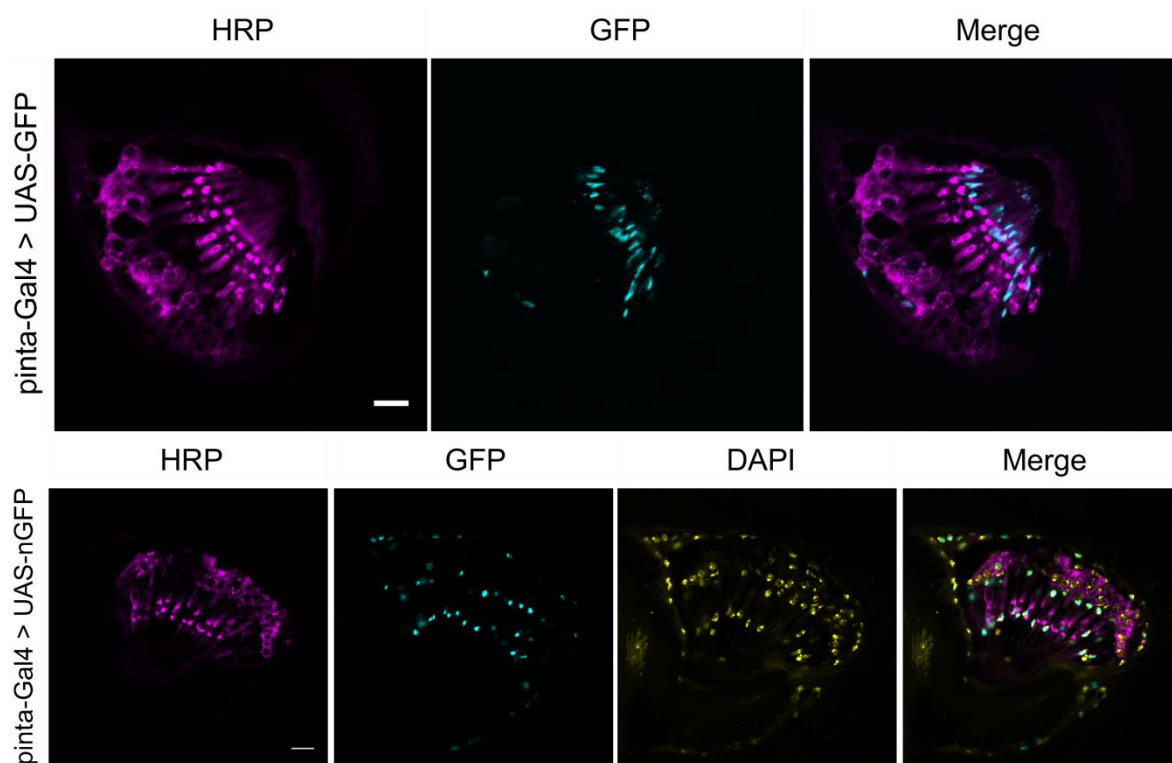


Figure 18. *pinta* expression pattern in Johnston's organ.

Top panel: Immunohistochemical staining of 2nd antennal segment slices. Neurons are stained with HRP - magenta, GFP signal is shown in cyan. An overlay is shown on the right. Scale bar = 10 μ m.

Bottom panel: *pinta-Gal4 > UAS-nRFP*, neurons of Ich5 organ marked with anti-HRP neuronal marker showed in magenta. RFP signal showed in cyan. DAPI shown in yellow. Overlap picture on the right. Scale bar = 10 μ m

1.2.3.2 *ninaG* function and expression in chordotonal organs

The next protein participating in visual chromophore synthesis is NINAG, an enzyme that belongs to the glucose-methanol-choline oxidoreductase family that mediates oxidation and hydroxylation of small organic molecules (Sarfare et al., 2005). In flies, NINAG acts in the conversion of (3R)-3-hydroxyretinol to the 3S enantiomer in the last step of chromophore production. However, in *ninaG* mutant flies only Rh1 synthesis is abolished because only Rh1 uses 3S retinal enantiomer (Ahmad et al., 2006).

1.2 Results

ninaG null mutant flies (*ninaG*^{P330}) were analyzed in free fluctuation measurements and subsequently exposed to pure tones to assess the amplification gain and the antennal nerve response. Disrupting *ninaG* gene led to strong auditory defects in both antennal mechanics and sound evoked antennal nerve responses. Compared to controls, the free fluctuations of the antennal sound receiver showed a severe reduction in power (60 ± 19 nm²/Hz) and a shift of best frequency towards higher values (542 ± 10 Hz) (Figure 19A). These auditory defects were associated with almost complete loss of amplification (gain = 1.8 ± 0.4) (Figure 19B). Moreover, sound-evoked antennal nerve responses were highly affected as maximum CAP amplitudes only reached 3.4 mV, suggesting severe defects in sound detecting JO neurons (Figure 19D). Compared to controls, higher sound particle velocities were necessary to evoke antennal nerve responses (SPV threshold = 0.15 mm/s \pm 0.039 mm/s) (Figure 19C). However, smaller antennal displacements were needed to elicit a nerve response (displacement threshold = 43 ± 6 nm) (Figure 19C).

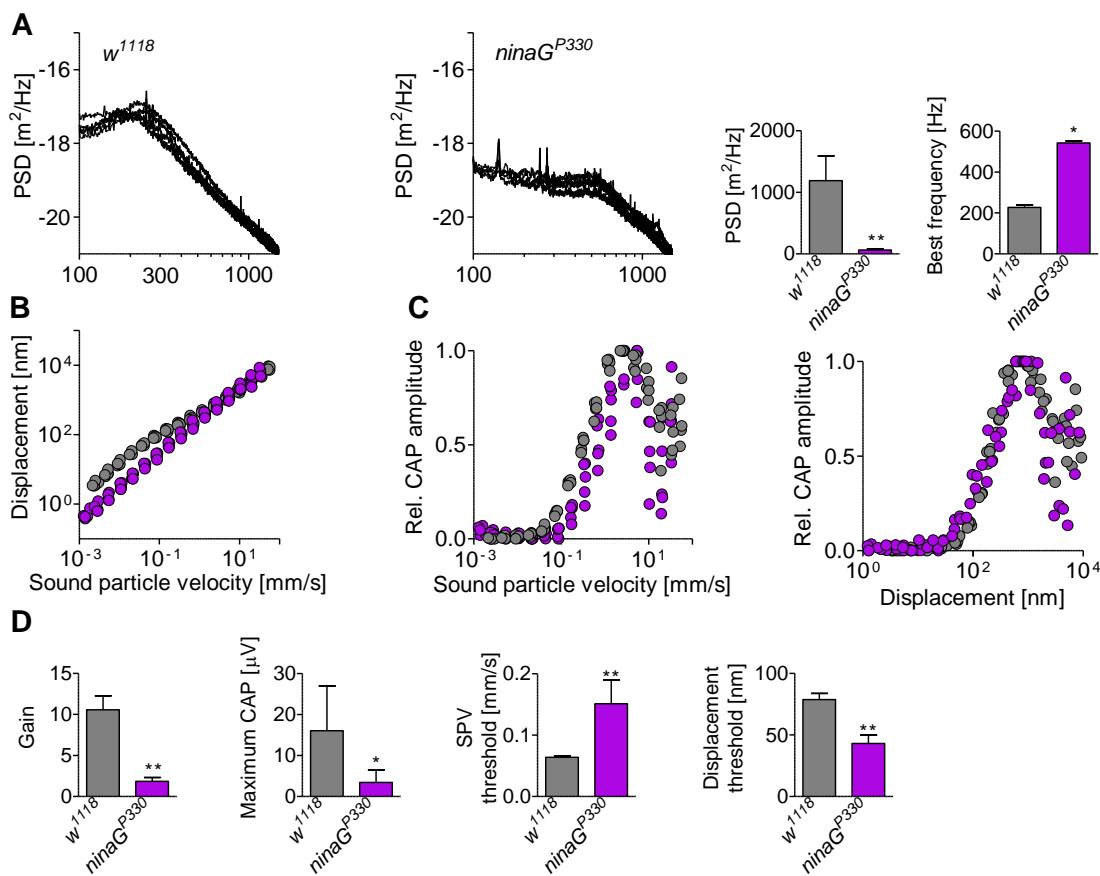


Figure 19. Auditory phenotype of *ninaG* mutant flies

- A)** Left: power spectral density (PSD) of the free mechanical fluctuation of the antenna in control and *ninaG^{P330}* (N=5 per strain). Right: respective fluctuation powers and antennal best frequencies.
- B)** Sound receiver displacement in response to sound stimuli. Superimposed data, control (gray) and *ninaG^{P330}* magenta.
- C)** Left: Relative amplitude of toned-evoked CAPs as a function of the particle velocity of the tone. Right: CAP amplitude plotted against the respective antennal displacement.
- D)** Respective gains, maximum CAPs amplitudes, sound particle velocity thresholds and antennal displacement thresholds.

Data are presented as a mean values \pm 1 SD, N = 5, *P < 0.05 **P < 0.01, two-tailed Mann Whitney U-test.

1.2 Results

To test whether chordotonal organs might express *ninaG*, a promoter fusion construct expressing GAL4 (*ninaG-Gal4*) was generated and subsequently used to drive a hexameric *20UAS-6xGFP* fluorescent reporter. In larvae, strong GFP signals were observed outside of *lch5* neuronal cell bodies at their axonal side, most likely in supporting ligament cells (Figure 20 bottom). To test this notion, the wild type larvae were stained with an antibody against α Tub85E, which is known to exclusively label accessory and attachment cells of chordotonal organs (Halachmi et al., 2016). As expected, ligament cell labeled by anti- α Tub85E antibody strongly resembled the structure observed in *ninaG-Gal4 UAS-GFP* larvae, further suggesting that the ligament cells of *lch5* express *ninaG* (Figure 20 top).

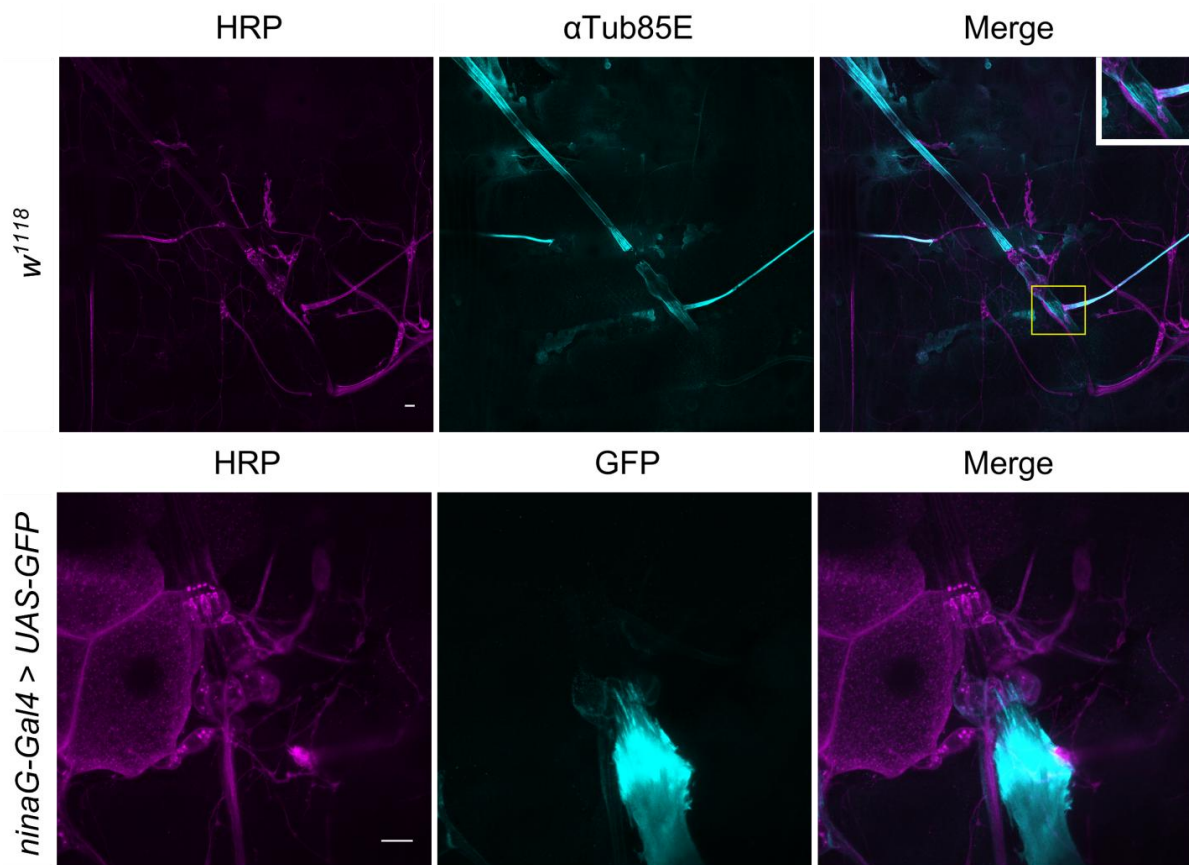


Figure 20. α Tub85E and *ninaG* expression pattern in larval *lch5* chordotonal organ.

Top: Antibody staining against chordotonal organ specific protein α Tub85E (cyan), neurons marked by HRP (magenta). Bottom: anti GFP staining on *ninaG-Gal4 > UAS-GFP* larvae *lch5* organ (cyan), neurons marked by HRP (magenta). Scale bar = 10 μ m.

The same approach was used to study the *ninaG* expression pattern in Johnston's organ. In *ninaG-Gal4 > UAS-GFP* flies, signal was detected around neuronal cell bodies, recapitulating the staining pattern of the antibody α Tub85E (Figure 21). *ninaG* is thus expressed in ligament cells, in both *lch5* and JO.

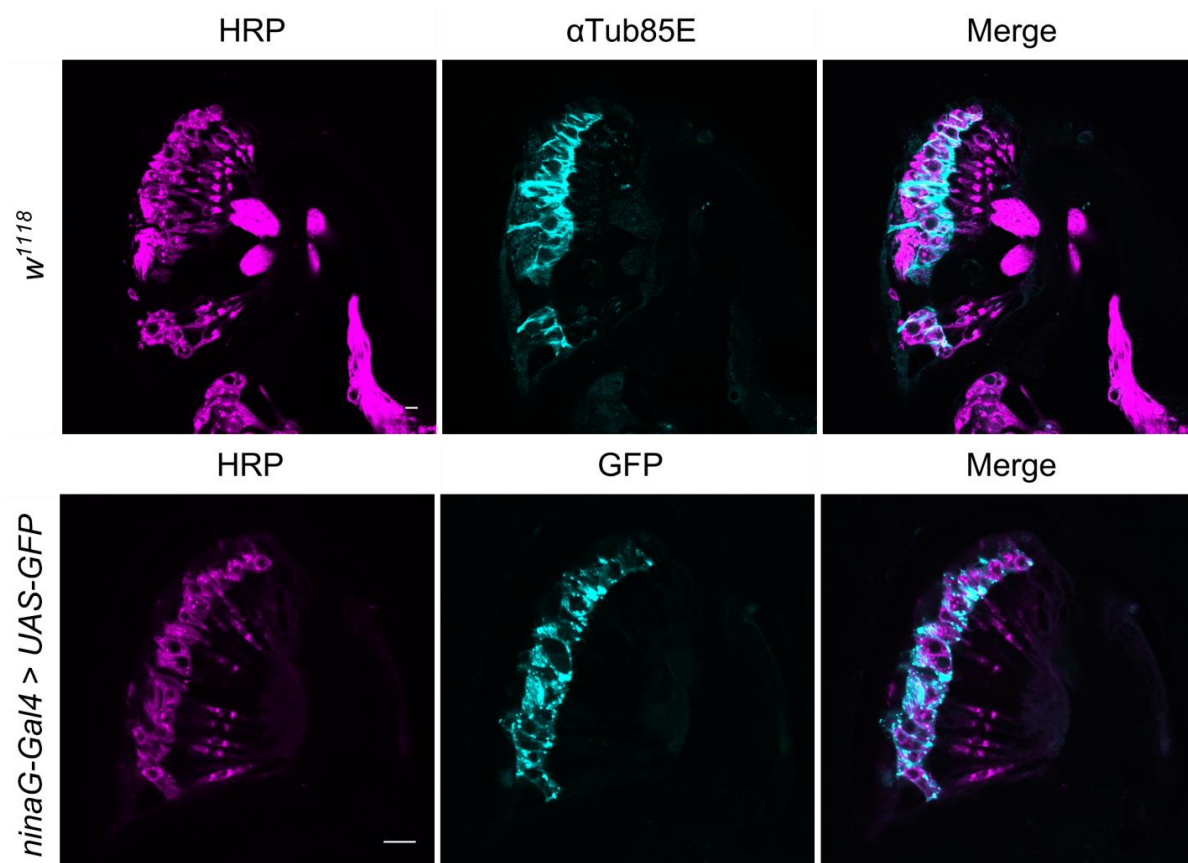


Figure 21. *ninaG* expression pattern in adult JO.

Top: Antibody staining against chordotonal organ specific protein α Tub85E (cyan), neurons marked by HRP (magenta). Bottom: anti-GFP staining on *ninaG-Gal4 > UAS-GFP* flies (cyan), neurons marked by HRP (magenta). Scale bar = 10 μ m.

1.2.3.3 Genes of chromophore recycling pathway in fly hearing

So far, I investigated all of the known proteins participating in “de novo” chromophore synthesis. However, lately it has been shown that *Drosophila* photoreceptors are also able to regenerate photoisomerized 3-OH-all-trans retinal back to its cis configuration through a visual cycle as known from the mammalian retina (Wang et al., 2010). In *Drosophila*, this visual cycle involves enzymatic activity of pigment cell dehydrogenase (Pdh) (Wang et al., 2010) and retinal dehydrogenase B (RDHB) (Wang et al., 2012) that are expressed in retinal pigment cells (RPC). To determine whether these proteins are necessary for proper JO function, respective mutant flies (*Pdh*¹ and *rdhB*¹) were analyzed.

Antennal free fluctuation measurements revealed massive defects in JO neurons motility in both mutants tested. The fluctuation power of *Pdh*¹ and *rdhB*¹ mutants was reduced to 323 ± 147 and 69 ± 37 nm²/Hz respectively (Figure 22A, E). Together with this low power, also the antennal best frequency was shifted to higher values: 386 ± 15 Hz for *Pdh*¹ and 581 ± 58 Hz for *rdhB*¹ mutants (Figure 22A, E). Low fluctuation powers indicate reduced mechanical amplification, and sound receiver responses to pure tones showed almost linear scaling (Figure 22B, E). The amplification gains reached 3.6 ± 0.7 for *Pdh* mutants and 1.5 ± 0.1 for *rdhB*¹ mutants (Figure 22E). Maximum CAP amplitudes measured from antennal nerve were greatly diminished in *rdhB*¹ mutants (2.3 ± 0.1 μV) (Figure 22E), indicating that besides defects in amplification also current responses are greatly affected. Furthermore, considerably higher sound particle velocities were needed to exceed the response threshold (0.23 ± 0.11 mm/s) (Figure 22C, E). *Pdh*¹ mutant flies showed slightly larger CAP amplitudes compared to *rdhB*¹, but they were still noticeable smaller than in controls. Maximum CAP amplitudes reached only 6.3 ± 2.2 μV, and the antennal displacement threshold (49 ± 11 nm) was increased (Figure 22D, E).

The auditory defects seen in *Pdh*¹ mutant flies were reversed to wild-type levels when a genomic *Pdh* rescue construct, *P{Pdh⁺}*, was introduced into the *Pdh*¹ mutant background.

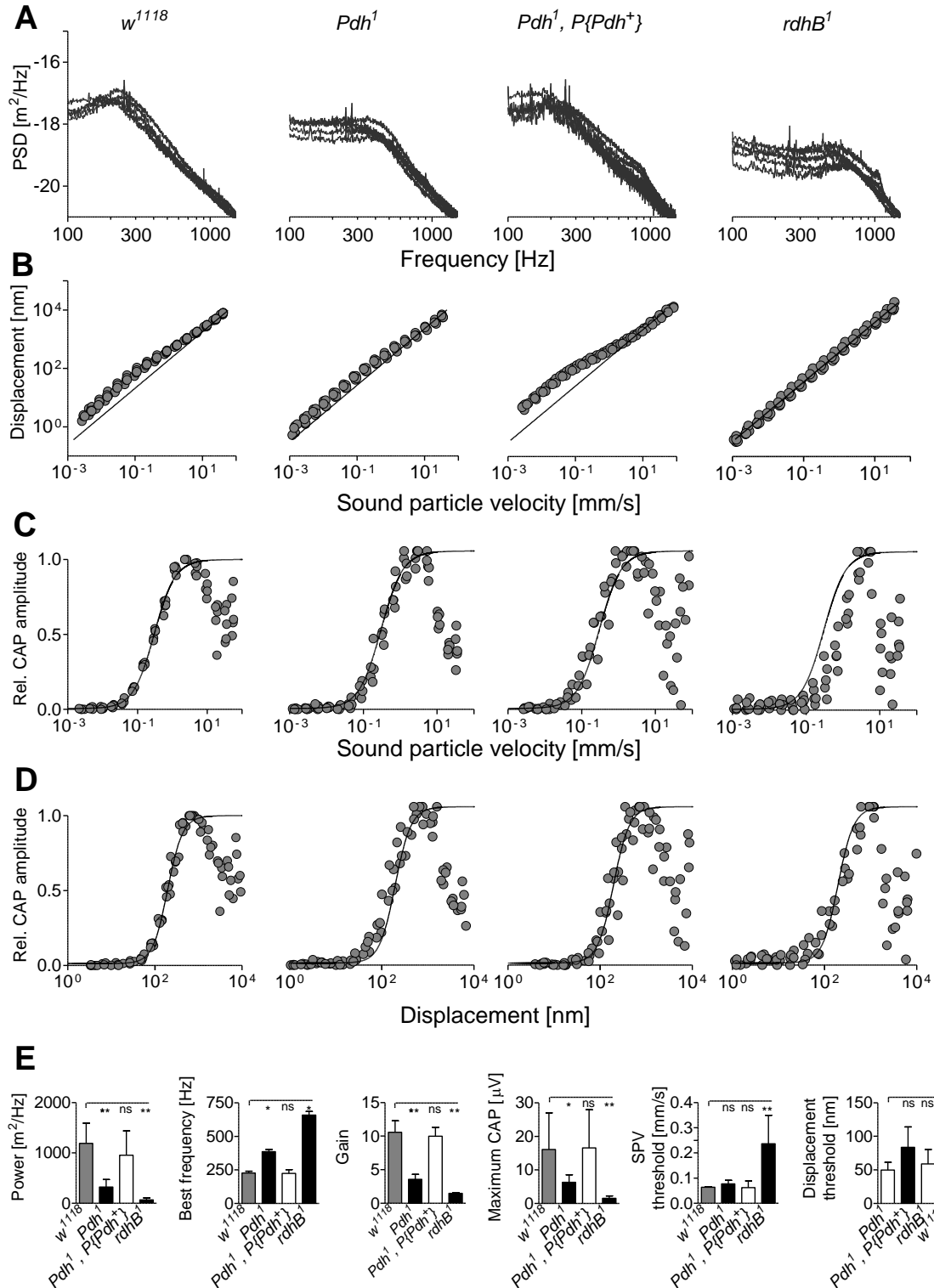


Figure 22. Auditory performance of the mutant flies implicated in chromophore recycle.

A) Power spectral density (PSD) of the free mechanical fluctuation of the antenna in *w¹¹¹⁸* control flies; *pdh¹* mutants; *pdh¹, P{pdh⁺}* genomic rescue and *rdhB¹* mutants flies (N=5 per strain).

1.2 Results

- B)** Tone-evoked antennal displacement as a function of the particle velocity of the tone. The black line indicates linearity.
- C)** Relative amplitude of toned-evoked CAPs as a function of the particle velocity of the tone.
- D)** Relative CAPs amplitudes plotted against the respective antennal displacement.
- E)** Respective: fluctuation powers, antennal best frequencies, mechanical amplification gains, maximum CAP amplitudes, sound particle velocity thresholds and displacement thresholds.

Data are presented as a mean values \pm 1 SD, N = 5, *P < 0.05, **P < 0.01, ns = not significant, two-tailed Mann Whitney U-test.

The promoter fusion construct *Pdh-Gal4* was generated to reveal the cell types where *Pdh* is expressed, however, no signal was detected in Ich5 chordotonal organ and in adult JO. The only visible GFP signals came from the adult eye and ocelli (Figure 23), where *Pdh* is reportedly expressed in retinal pigment cells (Wang et al., 2010).

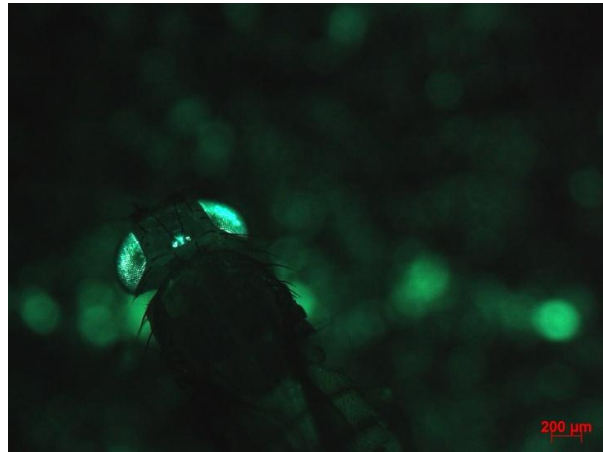


Figure 23. *Pdh-GAL4* expression in the eye of *Drosophila*.

Overview of adult fly expressing *UAS-GFP* in the pattern of *Pdh-Gal4*. Picture was taken from epifluorescent microscope with GFP filter.

To find out whether *rdhB* is expressed in chordotonal neurons, previously published *rdhB-Gal4* (Wang et al., 2012) was used to drive expression of *UAS-GFP* reporter. After

immunohistochemical staining a weak GFP signals were detected in JO neurons cell bodies (Figure 24).

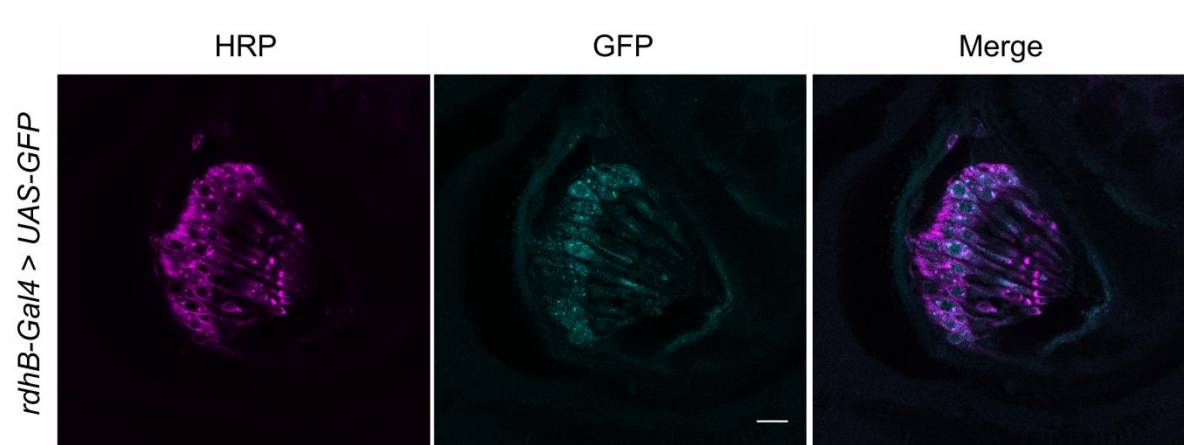


Figure 24. rdhB-Gal4 expression pattern in adult JO

Anti-GFP staining on *ninaG-Gal4 > UAS-GFP* flies (cyan), neurons marked by HRP (magenta). Scale bar = 10 μ m.

1.2.4. Possible roles of Rhodopsin1 in *Drosophila* hearing

The main visual rhodopsin Rh1 is encoded by *ninaE* gene and is found in 6 out of the 8 photoreceptor cell types in the fly eye. Rh1 is crucial for vision and the maintenance of proper photoreceptor architecture. In the past years nonvisual Rh1 functions have been reported in the context of thermosensation (Shen et al., 2011) and proprioception (Zanini et al., 2018). These studies, however, focused exclusively on Rh1 functions in 3rd instar larvae, no research was done on adult *Drosophila*. Giving that larval proprioceptive lch5 chordotonal organ requires Rh1 for controlling locomotion (Zanini et al., 2018), and adult hearing uses morphologically similar neurons, I checked whether *Rh1* is expressed in JO and, if so, if it has any function there. Initially, Rh1 was not detected in the screen of the genes expressed in adult JO (Senthilan et al., 2012). However, I decided to reassess this result using the reverse transcription polymerase reaction (RT-PCR) on cDNA obtained from the 2nd antennal segment. *Rh1* mRNA transcripts were detected in Johnston's organ (Figure 25).

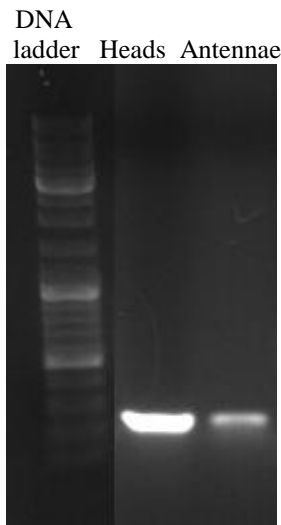


Figure 25. Rhodopsin1 RT-PCR analysis.

mRNA expression of *rh1* was checked by performing PCR on cDNA from heads (2nd row) and antenna (3rd row) of wild-type flies.

1.2.4.1. Probing Johnston's organ function in *ninaE*¹⁷ mutants

Assuming that *rh1* is expressed in *Drosophila* antennae the intriguing question was whether it contributes to auditory functions like *rh5* and *rh6*. To evaluate this, I analyzed hearing in *ninaE*¹⁷ null mutants lacking the Rh1 opsin (O'Tousa et al., 1985). Antennal free fluctuation measurements revealed a substantial drop in power ($368 \pm 270 \text{ nm}^2/\text{Hz}$) and a slight increase in the antennal best frequency ($295 \pm 26 \text{ Hz}$) when compared to its genetic background *CantonS* (Power = $1272 \pm 569 \text{ nm}^2/\text{Hz}$ and Ibf = $210 \pm 29 \text{ Hz}$) (Figure 26A and E). When exposed to pure tones, the antennal sound receiver of *Rh1* mutants showed reduced amplification gain (4.3 ± 0.9) compared to control flies (10.8 ± 2.7) (Figure 26B and E). Maximum CAP amplitudes of the mutants resembled those of controls (21.4 ± 12.1 and $14.4 \pm 4.9 \mu\text{V}$ respectively) (Figure 26E). Difference between mutants and controls, however, were also found with respect to sound particle velocity thresholds 0.1 ± 0.01 and 0.05 ± 0.01 respectively (Figure 26C and E). Displacement thresholds, however, seemed to be unaffected by *ninaE*¹⁷ mutation (Figure 26D and E).

Notwithstanding these apparent phenotypes, no hearing defects were seen when the *ninaE*¹⁷ mutation was uncovered with the *ninaE* deficiency *Df(3R)Exel6174*. Moreover, no auditory defects were also detectable when the genetic background was changed to *yw*. These results strongly indicate that auditory defects seen in *cs; ninaE*¹⁷ mutant flies were not caused by the *Rh1* mutation itself, but rather site mutations within *CantonS* genetic background. Thus, in contrast to *Rh5* and *Rh6* mutant flies where strong auditory defects that could be rescued have been documented (Senthilan et al., 2012), the main visual opsin Rh1 seems dispensable for fly hearing.

1.2 Results

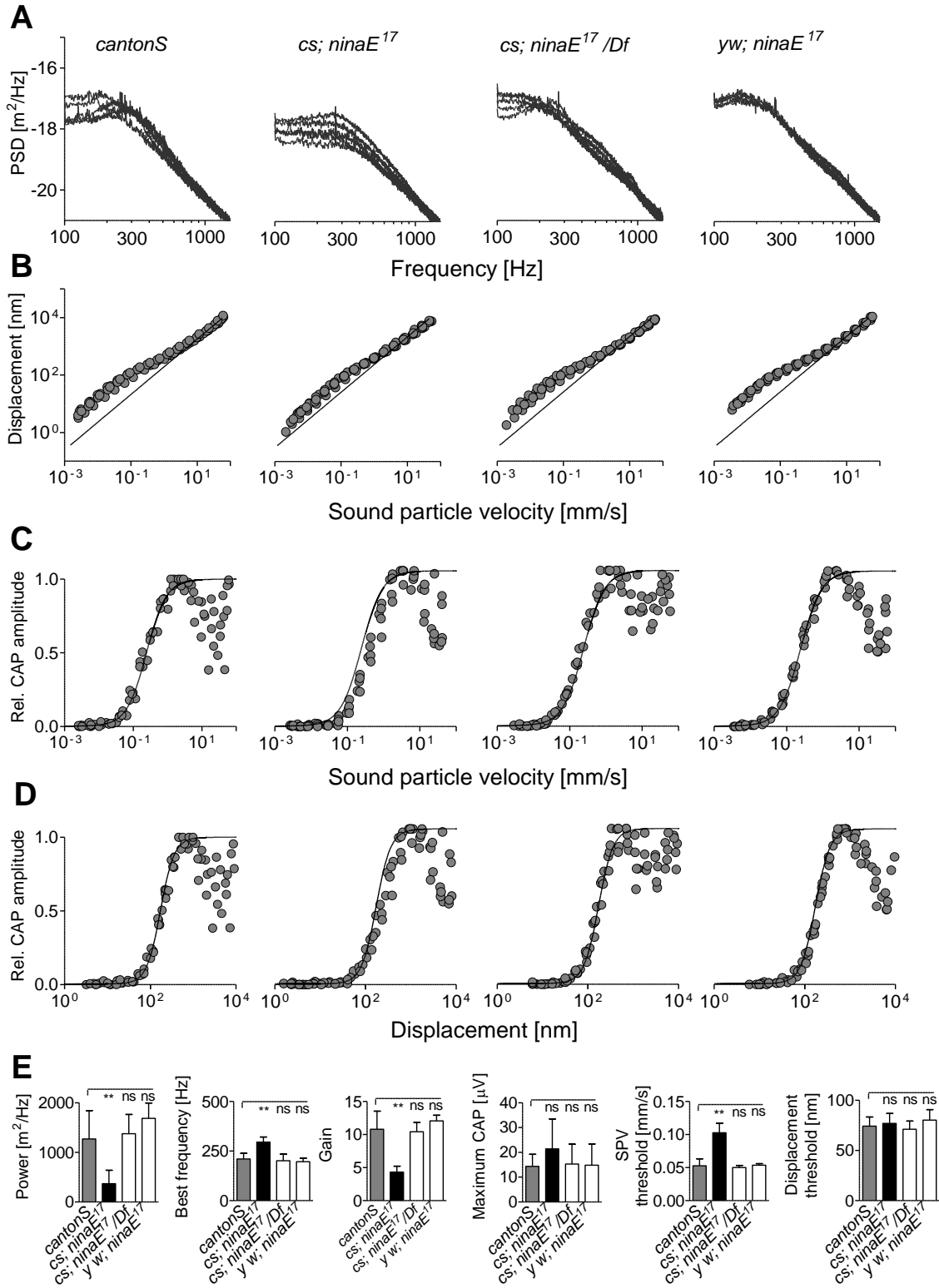


Figure 26. Auditory performance of various *ninaE¹⁷* mutant strains

- A)** Power spectral density (PSD) of the free mechanical fluctuation of the antenna in cantonS control flies, *ninaE¹⁷* in cantonS genetic background (*cs; ninaE¹⁷*), *ninaE¹⁷* uncovered by deficiency *cs; ninaE¹⁷/Df* and *ninaE¹⁷* with genetic background changed to *yw* (*yw; ninaE¹⁷*) flies (N=5 per strain).
- B)** Tone-evoked antennal displacement as a function of the particle velocity of the tone. The black line indicates linearity.
- C)** Relative amplitude of toned-evoked CAPs as a function of the particle velocity of the tone.
- D)** Relative CAPs amplitudes plotted against the respective antennal displacement.
- E)** Respective: fluctuation powers, antennal best frequencies, mechanical amplification gains, maximum CAP amplitudes, sound particle velocity thresholds and displacement thresholds.

Data are presented as a mean values \pm 1 SD, N = 5, *P < 0.05, **P < 0.01, ns = not significant, two-tailed Mann Whitney U-test.

1.3. Discussion

Drosophila opsins, besides being light sensors, also have non-visual roles in larval thermosensation, proprioception and adult hearing (Senthilan et al., 2012; Shen et al., 2011; Sokabe et al., 2016). Without Rh5 or Rh6 Johnston's organ function is severely impaired, as witnessed by abolished mechanical amplification as well as defects in signal transduction (Senthilan et al., 2012). Initial studies suggested that all these non-visual opsins functions are chromophore-dependent as disrupting chromophore synthesis by eliminating the Santa-Maria scavenger receptor cause similar sensory defects as seen in opsin mutants alone.

In this thesis I tested the hypothesis that the chromophore is required for non-visual opsin functions. I studied all genes known to participate in chromophore synthesis, checking their functional contribution to *Drosophila* hearing. Additionally, I investigated the impact of the *santa-maria*¹ mutation on JO function and morphology. I also tested whether proteins involved in chromophore recycling are necessary for fly audition. Finally, I checked if the main visual opsin of adult flies, Rh1, is needed for hearing.

1.3.1. Eliminating key genes of chromophore synthesis left hearing unaffected

Dietary uptake of β -carotene is crucial for the de novo synthesis of the chromophore. In flies, the first step in chromophore synthesis, the uptake of β -carotene into gut cells, depends on NINAD, a class B scavenger receptor (Giovannucci and Stephenson, 1999). In *ninaD*¹ null mutant flies, this chromophore uptake is disrupted, yet hearing was normal, resembling that of controls. Upon uptake in the gut, β -carotene is cleaved into retinal by NINAB (Oberhauser et al., 2008), which also is dispensable for fly audition. Hence, disrupting β -carotene uptake and cleavage leaves hearing unaffected, suggesting that auditory opsin functions are independent of the chromophore. Support for this chromophore-independence comes from nutritional approaches, in which the animals were raised for several generations on a medium depleted of provitamin A (β -carotene).

Removing the chromophore substrate greatly reduces rhodopsin levels as evidenced by loss of PDA phenotype in photoreceptor cells (Pak et al., 2012). However, hearing remained unaffected, further suggesting that hearing requires opsin apoproteins without chromophore.

In flies, this is the first evidence for a chromophore-independent opsin function. In photoreceptor cells, the chromophore is crucial for opsin maturation and trafficking in the ER (Colley et al., 1991). Thus, it was concluded that even though non-visual opsin functions are independent of light, they still need the chromophore for opsin synthesis (Voolstra et al., 2010). Based on my results, it seems that in hearing, opsins can be metabolized without chromophore, or there is another molecule that can play a similar role as retinal in photoreceptor cells. In either case, more research will be needed to check whether the retinal binding pocket of different opsins is free or occupied by another cofactor.

1.3.2. Santa-Maria scavenger receptor is crucial for JO function

Previous studies had been shown that the *santa-maria*¹ mutation severely impacts audition in adult flies and locomotion in larvae (Senthilan et al., 2012; Zanini et al., 2018), as well as larval thermosensation (Shen et al., 2011; Sokabe et al., 2016). Consistent with these studies, hearing in *santa-maria* mutant flies was found to be defective, with SANTA-MARIA being required for JO neuron motility and, thus, mechanical signal amplification. Also transduction seems affected as louder sounds and larger antennal displacements are required to evoke CAP responses in the antennal nerve, and also maximum CAP amplitudes are slightly lower than in controls.

Using a *santa-maria* T-GEM line, the native pattern of *santa-maria* expression was revealed. This driver showed stronger and broader expression than previously reported *santa-maria-Gal4* (Wang et al., 2007), labelling accessory glia cells of chordotonal organs and other sensory neurons in both larvae and the adult stage. Also hindgut seem to express

santa-maria – an expression that might have implications on chromophore synthesis and that had been excluded based on the old driver line (Wang et al., 2007).

The strong auditory phenotype of *santa-maria*¹ mutants is partially rescued when *UAS-santa-maria* is driven by *repo-Gal4* that targets all glia except for midline glia (Stork et al., 2012). Also the chordotonal neuron-specific driver *Dnai2-Gal4* (Karak et al., 2015) is able to partially rescue hearing, suggesting that also these receptors express *santa-maria* at low levels, or that ectopic expression of *santa-maria* in the chordotonal receptors can compensate for its loss in chordotonal organ glial cells.

Mutations in opsins reportedly cause mislocalization of NOMPC and IAV TRP channels in the cilia of larval proprioceptor cells (Zanini et al., 2018). In the JO of *santa-maria*¹ mutants, no such mislocalization was detected, neither in larval proprioceptors nor in JO receptor cells. This suggests that, in mechanoreceptors, SANTA-MARIA and opsins have unrelated functions, yet what these functions are still remains unclear. It is known that in vertebrates class B scavenger receptors type I (SR-BI) are able to recognize a broad array of ligands like oxidized low density lipoprotein (LDL), high density lipoprotein (HDL), native lipoproteins, and fatty acids (Steinbrecher, 1999). Giving that, one might speculate that Santa-Maria mediates for example cholesterol transport in chordotonal neurons, helping to maintain a proper plasma membrane composition and membrane tension necessary for mechanotransduction channel gating. This could explain why, even though TRP channels are correctly localized in *santa-maria*¹ mutants, JO function is impaired.

1.3.3. Auditory organ function is dependent on the proteins previously implicated in chromophore processing

In my study, I also showed that proteins previously implicated in all-trans retinal binding and processing, PINTA and NINAG, are involved in hearing. In absence of these proteins, JO neurons lack motility witnessed by the loss of mechanical amplification. Whereas electrical JO responses of *pinta*¹ mutants are affected only slightly, *ninaG*^{P330} flies show strong defects with respect to CAP amplitudes and thresholds. Like *santa-maria*, both

genes are expressed in accessory cells of chordotonal organs. *Pinta* was detected in cap cells and scolopale cells, and *ninaG* is affiliated with ligament cells in chordotonal organs of both larvae and adult flies. In vision, the precise role of PINTA is largely unclear, besides the fact that it preferentially binds all-trans retinol in retinal pigment cells and is necessary for chromophore synthesis (Pak et al., 2012). The presence of a CRAL-TRIO domain suggests that PINTA might bind small lipophilic molecules other than retinol. Judging from the *pinta*¹ hearing phenotype and expression pattern it may be involved in trafficking small molecules between the cap and scolopale cells.

The NINAG enzyme is also required JO neurons motility, active antennal amplification and proper electrical sound responses. NINAG belongs to a glucose-methanol-choline oxidoreductase (GMC) class of oxidoreductases (Ahmad et al., 2006). These proteins are known to act on CH-OH group of donors performing redox reactions on a wide range of organic metabolites, however most of these metabolites still remain unknown (Sarfare et al., 2005). The exact function of NING in ligament cells likewise remains unclear. It might act in the oxidation of membrane lipids, which has a major impact on membrane physiochemical properties, both in neurons and in glial cells (Fantini et al., 2015). Possibly, NINAG participates in metabolic reactions that supply JO neurons with necessary nutrients, and further studies will be required to unravel its mechanosensory role.

1.3.4. Genes of chromophore recycling pathway are functionally involved in hearing

Analogous to vertebrates, *Drosophila* is endowed with an enzymatic visual cycle that recycles the chromophore after its release from light-activated rhodopsin. The two enzymes participating in this pathway, PDH and RDHB, are also needed for hearing. Defects in JO performance in *Pdh*¹ mutants resemble those seen in *pinta*¹ mutants, with both mutant lines showing moderately reduced mechanical amplification gains. Sound-evoked CAPs were only partially affected by the loss of PDH, and normal auditory function was restored by a genomic *Pdh* rescue. *rdhB*¹ mutants showed similarly strong auditory

2.2 Results

defects as seen in *ninaG*^{P330} mutants, including strongly reduced mechanical amplification, CAP amplitudes, and auditory sensitivity.

Unfortunately, I was not able to detect *Pdh* expression in chordotonal organs. The only detectable GFP signals driven by promoter fusion construct *Phd-Gla4* occurred in the retinal pigment cells. One explanation for the lack of signals in the mechanosensory organs can be that a respective part of the promoter/enhancer of *Pdh* is located further away in the genome than the 2kb upstream of first ATG used to generate the Gal4 line. Another issue is that *Pdh* gene has 4 isoforms and it is possible that they are expressed via different promoters. Thus, a new Gal4 line should be generated to fully mimic *Pdh* expression pattern. RDHB, in turn, seems to occur in adult JO neurons, where faint GFP signals were detected using a previously published *rdhB-Gal4* line (Wang et al., 2012).

PDH is a member of Short-chain dehydrogenase/reductase (SDR) proteins that exhibit retinol dehydrogenase and alcohol dehydrogenase (NAD) activity (Kallberg et al., 2002). PDH also shows considerable protein sequence homology (34% identity and 54% similarity (Gramates et al., 2017)) to mammalian Hydroxyprostaglandin dehydrogenase 15-(NAD) (HPGD) enzyme that participates in prostaglandins (PGs) metabolism (Clish et al., 2000). In flies, these highly conserved lipid signaling molecules were implicated in actin cytoskeletal remodeling in follicle cells (Groen et al., 2012). Moreover, recently HPGD was found to be expressed in mouse hair cells (Scheffer et al., 2015). There is a possibility that PDH also participates in PG metabolism, however nothing is known about PGs signaling in chordotonal organs.

Similarly to PDH, RDHB belongs to SDR class of enzymes and its only known function is the dehydrogenation of 11-cis-hydroxyretinol. When checked for orthologs, RDHB shares 57% similarity and 37% identity with mammalian DHRS11 (Gramates et al., 2017). This latter protein is widely expressed in human tissues, including: testis, small intestine, colon, and kidney where it catalyzes a broad range of reactions, mainly on steroids (Endo et al., 2016). In flies, RDHB might not only participate in chromophore synthesis but in some other enzymatic reactions, most probably on membrane lipids changing their composition and properties.

1.3.5. Rhodopsin1 has no function in JO

The main visual rhodopsin of adult flies, Rh1, was previously shown to be involved in larval thermosensation and proprioception (Shen et al., 2011; Zanini et al., 2018). Accordingly, it seemed likely that it also plays functions in JO, in particular because larval and adult chordotonal organs are very similar in terms of both genetics and morphology. RT-PCR analysis confirmed that *rh1* mRNA occurs in the adult JO, and *cs;ninaE¹⁷* mutant flies displayed moderately impaired JO function. When *ninaE¹⁷* mutation was uncovered by *ninaE* deficiency or put into other genetic background (*yw*), however, hearing remained normal, indicating that there is a site mutation in *cs;ninaE¹⁷* that is affecting hearing. Thus, even though Rh1 is crucial for larval chordotonal receptor function, it seems rather dispensable for the function of JO. That *rh1* mRNA can be detected in JO clearly does not mean that Rh1 functions in hearing, and I also cannot fully exclude contamination from the eye when separating second antennal segments by sieving.

Chapter 2: Identifying novel genes in *Drosophila* hearing.

2.1. Introduction:

The first genetic screen for genes that are expressed in Johnston's organ was performed by Senthilan and colleagues 2012. Among the 274 identified genes the authors focused on 42 of them, describing their functional contribution to fly hearing. David Piepenbrock in his doctoral dissertation (Piepenbrock, 2013) characterized auditory phenotype of 92 more mutant fly strains. He found most of them to have defective JO functions manifested in the wide range of hearing phenotypes. Following this direction I decided to deeply characterize a couple of genes that appeared to be interesting.

My approach was to carefully study the screening list and pick the genes to study their expression pattern and hearing phenotypes based on following criteria:

- The genes that are highly abundant in Johnston's organ
- The genes that were not characterized previously or the knowledge about them is very limited
- The genes that contain suitable MiMIC insertions

2.1.1. MiMIC as a powerful tool in *Drosophila* genetics

2.1.1.1. MiMIC features

The Minos-Mediated Integration Cassette (MiMIC) is a specifically engineered transposable element that provides a very powerful tool in *Drosophila* genetics (Venken et al., 2011). One of the main features of MiMIC elements is the presence of two inverted Φ C31 *attP* sites that flank the whole cassette, allowing for site-specific recombination

through recombinase-mediated cassette exchange (RMCE) (Baer and Bode, 2001). Another feature is the presence of a mutagenic gene-trap cassette that consists of a splice acceptor (SA), stop codons in all three reading frames, and a strong SV40 polyadenylation signal sequence (Venken et al., 2011). Thus, a MiMIC insertion in a coding intron and in proper orientation is highly mutagenic, leading to the truncation of transcripts.

2.1.1.2. RMCE

Exploiting the RMCE it is possible to replace MiMIC cassette with any other DNA fragment flanked by *attB* sites. One of these specifically engineered DNA cassette is “Trojan exon” that consists of splice acceptor, T2A self cleaving peptide and Gal4 effector followed by pA signal (Diao and White, 2012; Diao et al., 2015c). Exchanging correctly positioned MiMIC transposon with Trojan-Gal4 allows for expressing Gal4 in pattern of a native gene. The other possibility is to swap MiMIC with cassette containing green fluorescent protein. In this approach the protein product is tagged with GFP allowing for subcellular localization analysis.

2.2. Results

2.2.1. Selection of candidate genes

The candidate “hearing genes” were picked based on Senthilan genetic screen (Senthilan et al., 2012), RNA-seq data from Natasha Zhang (unpublished data) and criteria that were mentioned above. The two candidate genes were *CG13636* (*sosie*) and *CG14085* (Figure 27).

Affymetrix ID	Public ID	Gene symbol	Gene name	Average p-value	p-value contr1/mut	p-value contr2/mut	JO/Brain expression
1637514_at	CG14142	CG14142	CG14142	2.88E-07	1.64E-08	4.93E-07	3.069266639
1636816_at	CG13133	CG13133	CG13133	1.50E-06	8.34E-07	2.10E-06	3.808554816
1631403_at	CG14445	CG14445	CG14445	1.97E-06	5.84E-07	3.36E-06	3.197957601
1626959_at	CG13518	Olp58b	Olfant-receptor-binding protein 58b	3.46E-06	4.39E-06	1.92E-06	1.858256466
1633919_at	CG56542	s10	reteneal protein 10	6.62E-06	7.42E-07	1.25E-05	2.122633121
1641736_at	CG13636	CG13636	CG13636	6.36E-06	1.12E-05	2.68E-06	1.078566753
1635518_at	CG13950	CG13950	CG13950	7.31E-06	2.31E-06	1.23E-05	3.652136926
1640214_at	CG13216	Nsun	Nicotinamide amidase	3.19E-06	6.37E-06	1.14E-05	2.263828729
1631175_at	CG10283	CG10283	CG10283	1.11E-05	4.16E-06	1.80E-05	0.868563019
1627074_at	CG10185	CG10185	CG10185	1.71E-05	2.83E-05	5.20E-06	3.464006559
1636405_at	CG4329	CG4329	CG4329	1.89E-05	1.38E-05	1.80E-05	2.280071502
1628647_at	CG5430	s5	reteneal protein 5	2.73E-05	5.22E-06	4.34E-05	2.688555972
1639333_at	CG3935	sl	slitlike2	3.07E-05	5.60E-05	5.46E-06	1.433276264
1639553_at	CG10062	CG10062	CG10062	3.90E-05	5.45E-06	7.25E-05	1.367668045
1635773_at	CG11041	CG11041	CG11041	4.21E-05	6.53E-05	1.89E-05	3.51589191
1639363_at	CG33472	qvr	quiver	4.52E-05	6.56E-05	2.47E-05	0.832136795
1623363_at	CG1672	gl	gluss	4.54E-05	3.48E-07	3.05E-05	1.00437938
1639022_at	CG12836	CG12836	CG12836	5.08E-05	6.34E-05	3.81E-05	2.193153851
1640774_at	CG11111	Mob2	Mob2	5.24E-05	6.07E-05	4.41E-05	0.340157877
1640649_at	CG15878	CG15878	CG15878	5.55E-05	4.82E-05	6.27E-05	2.309150328
1630369_at	CG116	Pbp4	Phenoxane-binding protein-related protein 4	6.22E-05	4.25E-05	8.18E-05	3.534795243
1641395_at	CG14342	CG14342	CG14342	6.28E-05	2.38E-05	9.58E-05	2.163360151
1641605_at	CG12129	PIP82	PIP82	6.52E-05	3.33E-06	1.21E-04	0.364515777
1641423_at	CG5611	foi	Fear of intimacy	6.66E-05	3.30E-05	4.01E-05	1.238855536
1636576_at	CG3620	norpA	no receptor potential A	7.72E-05	1.40E-04	1.45E-05	0.888502597
1630116_at	CG3620	norpA	no receptor potential A	7.78E-05	4.00E-05	1.8E-04	0.37041297
1639795_at	CG11219	CG11219	CG11219	8.70E-05	3.11E-05	1.43E-04	4.236065203
1634172_at	CG14085	CG14085	CG14085	3.09E-05	1.18E-04	6.37E-05	2.143186533
1628723_at	CG31019	CG31019	CG31019	3.43E-05	1.17E-04	7.21E-05	2.127664812
1640182_at	CG5842	nan	nanchang	1.08E-04	1.17E-05	2.04E-04	1.395344931
1630904_at	CG3723	Dhs33AB	Dysin heavy chain at 93AB	1.09E-04	1.86E-04	3.21E-05	2.077110575
1637870_at	CG5308	4pr5	4pr5	1.10E-04	1.41E-04	7.97E-05	0.818300174
1640370_at	CG3313	CG3313	CG3313	1.12E-04	1.37E-04	8.69E-05	1.450950162
1626722_at	CG14087	CG14087	CG14087	1.13E-04	1.62E-04	6.31E-05	0.834418867
1631168_at	CG5687	CG5687	CG5687	1.14E-04	1.73E-04	5.44E-05	1.345839368
1638091_at	CG15143	CG15143	CG15143	1.18E-04	1.89E-04	4.77E-05	1.534023939
1638110_at	CG40467	CG40467	CG40467	1.20E-04	4.72E-05	1.93E-04	0.330087436
1624383_at	HD09346			1.25E-04	1.61E-04	8.87E-05	1.322329249
1633313_at	CG19768	Aak2	Aaklyin 2	1.35E-04	1.88E-04	8.17E-05	0.971298961
1632968_at	CG6053	CG6053	CG6053	1.40E-04	1.42E-04	0.000158488	2.469562475
1630118_at	CG5829	Dyb	Dystronobrevin-like	1.54E-04	1.07E-04	0.000200437	0.179143729
1636288_at	CG31732	ywi1	ywi1 gppain	1.59E-04	2.25E-04	3.36E-05	1.608681123
1636865_at	CG3250	Ov-C	Ov-C	1.67E-04	1.58E-04	0.000174962	2.2658434063
1634272_at	CG18516	CG18516	CG18516	1.68E-04	5.64E-05	0.000278846	4.344801648
1636574_at	CG3935	CG3935	CG3935	2.10E-04	3.85E-05	0.0003907	0.35474114
1628369_at	CG2825	boss	bride of areolase	2.17E-04	1.35E-05	0.000420452	0.313389059

Figure 27. Screenshot showing list of the genes detected in *Drosophila* JO from Senthilian et al., 2012.

Highlighted are the two genes that met chosen criteria: *CG13636* (*sosie*) and *CG14085*. Modified from Senthilian et al., 2012.

2.2.2. *Sosie*

sosie gene has 3 annotated transcripts that encode 3 protein variants. The biggest, *sosie-PA* has a predicted molecular mass of 20kDa and consists of 186 amino acids. The other two isoforms are 8.2 kDa proteins consisting of 74 amino acids. The protein is insect-specific and no orthologs can be found in non-insect species. Previously, *Sosie* was reported to localize to membranes in the germ line and follicle cells where it is responsible for epithelial integrity and cell migration (Urwyler et al., 2012). Moreover, *Sosie* was shown to be crucial for maintaining the normal localization of the cortical F-actin cytoskeleton, most probably by organizing or supporting β_H -Spectrin localization and interactions with the actin organizing genes *cheerio* and *chic* (Urwyler et al., 2012).

Within the *sosie* gene there is one *MiMIC* insertion, (*Mi{MIC}sosie^{Mi1265}*), which is inserted into a coding intron in the same orientation as the gene. Thus, this *MiMIC* transposon should act as a mutator gene trap that truncates the *sosie-PA* transcript variant.

2.2.2.1. Hearing in *sosie* mutant flies is severely impaired

Homozygous *sosie^{MiMIC}* flies are viable and do not display any obvious mutant phenotype e.g. walking or coordination problems. However, the free fluctuations of their sound receiver are severely impaired. Compared to controls, the fluctuation power was reduced to $220 \pm 197 \text{ nm}^2/\text{Hz}$, with the fluctuations displaying a very pronounced peak at $772 \pm 149 \text{ Hz}$ (Figure 28A). In line with the altered fluctuations, mechanical amplification was virtually lost, with amplification gains of 1.5 ± 0.2 (Figure 28B). Electrophysiological recordings from the antennal nerve revealed virtually no sound-evoked CAPs responses (Figure 28C). The maximum CAPs amplitude was as low as $1 \pm 0.1 \mu\text{V}$, and when relative response amplitudes were plotted against the sound particle velocity or the antennal displacement, data scattered and no clear response could be seen (Figure 28C).

2.2 Results

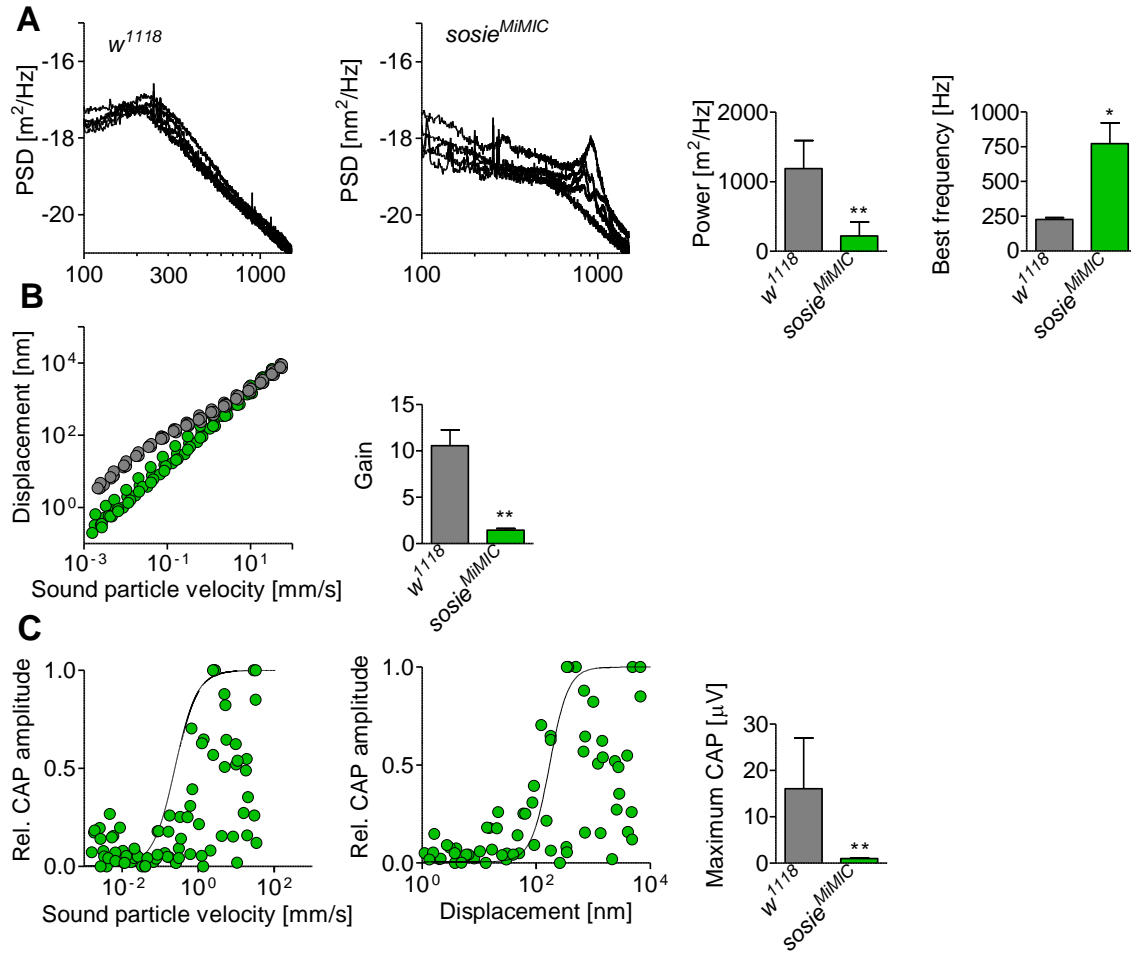


Figure 28. Laser Doppler Vibrometer analysis of auditory defects in *sosie* mutant flies.

- A)** Left: power spectral density (PSD) of the free mechanical fluctuation of the antenna in the w^{1118} controls and $sosie^{MiMIC}$ mutants (N=5 per strain). Right: respective fluctuation powers and antennal best frequencies.
- B)** Left: Tone-evoked antennal displacement as a function of the particle velocity of the tone. In grey controls and in green $sosie^{MiMIC}$ mutants. Right: respective mechanical amplification gains.
- C)** Left: Relative amplitude of toned-evoked CAPs as a function of the particle velocity of the tone and respective particle velocity thresholds. Middle: CAP amplitude plotted against the respective antennal displacement and corresponding displacement thresholds. Right: Maximum CAP responses.

Data are presented as a mean values \pm 1 SD, N=5, *P < 0.05, **P < 0.01 two-tailed Mann Whitney U-test.

2.2.2.2. Sosie is present in auditory neurons

To assess the cell types that express *sosie*, a *sosie^{Trojan}-Gal4* was generated. Therefore, RMCE between *Mi{MIC}sosie^{M11265}* and the Trojan-exon was performed using a “triplet donor” *in vivo* approach (Diao et al., 2015c). Then, *sosie^{Trojan}-Gal4* was crossed to *UAS-YFP* flies to check for expression in larval and adult chordotonal organs. In larvae, GFP signals were clearly visible even without immunohistochemical staining. *sosie^{Trojan}-Gal4* showed a broad expression pattern in the nervous system, including lch5 chordotonal organ neurons (Figure 29 top). In adults, GFP signals were found in 2nd antennal segment neurons (Figure 29 bottom). Interestingly, not all neurons seem to be expressing *sosie* as indicated by arrows (Figure 29 bottom left).

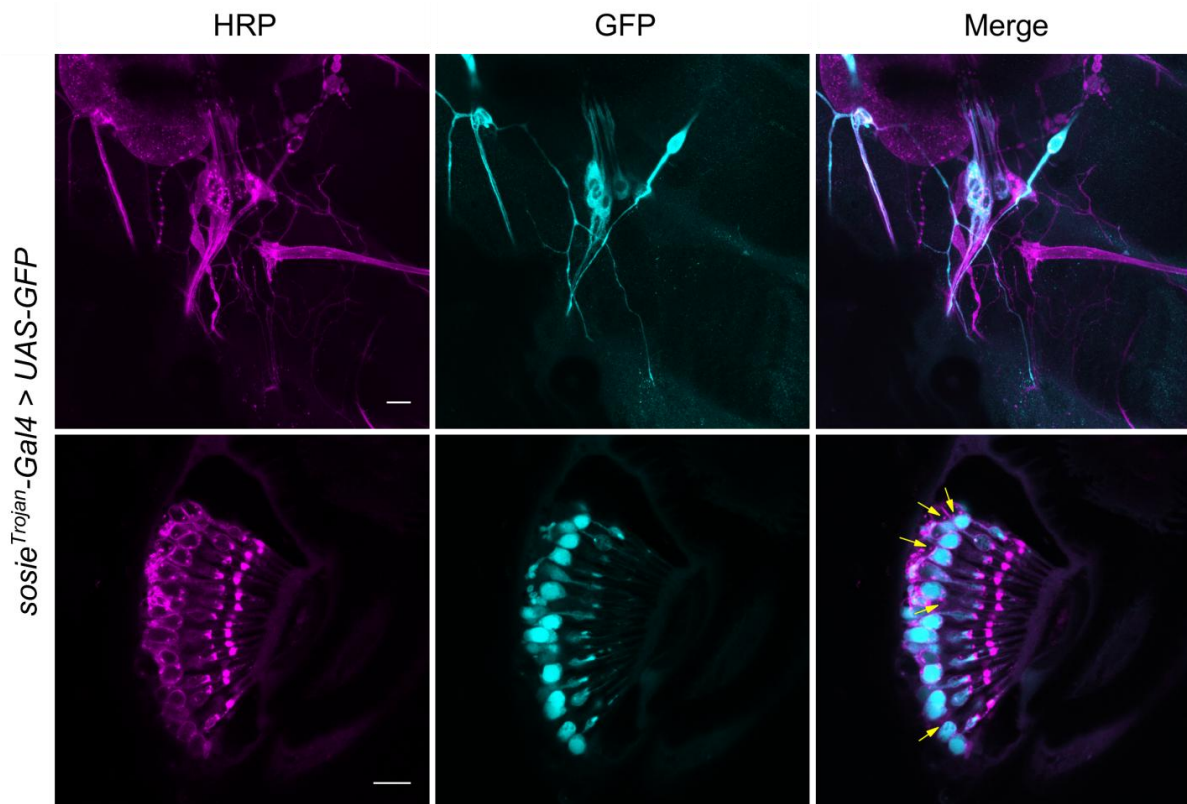


Figure 29. *sosie^{Trojan}-Gal4* expression pattern in larval and adult chordotonal organs

Top: Immunohistochemical staining of larval lch5 chordotonal organ. Neurons are stained with HRP - magenta, GFP signal is shown in cyan. Overlap picture on the right. Scale bar = 10 μ m.

Bottom: Adult 2nd antennal segment staining. Neurons are stained with HRP - magenta, GFP signal is shown in cyan. Overlap picture on the right (arrowheads indicate neurons that are not stained). Scale bar = 10 μ m.

2.2.2.3. Morphology of JO neurons in *sosie* mutants

Auditory impairments in *sosie*^{MiMIC} mutants might reflect defects in F-actin organization, similar to what previously observed in oocytes. To check this possibility, sliced 2nd antennal segments of *sosie*^{MiMIC} mutant flies were stained with the neuronal marker anti-HRP and phalloidin, which stains F-actin. However, no structural defects of the neurons or the adjacent actin- rich scolopale rods could be detected (Figure 30).

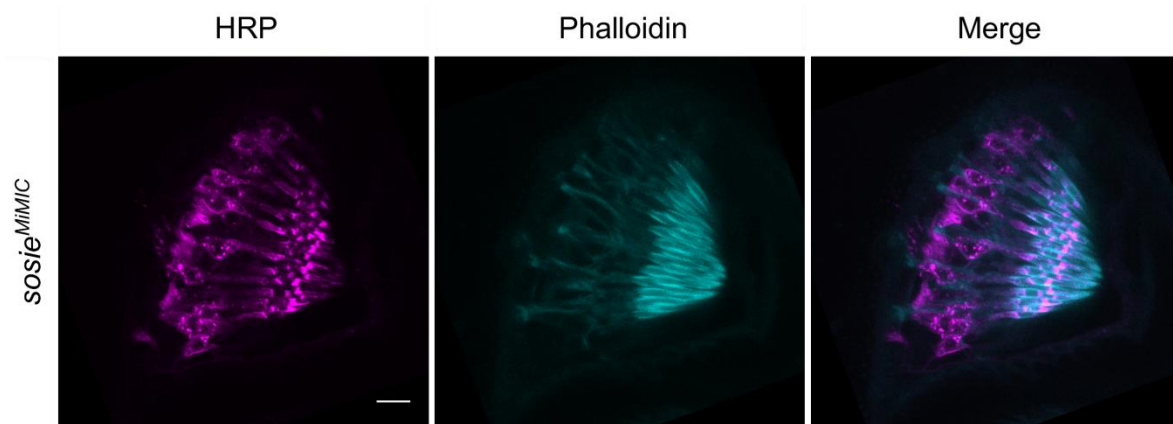


Figure 30. Johnston's organ staining of *sosie*^{MiMIC} mutants

Adult 2nd antennal segment staining. Neurons are stained with HRP - magenta, phalloidin is shown in cyan. Overlap picture on the right. Scale bar = 10 μ m.

2.2.3 *CG14085* – the unknown *Drosophila* gene

CG14085 gene encodes one protein variant of a predicted mass of 98kD that previously was not characterized. The protein is categorized as “Protein of unknown function DUF4495” family which shares two conservative motifs: QMW and DLW that can be found in eukaryotes. In order to make a prediction of *CG14085* protein model the phyre2 online software was used (Kelly et al., 2015). Based on its analysis, predicted secondary structure of *CG14085* protein is still mysterious due to relatively low alignment coverage and identity percentage with other known protein domains as summarized in Table 1.

Allignment coverage	Confidence	% identity	Protein data base (PDB) molecule
6%	44.6	11	Putative phospholipase b-like 2
9%	37.3	11	Tutd, benzylsuccinate alpha-gamma complex
6%	34.2	11	Putative phospholipase b-like 2
5%	33.7	23	RNA-binding domain

Table 1. Summarized analysis of *CG14085* protein domains obtained from phyre2 software

2.2.3.1 Hearing deficits in *CG14085* mutant flies

To test whether *CG14085* has a function in fly auditory system a MiMIC line *CG14085*^{Mi11086} was used. In this strain MiMIC transposon is placed in coding intron between 2nd and 3rd exon in correct orientation, which should result in truncated transcript. Homozygous animals are viable and do not show any noticeable impairments. When it comes to auditory performance, mutants show considerably higher fluctuation power ($6333 \pm 1730 \text{ nm}^2/\text{Hz}$) together with reduced antennal best frequency ($132 \pm 20 \text{ Hz}$) (Figure 31A). As a consequence of excessive JO neurons motility, amplification gain increased to 26 ± 5 (Figure 31B). Maximum sound-evoked action potentials recorded from antennal nerve were significantly lower reaching $7.4 \pm 0.9 \text{ mV}$. The *CG14085*^{MiMIC} mutation strongly impaired sensitive hearing as both sound particle velocity threshold and displacement threshold increased to $0.118 \pm 0.044 \text{ mm/s}$ and $179 \pm 43 \text{ nm}$ respectively (Figure 31C).

2.2 Results

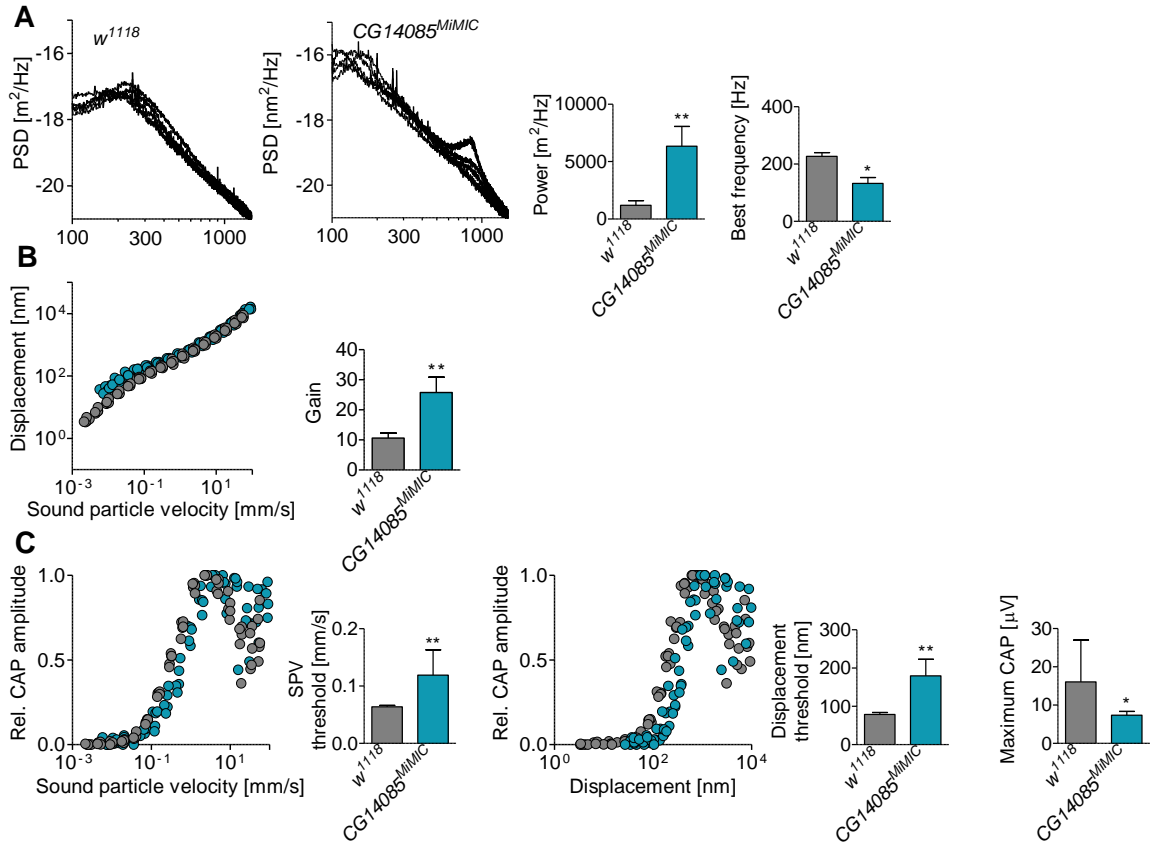


Figure 31. Auditory phenotype of $CG14085^{MiMIC}$ mutant flies.

- A)** Left: power spectral density (PSD) of the free mechanical fluctuation of the antenna in the w^{1118} controls and $CG14085^{MiMIC}$ mutants (N=5 per strain). Right: respective fluctuation powers and antennal best frequency.
- B)** Left: Tone-evoked antennal displacement as a function of the particle velocity of the tone. $CG14085^{MiMIC}$ mutants in blue and controls in gray. Right: respective mechanical amplification gains.
- C)** Left: Relative amplitude of toned-evoked CAPs as a function of the particle velocity of the tone and respective particle velocity thresholds. Right: CAPs amplitude plotted against the respective antennal displacement and corresponding displacement thresholds together with maximum CAPs.

Data are presented as a mean values \pm 1 SD, N=5, * $P < 0.05$, ** $P < 0.01$ two-tailed Mann Whitney U-tests against w^{1118} controls and $CG14085^{MiMIC}$ mutants.

2.2.2.2. *CG14085* is expressed in chordotonal organs

To investigate whether *CG14085* is expressed in *Drosophila* chordotonal organs MiMIC cassette was replaced with *Trojan-Gal4* through in vivo RMCE. When crossed to *UAS-GFP* reporter fluorescent signals can be observed both in larval lch5 chordotonal organ neurons and in adult JO neurons (Figure 32). It is worth to mention that *CG14085* expression pattern seem to be chordotonal neurons specific, as I could not detect GFP signals in other neurons or cells.

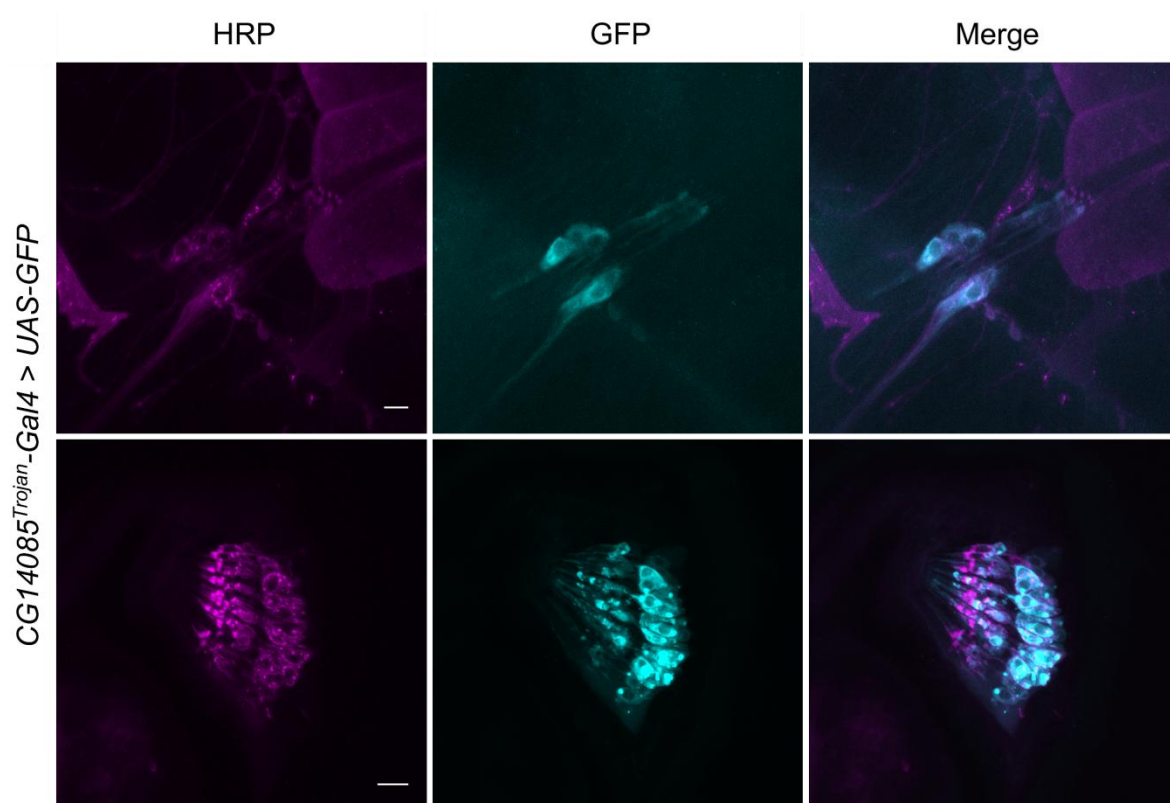


Figure 32. *CG14085* expression pattern in chordotonal organs.

Top: Immunohistochemical staining of larval lch5 chordotonal organ. Neurons are stained with HRP - magenta, GFP signal is shown in cyan. Overlap picture on the right. Scale bar = 10 μ m.

Bottom: Adult 2nd antennal segment staining. Neurons are stained with HRP - magenta, GFP signal is shown in cyan. Overlap picture on the right. Scale bar = 10 μ m.

2.3 Discussion

The aim of my study was to characterize the novel genes involved in hearing process in *Drosophila*. In order to identify them I used a data from previously published genetic screen (Senthilan et al., 2012) and recent RNA-seq data (unpublished, Zhang) of the genes expressed in 2nd antennal segment. I also wanted to implement and take advantage of recently developed MiMIC genetic technique.

I decided to focus on two potential “hearing” genes that were highly enriched in Johnston’s organ. I found that *sosie*, which was previously implicated in *Drosophila* oogenesis (Urwyler et al., 2012), is also functionally involved in hearing. *Sosie*^{MiMIC} mutants have severe defects in JO function, where mechanosensory neurons lack motility witness by loss of mechanical amplification. Additionally, sound-evoked CAPs recorded from the antennal nerve are almost abolished, suggesting that not only antennal mechanics is impaired but also electric signal transduction and propagation. *Sosie* seems to operate in JO neurons as confirmed by *sosie*^{Trojan-Gal4} line. Yet, what is the cause of such a strong auditory phenotype is elusive. Since previous studies linked *Sosie* with cortical F-actin organization through β_H -Spectrin in nurse cells during oogenesis (Urwyler et al., 2012), it also might play similar role in chordotonal neurons. Nonetheless, *sosie* mutants display typical F-actin organization in scolopale rods and ligament cells, thus mechanosensory role of *Sosie* seems to be not related with actin modeling.

The second gene selected for the analysis was *CG14085* that encodes largely unknown protein. According to my results, *CG14085* is required for normal mechanosensory function of antennal ear. *CG14085*^{MiMIC} mutant flies display excessive antennal fluctuation power and slightly shifted individual best frequency. As a consequence, mechanical amplification gains are ca. 3 times higher than in wild types. The gene is also expressed in chordotonal neurons cell bodies as shown by *CG14085*^{Trojan-Gal4} line. There is little known about *CG14085* protein structure, biological process, molecular function and cellular localization besides the fact that it contains a conserved sequence motif QMW and DLW and belongs to the protein of unknown function DUF4495 family. According to flybase *CG14085* is an ortholog of human KIAA0825 with 38% similarity and 22% identity.

KIAA0825 is considered as a possible risk factor in Type II diabetes that might increase the glucose levels in the blood (Li et al., 2016). It is predicted to shuttle back and forth across the nuclear membrane (Nakai and Horton, 1999). However, the precise function of this protein in humans remains unknown. The hearing performance of *CG14085^{MiMIC}* mutants closely resembles the auditory defects seen in *nan* and *iav* mutants. In *Drosophila* these TRPV channels are believed to negatively control NOMPC dependent amplification, thus *nan* or *iav* mutant flies exhibit excessive antennal fluctuations and mechanical amplification (Göpfert et al., 2006). Having this in mind, one possibility might be that CG14085 influence NAN or Iav functions.

To narrow down the exact function of *Sosie* and *CG14085* in JO mechanosensory neurons further research need to be done. This includes generation of *UAS-sosie::GFP* and *UAS-CG14085::GFP* lines which could help to reveal cellular localization of both proteins. The other possibility might be to swap MiMIC with GFP cassette; however expressing GFP within the protein sequence could result in incorrect localization or even protein degradation. GFP tagged protein would open possibility to perform co-immunoprecipitation in order to find interaction partners. Both genes are excellent candidates for further research in *Drosophila* hearing.

3. Summary

During the past years, rhodopsins, besides serving vision, have been implicated in thermo- and mechanosensation. Two out of seven *Drosophila* rhodopsins (Rh5, Rh6) were shown to be crucial for proper JO function in fly hearing. However, little was known about whether these non-visual functions involve the light-sensitive retinal chromophore or opsin apoprotein alone. In this thesis I showed that depriving wild-type flies from dietary carotenoids as well as disrupting proteins responsible for β -carotene uptake and cleavage do not impact *Drosophila* mechanosensory JO function, documenting biological function for opsin apoproteins alone. Rather surprisingly, fly hearing turned out to be nonetheless impaired in the flies lacking chromophore processing proteins and visual cycle enzymes. Moreover, expression studies revealed that respective proteins are present in accessory cells of chordotonal mechanosensory organs. Exact function of these proteins in *Drosophila* hearing is still elusive and will require further studies. I also looked at possible functions of Rh1 in adult hearing, but unlike Rh5 and Rh6, the fly's main visual opsin seems to be dispensable for JO function.

In the second part of my thesis I focused on *sosie* and *CG14085* that were identified as putative genes for hearing in JO gene expression screens. Testing MiMIC mutants, I found that both genes are required for JO function, with *sosie*^{MiMIC} flies showing abolished mechanical amplification and *CG14085*^{MiMIC} mutants displaying excessive amplification. Replacing MiMIC cassettes with Trojan-Gal4 through RMCE revealed that both genes are expressed in chordotonal sensory neurons, both in larval *lch5* organs and in JO. Apart from an initial characterization of *sosie* and *CG14085* as “hearing genes”, I showed that MiMIC is a powerful and versatile screening tool that can be applied for describing new genes in *Drosophila* audition.

Bibliography:

- Ahmad, S.T., Joyce, M. V., Boggess, B., and O'Tousa, J.E. (2006). The role of *Drosophila* ninaG oxidoreductase in visual pigment chromophore biogenesis. *J. Biol. Chem.* *281*, 9205–9209.
- Albert, J.T., and Göpfert, M.C. (2015). Hearing in *Drosophila*. *Curr. Opin. Neurobiol.* *34*, 79–85.
- Albert, J.T., Nadrowksi, B., and Göpfert, M.C. (2007a). *Drosophila* mechanotransduction linking proteins and functions. *Fly (Austin)*. *1*, 238–241.
- Albert, J.T., Nadrowski, B., and Göpfert, M.C. (2007b). Mechanical Signatures of Transducer Gating in the *Drosophila* Ear. *Curr. Biol.* *17*, 1000–1006.
- Azusa Kamukouchi, Tkashi Shimada, K.I. (2006). Comprehensive Classification of the Auditory Sensory Projections in the Brain of the Fruit Fly *Drosophila melanogaster*. *J. Comp. Neurol.* *499*, 317–356.
- Baer, A., and Bode, J. (2001). Coping with kinetic and thermodynamic barriers: RMCE, an efficient strategy for the targeted integration of transgenes. *Curr. Opin. Biotechnol.* *12*, 473–480.
- Bokolia, N.P., and Mishra, M. (2015). Hearing molecules, mechanism and transportation: Modeled in *Drosophila melanogaster*. *Dev. Neurobiol.* *75*, 109–130.
- Brewster, R., and Bodmer, R. (1995). Origin and specification of type II sensory neurons in *Drosophila*. *Development* *121*, 2923–2936.
- Caldwell, J.C., and Eberl, D.F. (2002). Towards a molecular understanding of *Drosophila* hearing. *J. Neurobiol.* *53*, 172–189.
- Caldwell, J.C., Miller, M.M., Wing, S., Soll, D.R., and Eberl, D.F. (2003). Dynamic analysis of larval locomotion in *Drosophila* chordotonal organ mutants. *Proc. Natl. Acad. Sci.* *100*, 16053–16058.
- Clish, C.B., Levy, B.D., Chiang, N., Tai, H.H., and Serhan, C.N. (2000). Oxidoreductases

in lipoxin A4 metabolic inactivation: A novel role for 15-oxoprostaglandin 13-reductase/leukotriene B4 12-hydroxydehydrogenase in inflammation. *J. Biol. Chem.* *275*, 25372–25380.

Colley, N.J., Baker, E.K., Stamnes, M.A., and Zuker, C.S. (1991). The cyclophilin homolog *ninaA* is required in the secretory pathway. *Cell* *67*, 255–263.

Diao, F., and White, B.H. (2012). A novel approach for directing transgene expression in *Drosophila*: T2A-Gal4 in-frame fusion. *Genetics* *190*, 1139–1144.

Diao, F., Ironfield, H., Luan, H., Diao, F., Shropshire, W.C., Ewer, J., Marr, E., Potter, C.J., Landgraf, M., and White, B.H. (2015a). Plug-and-play genetic access to *drosophila* cell types using exchangeable exon cassettes. *Cell Rep.* *10*, 1410–1421.

Diao, F., Ironfield, H., Luan, H., Diao, F., Shropshire, W.C., Ewer, J., Marr, E., Potter, C.J., Landgraf, M., and White, B.H. (2015b). Plug-and-play genetic access to *drosophila* cell types using exchangeable exon cassettes. *Cell Rep.* *10*, 1410–1421.

Diao, F., Ironfield, H., Luan, H., Diao, F., Shropshire, W.C., Ewer, J., Marr, E., Potter, C.J., Landgraf, M., and White, B.H. (2015c). Plug-and-play genetic access to *Drosophila* cell types using exchangeable exon cassettes. *Cell Rep.* *10*, 1410–1421.

Dickson, B.J. (2008). Wired for sex: The neurobiology of *Drosophila* mating decisions. *Science* (80-.). *322*, 904–909.

Dolph, P.J., Ranganathan, R., Colley, N.J., Hardy, R.W., Socolich, M., and Zuker, C.S. (1993). Arrestin Function in Inactivation of G-Protein Coupled Receptor Rhodopsin *In vivo*. *Science* (80-.). *260*, 1910–1916.

Effertz, T., Wiek, R., and Göpfert, M.C. (2011). NompC TRP channel is essential for *Drosophila* sound receptor function. *Curr. Biol.* *21*, 592–597.

Effertz, T., Nadrowski, B., Piepenbrock, D., Albert, J.T., and Göpfert, M.C. (2012). Direct gating and mechanical integrity of *Drosophila* auditory transducers require TRPN1. *Nat. Neurosci.* *15*, 1198–1200.

- Endo, S., Miyagi, N., Matsunaga, T., Hara, A., and Ikari, A. (2016). Human dehydrogenase/reductase (SDR family) member 11 is a novel type of 17 β -hydroxysteroid dehydrogenase. *Biochem. Biophys. Res. Commun.* *472*, 231–236.
- Fantini, J., Yahi, N., Fantini, J., and Yahi, N. (2015). Lipid Metabolism and Oxidation in Neurons and Glial Cells. *Brain Lipids Synaptic Funct. Neurol. Dis.* *53–85*.
- Fritzschn, B., Beisel, K.W., Pauley, S., and Soukup, G. (2007). Molecular evolution of the vertebrate mechanosensory cell and ear. *Int. J. Dev. Biol.* *51*, 663–678.
- Giovannucci, D.R., and Stephenson, R.S. (1999). Identification and distribution of dietary precursors of the *Drosophila* visual pigment chromophore: Analysis of carotenoids in wild type and *ninaD* mutants by HPLC. *Vision Res.* *39*, 219–229.
- Göpfert, M.C., and Robert, D. (2001). Turning the key on *Drosophila* audition. *Nature* *411*, 908.
- Göpfert, M.C., and Robert, D. (2002). The mechanical basis of *Drosophila* audition. *J. Exp. Biol.* *205*, 1199–1208.
- Göpfert, M.C., and Robert, D. (2003). Motion generation by *Drosophila* mechanosensory neurons. *Proc. Natl. Acad. Sci. U. S. A.* *100*, 5514–5519.
- Göpfert, M.C., Humphris, A.D.L., Albert, J.T., Robert, D., and Hendrich, O. (2005). Power gain exhibited by motile mechanosensory neurons in *Drosophila* ears. *Proc. Natl. Acad. Sci. U. S. A.* *102*, 325–330.
- Göpfert, M.C., Albert, J.T., Nadrowski, B., and Kamikouchi, A. (2006). Specification of auditory sensitivity by *Drosophila* TRP channels. *Nat. Neurosci.* *9*, 999–1000.
- Gramates, L.S., Marygold, S.J., Dos Santos, G., Urbano, J.M., Antonazzo, G., Matthews, B.B., Rey, A.J., Tabone, C.J., Crosby, M.A., Emmert, D.B., et al. (2017). FlyBase at 25: Looking to the future. *Nucleic Acids Res.* *45*, D663–D671.
- Grebler, R., Kistenpennig, C., Rieger, D., Bentrop, J., Schneuwly, S., Senthilan, P.R., and Helfrich-Förster, C. (2017). *Drosophila* Rhodopsin 7 can partially replace the structural role

of Rhodopsin 1, but not its physiological function. *J. Comp. Physiol. A Neuroethol. Sensory, Neural, Behav. Physiol.* *203*, 649–659.

Greenspan, R.J. (2000). Courtship in *Drosophila*.

Groen, C.M., Spracklen, A.J., Fagan, T.N., and Tootle, T.L. (2012). *Drosophila* Fascin is a novel downstream target of prostaglandin signaling during actin remodeling. *Mol. Biol. Cell* *23*, 4567–4578.

Halachmi, N., Nachman, A., and Salzberg, A. (2016). A newly identified type of attachment cell is critical for normal patterning of chordotonal neurons. *Dev. Biol.* *411*, 61–71.

Hartenstein, V. (1988). Development of *Drosophila* larval sensory organs: spatiotemporal pattern of sensory neurones, peripheral axonal pathways and sensilla differentiation. *Development* *102*, 869–886.

Jarman, A.P., and Groves, A.K. (2013). The role of Atonal transcription factors in the development of mechanosensitive cells. *Semin. Cell Dev. Biol.* *24*, 438–447.

Kallberg, Y., Oppermann, U.D.O., and Jörnvall, H. (2002). Short chain dehydrogenasereductase (SDR) relationships: A large family with eight clusters common to human, animal, and plant genomes. *Protein Sci.* *11*, 636–641.

Kamikouchi, A., Inagaki, H.K., Effertz, T., Hendrich, O., Fiala, A., Göpfert, M.C., and Ito, K. (2009). The neural basis of *Drosophila* gravity-sensing and hearing. *Nature* *458*, 165–171.

Karak, S., Jacobs, J.S., Kittelmann, M., Spalthoff, C., Katana, R., Sivan-Loukianova, E., Schon, M.A., Kernan, M.J., Eberl, D.F., and Göpfert, M.C. (2015). Diverse Roles of Axonemal Dyneins in *Drosophila* Auditory Neuron Function and Mechanical Amplification in Hearing. *Sci. Rep.* *5*, 1–12.

Kelly, L.A., Mezulis, S., Yates, C., Wass, M., and Sternberg, M. (2015). The Phyre2 web portal for protein modelling, prediction, and analysis. *Nat. Protoc.* *10*, 845–858.

- Kiefer, C., Hessel, S., Lampert, J.M., Vogt, K., Lederer, M.O., Breithaupt, D.E., and Von Lintig, J. (2001). Identification and Characterization of a Mammalian Enzyme Catalyzing the Asymmetric Oxidative Cleavage of Provitamin A. *J. Biol. Chem.* 276, 14110–14116.
- Kiefer, C., Sumser, E., Wernet, M.F., and Von Lintig, J. (2002). A class B scavenger receptor mediates the cellular uptake of carotenoids in *Drosophila*. *Proc. Natl. Acad. Sci. U. S. A.* 99, 10581–10586.
- Kim, J., Chung, Y.D., Park, D.Y., Choi, S.K., Shin, D.W., Soh, H., Lee, H.W., Son, W., Yim, J., Park, C.S., et al. (2003). A TRPV family ion channel required for hearing in *Drosophila*. *Nature* 424, 81–84.
- Kwon, Y., Shim, H.S., Wang, X., and Montell, C. (2008). Control of thermotactic behavior via coupling of a TRP channel to a phospholipase C signaling cascade. *Nat. Neurosci.* 11, 871–873.
- Lane, M.A., and Bailey, S.J. (2005). Role of retinoid signalling in the adult brain. *Prog. Neurobiol.* 75, 275–293.
- Leung, N.Y., and Montell, C. (2017). Unconventional Roles of Opsins. *Annu. Rev. Cell Dev. Biol.* 33, annurev-cellbio-100616-060432.
- Li, J., Wei, J., Xu, P., Yan, M., Li, J., Chen, Z., and Jin, T. (2016). Impact of diabetes-related gene polymorphisms on the clinical characteristics of type 2 diabetes Chinese Han population. *Oncotarget* 7, 85464–85471.
- Lintig, J. Von, and Vogt, K. (2000). Filling the Gap in Vitamin A Research. *J. Biol. Chem.* 275, 11915–11920.
- Montell, C. (2012). *Drosophila* visual transduction. *Trends Neurosci.* 35, 356–363.
- Nadrowski, B., Albert, J.T., and Göpfert, M.C. (2008). Transducer-Based Force Generation Explains Active Process in *Drosophila* Hearing. *Curr. Biol.* 18, 1365–1372.
- Nakai, K., and Horton, P. (1999). PSORT: A program for detecting sorting signals in proteins and predicting their subcellular localization. *Trends Biochem. Sci.* 24, 34–35.

- O'Tousa, J.E., Baehr, W., Martin, R.L., Hirsh, J., Pak, W.L., and Applebury, M.L. (1985). The *Drosophila ninaE* gene encodes an opsin. *Cell* *40*, 839–850.
- O'Tousa JE1, Leonard DS, P.W. (1989). Morphological defects in oraJK84 photoreceptors caused by mutation in R1-6 opsin gene of *Drosophila*. No Title. *J Neurogenet.* *6(1)*, 41–52.
- Oberhauser, V., Voolstra, O., Bangert, A., von Lintig, J., and Vogt, K. (2008). NinaB combines carotenoid oxygenase and retinoid isomerase activity in a single polypeptide. *Proc. Natl. Acad. Sci.* *105*, 19000–19005.
- Ozaki, K., Nagatani, H., Ozaki, M., and Tokunaga, F. (1993). Maturation of major *drosophila* rhodopsin, *ninaE*, requires chromophore 3-hydroxyretinal. *Neuron* *10*, 1113–1119.
- Pak, W.L., Shino, S., and Leung, H.T. (2012). PDA (Prolonged Depolarizing Afterpotential)-defective mutants: The story of *nina*'s and *ina*'s - *Pinta* and *santa maria*, too. *J. Neurogenet.* *26*, 216–237.
- Robert, D., and Göpfert, M.C. (2002). Acoustic sensitivity of fly antennae. *J. Insect Physiol.* *48*, 189–196.
- Sakmar, T.P., Menon, S.T., Marin, E.P., and Awad, E.S. (2002). Rhodopsin: Insights from Recent Structural Studies. *Annu. Rev. Biophys. Biomol. Struct.* *31*, 443–484.
- Salcedo, E., Zheng, L., Phistry, M., Bagg, E.E., and Britt, S.G. (2003). Molecular basis for ultraviolet vision in invertebrates. *J. Neurosci.* *23*, 10873–10878.
- Sarfare, S., Ahmad, S.T., Joyce, M. V., Boggess, B., and O'Tousa, J.E. (2005). The *Drosophila ninaG* oxidoreductase acts in visual pigment chromophore production. *J. Biol. Chem.* *280*, 11895–11901.
- Scheffer, D.I., Shen, J., Corey, D.P., and Chen, Z.-Y. (2015). Gene Expression by Mouse Inner Ear Hair Cells during Development. *J. Neurosci.* *35*, 6366–6380.
- Scott, K., Becker, a, Sun, Y., Hardy, R., and Zuker, C. (1995). Gq alpha protein function in vivo: genetic dissection of its role in photoreceptor cell physiology. *Neuron* *15*, 919–927.

- Senthilan, P.R., Piepenbrock, D., Ovezmyradov, G., Nadrowski, B., Bechstedt, S., Pauls, S., Winkler, M., Möbius, W., Howard, J., and Göpfert, M.C. (2012). *Drosophila* auditory organ genes and genetic hearing defects. *Cell* 150, 1042–1054.
- Shen, W.L., Kwon, Y., Adegbola, A.A., Luo, J., Chess, A., and Montell, C. (2011). Function of rhodopsin in temperature discrimination in *Drosophila*. *Science* (80-.). 331, 1333–1336.
- Sokabe, T., Chen, H.C., Luo, J., and Montell, C. (2016). A Switch in Thermal Preference in *Drosophila* Larvae Depends on Multiple Rhodopsins. *Cell Rep.* 17, 336–344.
- Steinbrecher, U.P. (1999). Receptors for oxidized low density lipoprotein. *Biochim. Biophys. Acta* 1436, 279–298.
- Stork, T., Bernardos, R., and Freeman, M.R. (2012). Analysis of glial cell development and function in *Drosophila*. *Cold Spring Harb. Protoc.* 7, 1–17.
- Styczynska-Soczka, K., and Jarman, A.P. (2015). The *Drosophila* homologue of Rootletin is required for mechanosensory function and ciliary rootlet formation in chordotonal sensory neurons. *Cilia* 1–11.
- Todi, S. V., Sharma, Y., and Eberl, D.F. (2004). Anatomical and molecular design of the *Drosophila* antenna as a flagellar auditory organ. *Microsc. Res. Tech.* 63, 388–399.
- Urwyler, O., Cortinas-Elizondo, F., and Suter, B. (2012). *Drosophila sosie* functions with β _H-Spectrin and actin organizers in cell migration, epithelial morphogenesis and cortical stability. *Biol. Open* 1, 994–1005.
- Venken, K.J.T., Schulze, K.L., Haelterman, N.A., Pan, H., He, Y., Evans-Holm, M., Carlson, J.W., Levis, R.W., Spradling, A.C., Hoskins, R.A., et al. (2011). MiMIC: A highly versatile transposon insertion resource for engineering *Drosophila melanogaster* genes. *Nat. Methods* 8, 737–747.
- Vogt, K., and Kirschfeld, K. (1984). Chemical identity of the chromophores of fly visual pigment. *Naturwissenschaften* 71, 211–213.

- Voolstra, O., Oberhauser, V., Sumser, E., Meyer, N.E., Maguire, M.E., Huber, A., and Von Lintig, J. (2010). NinaB is essential for *Drosophila* vision but induces retinal degeneration in opsin-deficient photoreceptors. *J. Biol. Chem.* 285, 2130–2139.
- Wald, G. (1938). ON RHODOPSIN IN SOLUTION. *J Gen Physiol* 795–832.
- Wald, G. (1968). *Molecular Basis of Visual Excitation*. Pdf. 162.
- Wang, T. (2005). Rhodopsin Formation in *Drosophila* Is Dependent on the PINTA Retinoid-Binding Protein. *J. Neurosci.* 25, 5187–5194.
- Wang, T., Jiao, Y., and Montell, C. (2007). Dissection of the pathway required for generation of vitamin A and for *Drosophila* phototransduction. *J. Cell Biol.* 177, 305–316.
- Wang, V.Y., Hassan, B.A., Bellen, H.J., and Zoghbi, H.Y. (2002). *Drosophila* atonal fully rescues the phenotype of Math1 null mice: New functions evolve in new cellular contexts. *Curr. Biol.* 12, 1611–1616.
- Wang, X., Wang, T., Jiao, Y., von Lintig, J., and Montell, C. (2010a). Requirement for an Enzymatic Visual Cycle in *Drosophila*. *Curr. Biol.* 20, 93–102.
- Wang, X., Wang, T., Jiao, Y., von Lintig, J., and Montell, C. (2010b). Requirement for an Enzymatic Visual Cycle in *Drosophila*. *Curr. Biol.* 20, 93–102.
- Wang, X., Wang, T., Ni, J.D., von Lintig, J., and Montell, C. (2012). The *Drosophila* Visual Cycle and De Novo Chromophore Synthesis Depends on rdhB. *J. Neurosci.* 32, 3485–3491.
- Yack, J.E. (2004). The structure and function of auditory chordotonal organs in insects. *Microsc. Res. Tech.* 63, 315–337.
- Yoon, J., Matsuo, E., Yamada, D., Mizuno, H., Morimoto, T., Miyakawa, H., Kinoshita, S., Ishimoto, H., and Kamikouchi, A. (2013). Selectivity and Plasticity in a Sound-Evoked Male-Male Interaction in *Drosophila*. *PLoS One* 8, 1–13.
- Yorozu, S., Wong, A., Fischer, B.J., Dankert, H., Kernan, M.J., Kamikouchi, A., Ito, K., and Anderson, D.J. (2009). Distinct sensory representations of wind and near-field sound in

the *Drosophila* brain. *Nature* 458, 201–205.

Zanini, D., Giraldo, D., Warren, B., Katana, R., Andrés, M., Reddy, S., Pauls, S., Schwedhelm-Domeyer, N., Geurten, B.R.H., and Göpfert, M.C. (2018). Proprioceptive Opsin Functions in *Drosophila* Larval Locomotion. *Neuron* 98, 67–74.e4.

Zhang, W., Cheng, L.E., Kittelmann, M., Li, J., Petkovic, M., Cheng, T., Jin, P., Guo, Z., Göpfert, M.C., Jan, L.Y., et al. (2015). Ankyrin Repeats Convey Force to Gate the NOMPC Mechanotransduction Channel. *Cell* 162, 1391–1403.

List of figures:

Figure 1. Hearing organ of <i>Drosophila</i>	10
Figure 2. Chordotonal organs in <i>Drosophila</i>	11
Figure 3. Experimental setup to probe antennal mechanics and electrophysiology	20
Figure 4. Rhodopsin sketch	27
Figure 5. Biomechanical and sound evoked nerve responses analyses of wild-type and <i>santa-maria</i> ¹ mutant flies	34
Figure 6. <i>santa-maria-Gal4</i> expression pattern.	35
Figure 7. Epifluorescent image of the <i>santa-maria</i> ^{T-GEM} - <i>Gal4</i> expression pattern in larva	36
Figure 8. <i>santa-maria</i> ^{T-GEM} - <i>Gal4</i> expression in larval Ich5 chordotonal organ	36
Figure 9. <i>santa-maria</i> ^{T-GEM} - <i>Gal4</i> expression in Johnston's organ	37
Figure 10. Localization of TRP channels in Ich5 organ in wild type and <i>santa-maria</i> ¹ mutant larvae.	38
Figure 11. Localization of TRP channels in JO of wild type and <i>santa-maria</i> ¹ mutants	39
Figure 12. Laser Doppler analysis of <i>santa-maria</i> GAL4-UAS rescue	41
Figure 13. Auditory performance of <i>ninaD</i> ¹ and <i>ninaB</i> ^{360d} mutant flies	43
Figure 14. ERG recording from wild type and vitamin A depleted flies	45
Figure 15. LDV measurements of Vitamin A depleted flies	46
Figure 16. JO function in <i>pinta</i> ¹ mutants and rescue flies	48
Figure 17. <i>pinta</i> expression in larval Ich5 organs	50
Figure 18. <i>pinta</i> expression pattern in Johnston's organ	51
Figure 19. Auditory phenotype of <i>ninaG</i> mutant flies	52
Figure 20. α Tub85E and <i>ninaG</i> expression pattern in larval Ich5 chordotonal organ	54
Figure 21. <i>ninaG</i> expression pattern in adult JO	55
Figure 22. Auditory performance of the mutant flies implicated in chromophore recycle	57
Figure 23. <i>Pdh-GAL4</i> expression in the eye of <i>Drosophila</i>	58
Figure 24. <i>rdhB-Gal4</i> expression pattern in adult JO	59
Figure 25. Rhodopsin1 RT-PCR analysis	60
Figure 26. Auditory performance of various <i>ninaE</i> ¹⁷ mutant strains	62
Figure 27. Screenshot showing list of the genes detected in <i>Drosophila</i> JO from Senthilian et al., 2012.	27
Figure 28. Laser Doppler Vibrometer analysis of auditory defects in <i>sosie</i> mutant flies.	74
Figure 29. <i>sosie</i> ^{Trojan} - <i>Gal4</i> expression pattern in larval and adult chordotonal organs	75
Figure 30. Johnston's organ staining of <i>sosie</i> ^{MiMIC} mutants	76
Figure 31. Auditory phenotype of <i>CG14085</i> ^{MiMIC} mutant flies	78
Figure 32. <i>CG14085</i> expression pattern in chordotonal organs	79

List of abbreviations:

AAMC	antennal mechanosensory and motor center
<i>ato</i>	<i>atonal</i>
Ibf	individual best frequency
CAP	compound action potential
<i>cs</i>	<i>cantonS</i>
<i>Dnai2</i>	<i>dynein, axonemal, intermediate chain 2</i>
GFP	green fluorescence protein
<i>iav</i>	<i>inactive</i>
JO	Johnston's organ
Lch1	lateral chordotonal organ
Lch5	lateral pentalosclopidial chordotonal organ
MET	mechanoelectrical ion channel
MiMIC	Minos-Mediated Integration Cassette
<i>nan</i>	<i>nanchung</i>
<i>nina B/D/E/G</i>	<i>neither inactivation nor afterpotential B/D/E/G</i>
<i>nompC</i>	<i>no mechanoreceptor potential C</i>
<i>pdh</i>	<i>photoreceptor dehydrogenase</i>
<i>pinta</i>	<i>prolonged depolarization potential (PDA) is not apparent</i>
PLC	phospholipase C
PSD	power spectral density
<i>rdhB</i>	<i>retinol dehydrogenase</i>
Rh	Rhodopsin
RMCE	recombinase-mediated cassette exchange
<i>santa-maria</i>	<i>scavenger receptor acting in neural tissue and majority of rhodopsin is absent</i>
TRP	Transient receptor potential
TRPN	Transient receptor potential <i>nompC</i>
TRPV	Transient receptor potential vanilloid
VchA/B	ventral chordotonal organ A/B
WT	wild type

Curriculum Vitae

Personal details:

Name: Radoslaw Katana
Date of birth: November 24th, 1987
Place of birth: Zielona-Gora
Nationality: Polish

Education:

10.2013 – Present Phd student, Georg-August-Universität Göttingen
Department of Cellular Neurobiology
Phd thesis: “Chromophore-independent roles of *Drosophila* opsin
apoproteins and visual cycle components”

10.2010 – 09.2012 MSc, University of Wroclaw – Faculty of Biology,
Department of Animal Molecular Physiology,
Master’s thesis: „Phosphoglycerate mutase expression in the context
of synaptic plasticity in rat hippocampal slices”

10.2007 – 09.2010 Bachelor degree : University of Wroclaw – Faculty of Biology,
Specialization: Biology, Zoology

Publications:

Zanini, D., Giraldo, D., Warren, B., **Katana, R.**, Andrés, M., Reddy, S., Pauls, S., Schwedhelm-Domeyer, N., Geurten, B.R.H., and Göpfert, M.C. (2018). Proprioceptive Opsin Functions in *Drosophila* Larval Locomotion. *Neuron* 98, 67–74.e4.

Zazo Seco C, Castells-Nobau A, Joo SH, Schraders M, Foo JN, van der Voet M, Velan SS, Nijhof B, Oostrik J, de Vrieze E, **Katana R**, Mansoor A, Huynen M, Szklarczyk R, Oti M, Tranebjærg L, van Wijk E, Scheffer-de Gooyert JM, Siddique S, Baets J, de Jonghe P, Kazmi SA, Sadananthan SA, van de Warrenburg BP, Khor CC, Göpfert MC, Qamar R, Schenck A, Kremer H, Siddiqi S. A homozygous FITM2 mutation causes a deafness-dystonia syndrome with motor regression and signs of ichthyosis and sensory neuropathy. *Dis Model Mech.* 2017 Feb 1;10(2):105-118. doi: 10.1242/dmm.026476. Epub 2016 Dec 15.

Karak, S., Jacobs, J.S., Kittelmann, M., Spalthoff, C., **Katana, R.**, Sivan-Loukianova, E., Schon, M.A., Kernan, M.J., Eberl, D.F., and Göpfert, M.C. (2015). Diverse Roles of Axonemal Dyneins in *Drosophila* Auditory Neuron Function and Mechanical Amplification in Hearing. *Sci. Rep.* 5, 1–12.

Nesterov A, Spalthoff C, Kandasamy R, **Katana R**, Rankl NB, Andrés M, Jähde P, Dorsch JA, Stam LF, Braun FJ, Warren B, Salgado VL, Göpfert MC. TRP Channels in Insect Stretch Receptors as Insecticide Targets. *Neuron*. 2015 May 6;86(3):665-71. doi: 10.1016/j.neuron.2015.04.001.

Conference presentations:

09.2016 Neurofly 2016
16th European Neurobiology of *Drosophila* Conference,
Platanias, Chania, Greece. Poster: “Dissecting the auditory relevance
of the *Drosophila* visual chromophore pathway”.

Acknowledgements

Na wstępie chciałbym podziękować moim rodzicom, dzięki którym nie byłbym w tym miejscu w którym jestem. Chciałbym również podziękować moim przyjaciołom w szczególności: Piotrkowi, Przemkowi, Medykowi, Zajączowi i Mierzwiemu za ich wsparcie podczas mojego doktoratu.

I would like to thank Prof. Dr. Gopfert for giving me the credit and chance to start my research carrier in such a wonderful scientific environment. He was always there to support me, give advice and discuss the project. It was a great fun to attend two DFG conferences with him. I would also like to show my gratitude for the second member of my thesis committee member Prof. Dr. Andre Fiala for his scientific input into my project.

I would also like to thank my colleagues:

- Dr. Damiano Zanini, who was my “unofficial supervisor” and one of the best friends. Thank you for all your scientific help, and great time during Neurofly conference, that I will never forget. I was very lucky to come across such a great person.
- Dr. Diego Giraldo for being always there to talk and help. It was a great fun to hang around with you, watch football matches and discuss scientific and non-scientific things.
- Dr. David Pipenbrock who taught me LDV measurements, and helped me mentally during the first year of my phd.
- Dr. Marta Andreas for her involvement in the initial part of the project, help with molecular biology and being extremely nice and kind person.
- Dr. Somdatta Karak for her help and involvement in the project and being a mentor.
- Dr. Philipp Hehlert for his advises and long scientific and non-scientific discussions.
- Dr. Bart Geurten for help with building PDA setup.
- Marvin Seifert, it was a great pleasure to meet such a friendly person.

- Narges Bodaghabadi for being supportive and helping me during last weeks.

I would like to thank my office colleagues: Stephanie Pauls, Margareth Winkler, Nicola Schwedhelm-Domeyer for their technical support, help with german language and creating a kind and friendly atmosphere. I thank Gudrun Matthes for her help with all the formalities at the beginning of my phd. Last but not least, I would also like to thank all the other persons from the lab for being there, creating friendly and scientific atmosphere.